GEOLOGIC MAP OF THE ELDON 7.5-MINUTE QUADRANGLE, JEFFERSON, KITSAP, AND MASON COUNTIES, WASHINGTON

by Trevor A. Contreras, Eleanor Spangler, Logan A. Fusso, David A. Reioux, Gabriel Legorreta Paulin, Patrick T. Pringle, Robert J. Carson, Emily F. Lindstrum, Kenneth P. Clark, Jeffrey H. Tepper, Domenico Pileggi, and Shannon A. Mahan

WASHINGTON
DIVISION OF GEOLOGY
AND EARTH RESOURCES
Map Series 2012-03
December 2012

WASHINGTON STATE DEPARTMENT OF
Natural Resources
Peter Goldmark - Commissioner of Public Lands

DISCLAIMER

INDEMNIFICATION

Research supported by the U.S. Geological Survey, National Cooperative Geologic Mapping Program, under USGS award number G11AC20236. The views and conclusions contained in this document are those of the authors and should not be interpreted as necessarily representing the official policies, either expressed or implied, of the U.S. Government.

WASHINGTON STATE DEPARTMENT OF NATURAL RESOURCES

Peter Goldmark—Commissioner of Public Lands

DIVISION OF GEOLOGY AND EARTH RESOURCES

David K. Norman—State Geologist
John P. Bromley—Assistant State Geologist

Washington Department of Natural Resources
Division of Geology and Earth Resources

Mailing Address:
MS 47007
Olympia, WA 98504-7007

Street Address:
Natural Resources Bldg, Rm 148
1111 Washington St SE
Olympia, WA 98501

Phone: 360-902-1450
Fax: 360-902-1785
E-mail: geology@dnr.wa.gov
Website: http://www.dnr.wa.gov/ResearchScience/GeologyEarthSciences/Pages/Home.aspx

Publications List:
http://www.dnr.wa.gov/ResearchScience/Topics/GeologyPublicationsLibrary/Pages/pubs.aspx

Washington Geology Library Catalog:
http://www.dnr.wa.gov/ResearchScience/Topics/GeologyPublicationsLibrary/Pages/washbib.aspx

Washington State Geologic Information Portal:
http://www.dnr.wa.gov/ResearchScience/Topics/GeosciencesData/Pages/geology_portal.aspx

Suggested citation: Contreras, T. A.; Spangler, Eleanor; Fusso, L. A.; Reioux, D. A.; Legorreta Paulin, Gabriel; Pringle, P. T.; Carson, R. J.; Lindstrum, E. F.; Clark, K. P.; Tepper, J. H.; Pileggi, Domenico; Mahan, S. A., 2012, Geologic map of the Eldon 7.5-minute quadrangle, Jefferson, Kitsap, and Mason Counties, Washington: Washington Division of Geology and Earth Resources Map Series 2012-03, 1 sheet, scale 1:24,000, 60 p. text.

Published in the United States of America

Table of Contents

FIGURES

TABLES

PLATE

Geologic Map of the Eldon 7.5-minute Quadrangle, Jefferson, Kitsap, and Mason Counties, Washington

by Trevor A. Contreras[1], Eleanor Spangler[1], Logan A. Fusso[1], David A. Reioux[1], Gabriel Legorreta Paulin[2], Patrick T. Pringle[3], Robert J. Carson[4], Emily F. Lindstrum[5], Kenneth P. Clark[6], Jeffrey H. Tepper[6], Domenico Pileggi[7], and Shannon A. Mahan[8]

[1] Washington Division of
Geology and Earth Resources
MS 47007
Olympia, WA 98504-7007

[2] Universidad Nacional Autónoma de México
Instituto de Geografía
Ciudad Universitaria, Del Coyoacán
cp 04510, México, D.F.

[3] Centralia College
Earth Sciences Program
600 Centralia College Blvd
Centralia, WA 98531-4099

[4] Department of Geology
Whitman College
345 Boyer Ave
Walla Walla, WA 99362

[5] University of Hawaii at Hilo
Department of Geology
200 W Kawili St
Hilo, HI 96720-4091

[6] University of Puget Sound
Department of Geology
1500 N Warner St
Tacoma, WA 98416-1048

[7] University of Siena
Department of Earth Sciences
Via Laterina 8
53100 Siena, Italy

[8] U.S. Geological Survey
Box 25046, Denver Federal Center, MS 974
Denver, CO 80225-5046

INTRODUCTION

The map area, in the western Puget Lowland, straddles Hood Canal (Fig. 1) near the community of Eldon and contains the lower portion of the Hamma Hamma River. Most of the map area is covered by glacial sediment left by alpine glaciers of the Olympic Mountains and the Cordilleran ice sheet, which advanced south from Canada several times during the Pleistocene Epoch. This mapping was undertaken to identify the area's geologic hazards, including active faults and landslides, and to delineate the glacial stratigraphy and hydrologic characteristics of the Hood Canal area to assist scientists working on dissolved oxygen problems in Hood Canal.

Segments of the Seattle, Tacoma, Hood Canal, Saddle Mountain, and Dow Mountain faults and the Lucky Dog structure (Polenz and others, 2010a,b) are in the area (see Carson, 1973; Wilson, 1975; Wilson and others, 1979; Walsh and others, 1997; Witter and others, 2008; Blakely and others, 2009; and Lamb and others, 2012). How these faults interact is not yet well understood. The Seattle fault zone has been mapped as far west as Hood Canal (Lamb and others, 2012; Contreras and others, 2012b). Geophysical models by Lamb and others (2012) and Blakely and others (2009) suggest that the fault zone crosses Hood Canal and merges with faults to the southwest in a complex network of faults. Our mapping confirms these models and provides field evidence suggesting that east-trending faults and structures between Pleasant Harbor (to the north in the Brinnon quadrangle) and Ayock Point merge with northeast-trending faults that extend northward from the Saddle Mountain area (Hoodsport quadrangle). Additionally, evidence from faults that parallel Hood Canal suggests that faulting controls some parts of the canal, but the faults do not appear to be continuous, as previous maps have depicted (Contreras and others, 2010, 2012a; Polenz and others, 2012a).

Persistent landslides continue to damage property and infrastructure in the area. Landslides along U.S. Highway 101 between Lilliwaup and the Hamma Hamma River have occurred historically (Gryta, 1975) and continue to impact infrastructure and commerce. Many of these slides initiate on silts and clays of Whidbey Interglaciation age. Mapping by Contreras and others (2010) suggests that some ice-contact features previously interpreted as landslides are likely stable and widely distributed along Hood Canal.

Throughout the text, we refer to significant sites numbered 1 to 13 and indicated by orange diamonds on the map. Appendix F provides information on these sites. Other appendices include radiocarbon (^{14}C) and optically stimulated luminescence (OSL) dates, geochemical (Appendix C) and geophysical data (Appendix E), columnar and composite stratigraphic sections (Appendix B), and maps related to the extent of ice during the Vashon glaciation (Appendix D).

GEOLOGIC OVERVIEW

Bedrock in the quadrangle was mapped by Cady and others (1972), Carson (1976a,b), and Tabor and Cady (1978) as basalt and interbedded sedimentary rocks of the Eocene Crescent Formation. The formation is widely exposed in the northwestern part of the quadrangle and to the west and north. Determining the type of bedrock and thickness of glacial sediments beneath the map area is hampered by limited subsurface data and the structural complexity caused by the intersection of the Seattle and Tacoma faults with the Olympic Mountains (Fig. 1). Geophysical models (Lamb and others, 2012, 2009; Blakely and others, 2009; Karel and Liberty, 2008; Brocher and others, 2004; Haug, 1998) and geophysical data help constrain depth to bedrock and provide insight into faulting in the area. Lamb and others (2012) infer a strain transfer zone linking the Seattle and Dow Mountain faults within the map area. Their data indicate that bedrock in the Tacoma basin (near the south end of the map area) may be covered by more than 3280 ft of sediment.

Previous work (Bretz, 1913; Todd, 1939; Cady and others, 1972; Carson, 1976a; Gryta, 1975; Garling and others, 1965; Deeter, 1979; Wash. Dept. of Ecology, 1979, 1980) described the Pleistocene stratigraphy in the map area and provided subsurface information relating to groundwater. These authors documented repeated Pleistocene glacial incursions that deposited most of the quadrangle's unconsolidated sediment, and they attempted to classify and correlate these deposits within the Puget Lowland. Our map builds on previous work, but we broadly categorized deposits without tying them to specific formations or type sections unless we had enough age control to confidently do so.

Mapping in the adjacent Holly quadrangle (Contreras and others, 2012b) suggests that the Seattle basin extends west to at least Hood Canal. We based this conjecture on the extent of deposits of Whidbey Interglaciation age (Marine Oxygen Isotope Stage [MIS] 5; Fig. 2) at sea level north of the inferred location of the Seattle uplift, approximately the location of Holly, due east of Eldon. These silts are present in this map area in isolated outcrops on the west side of the canal, north of Ayock Point.

We broadly classify the various drifts as 'northern-sourced' or 'Olympic-sourced'. Northern-sourced drift generally contains granitic and metamorphic rock clasts, indicating deposition by the Cordilleran ice sheet, but it also typically contains abundant locally derived basalt clasts. Olympic-sourced drift contains basalt and sandstone (in addition to rare reworked granitic and metamorphic clasts), indicating deposition by alpine glaciers of the Olympic Mountains. The Cordilleran ice sheet overrode and incorporated sediment shed from the Olympic Mountains and deposited northern-sourced sediment in the Olympic foothills, resulting in occurrences of northern-sourced granitic and metamorphic rocks mingled with the dominantly basalt- and sandstone-rich Olympic-sourced drift.

DESCRIPTION OF MAP UNITS

Our map shows deposits of geotechnical and hydrological significance, generally having a thickness of at least 5 ft, although where stiff, impermeable, or geotechnically challenging (for example, till or peat), we locally mapped thinner deposits. In most areas, we relied considerably on geomorphology, field relations, and subsurface records. We used the Udden-Wentworth scale (Pettijohn, 1957) to classify unconsolidated sediments and Dickinson's (1970) terminology for sandstones. We estimated consistency and apparent density using suggested guidelines of the American Association of State Highway and Transportation Officials (1988). Assignment of volcanic rock names was made on the basis of whole-rock geochemistry and the total alkali-silica (TAS) diagram of Le Maitre (1989).

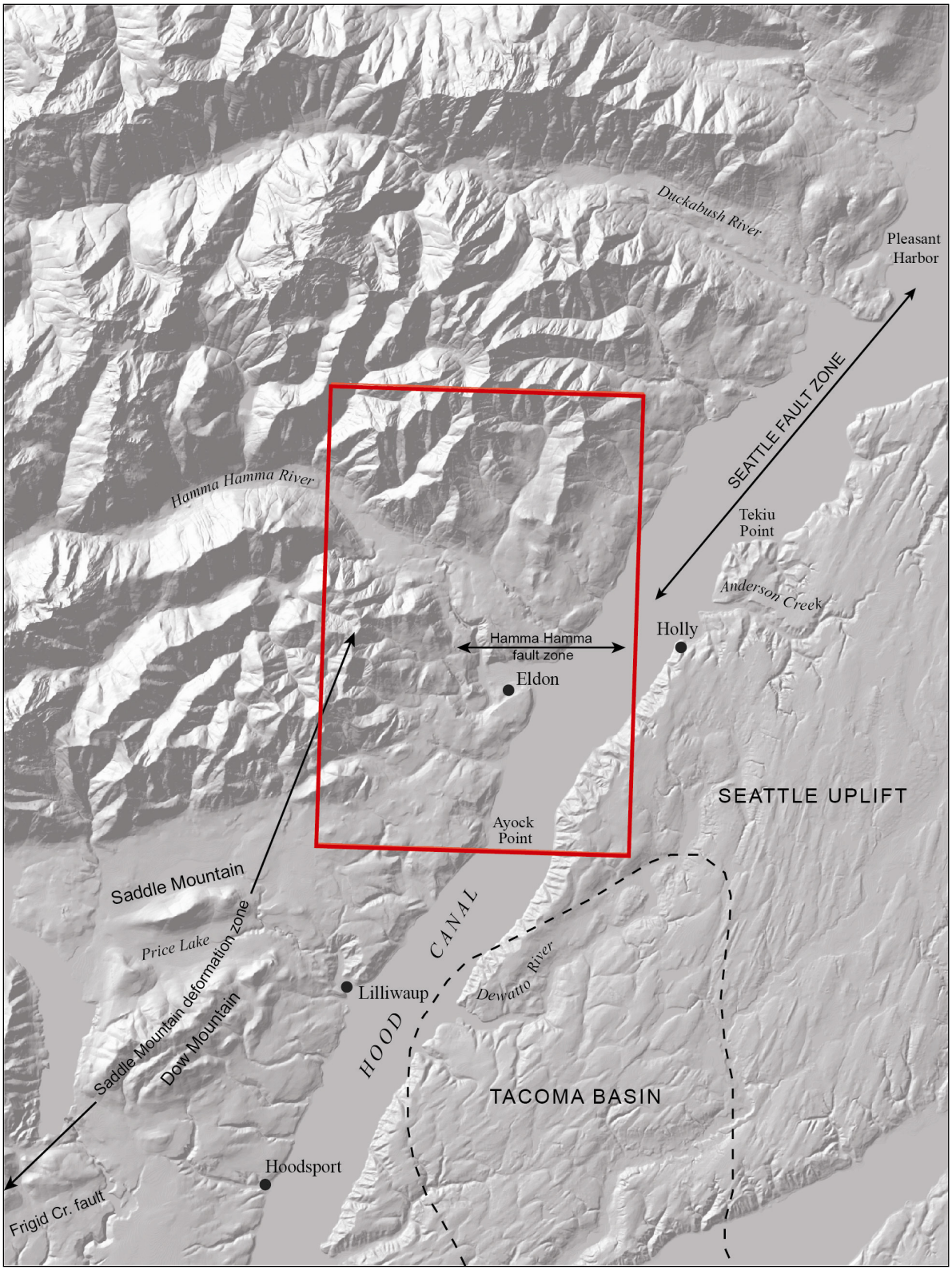

Figure 1. Shaded relief map of the Eldon quadrangle (red polygon) and surrounding area. Fault and deformation zones are shown as indicated by field investigations (Contreras and others, 2012a; Polenz and others, 2012c) and geophysical studies (Blakely and others, 2009; Lamb and others, 2012).

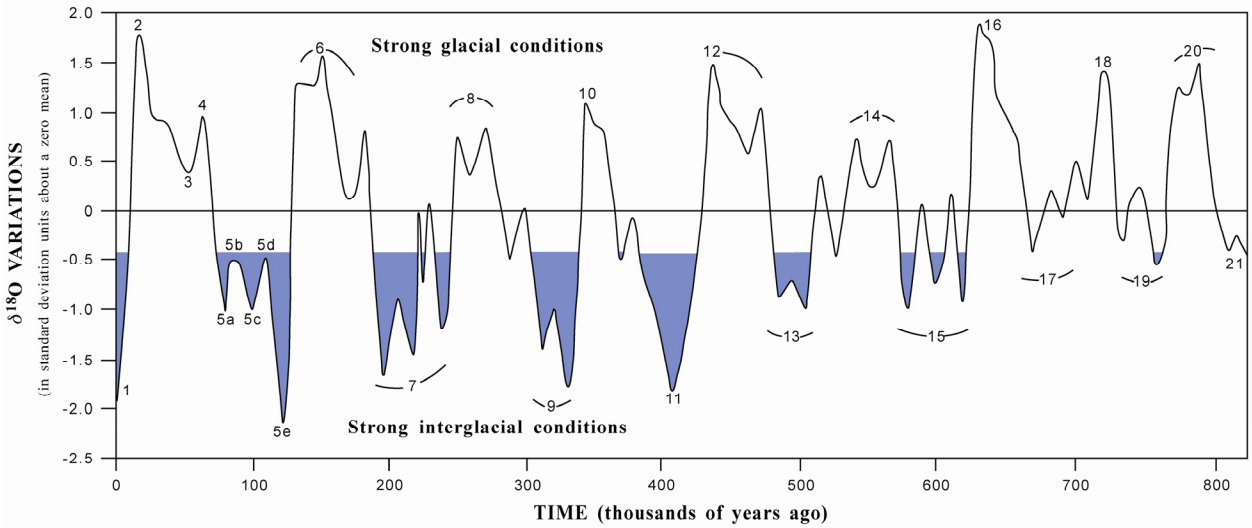

Figure 2. Marine oxygen-isotope stages for the past 800,000 years (redrawn from Morrison, 1991). The graph shows variations in the ratio of $^{18}O/^{16}O$ over time. The numbers within the graph are stage numbers; the even-numbered peaks (at top) are glacial maxima, and the odd-numbered troughs (at bottom) are interglacial minima. The blue areas indicate interglacial episodes defined by a cutoff at –0.5 $\delta^{18}O$ oxygen-isotope values (equivalent to Holocene interglacial values—the milder climate of the past 10 ka). Note that this last 800 ka of the Quaternary Period is dominated by times of glaciation.

We used the time scale of the U.S. Geological Survey Geologic Names Committee (2010). A USGS 7.5-minute topographic map of the Eldon quadrangle was used as a base map, but contact locations were generally refined by reference to a LiDAR (light detection and ranging, hereafter lidar) image, aerial photos, and field observations.

Quaternary Unconsolidated Deposits

HOLOCENE NONGLACIAL DEPOSITS

ml **Modified land**—Clay to boulder gravel and diamicton; locally derived but mixed and reworked by excavation and (or) redistribution that notably modifies topography; shown where fairly extensive, masking underlying geology, and geotechnically significant (>5 ft); excludes roads (except where connected to a larger modified area).

Qa **Alluvium**—Sand to cobble gravel, locally includes silt, clay, and peat; typically gray and generally unweathered; loose; clasts subrounded; moderately to well sorted; stratified to massive; includes some lacustrine and beach deposits and may include unrecognized older glacial outwash; consists of reworked glacial and nonglacial deposits.

Qm **Tide-flat deposits**—Sand to cobble gravel, locally includes silt, clay, and peat; typically tan and generally unweathered; loose; clasts subrounded; moderately to well sorted; stratified to massively bedded; occurs at the Hamma Hamma River delta; includes some lacustrine and beach deposits.

Qoa_m **Relict alluvium and salt-marsh deposits**—Silty sand and pebble to cobble gravel, locally includes silt, clay, peat, and detrital wood; typically tan and generally unweathered; loose; clasts subrounded; moderately to well sorted; stratified to massively bedded; may include older tide flats above current salt marsh. This unit occurs at the mouth of the Hamma Hamma River, where radiocarbon age estimates suggest land-level changes in the past 1000 years.

HOLOCENE TO LATEST PLEISTOCENE NONGLACIAL DEPOSITS

Qp **Peat**—Peat, muck, and organic-rich silt and clay; dark brown to black; very soft to medium-soft; typically in closed depressions. Unit Qp includes upland wetlands and flat surfaces in closed depressions, unless standing water was identified. We mapped some peat on the basis of topography and aerial photos.

Unit Qp overlies Vashon Drift and older glacial deposits and is Holocene but may include some late Pleistocene deposits.

Qls **Landslide deposits**—Clay, silt, sand, and gravels (diamicton); loose or soft; clasts are angular to rounded; unsorted to poorly sorted; nonstratified, but may locally retain primary bedding; includes exposures of underlying units in scarp areas. Absence of a mapped slide does not imply absence of landslide hazard; some slides are too small to show at map scale. Many previously mapped slides (Carson 1976a; Gerstel and Lingley, 2003) were not included in this unit in order to show underlying geology or because of lack of evidence of movement or a different interpretation of landforms; some landslides are mapped as unit Qmw. We did not include numerous debris flow chutes evident in the lidar elevation model. Some of our landslides on the west side of Hood Canal south of the Hamma Hamma River may be slump features in ice-contact deposits (unit Qgic). Some of these landforms are active landslides that damage U.S. Highway 101; others are relict stagnant-ice landforms. The active landslides initiate in unit Qc_w that perches water and causes failure of the overlying drift. Gryta (1975) has shown that a landslide along Jorsted Creek was active about 9000 years ago. We mapped additional landslides on the south side of Jorsted Creek; morphology and stratigraphy suggest these landslides could be the result of liquefaction and lateral spreading during earthquakes. This unit is mostly Holocene but may include some late Pleistocene deposits.

Qmw **Mass-wasting deposits**—Pebble to boulder gravel, sand, and diamicton, minor sand and gravel beds where modified by stream processes; loose; clasts subrounded; poorly to moderately sorted. This unit is mapped along mostly colluvium-covered slopes and includes debris fans, alluvial fans, and landslides where lidar shaded-relief suggested mass-wasting deposits large enough to show at map scale. Absence of a mapped mass-wasting deposit does not imply absence of slope instability or hazard. This unit is mostly Holocene but may include some late Pleistocene deposits.

Qaf **Alluvial fan deposits**—Sand and gravel and debris-flow diamicton; gray, weathering to brownish-orange; loose; clasts subrounded to rounded; typically poorly to moderately sorted; massive to weakly stratified. This unit forms concentric lobes where streams emerge from confining valleys. Debris flows and debris torrents may be a geologic hazard on some alluvial fans; the December 2007 storms added material to most fans in the area, damaged homes and infrastructure, and covered beaches and shellfish beds. The fan at the mouth of Waketickeh Creek contains unusually large boulders; Elmendorf and Kroeber (1992) noted that this creek formerly supported a salmon run. Unit Qaf is predominantly Holocene but likely includes some late Pleistocene deposits.

Qob **Older beach deposits**—Sand to boulder gravel with marine shell fragments; gray to brown-gray; loose; clasts typically subrounded; well sorted. Unit Qob is mapped only in the approximate location of Bretz's (1913) uplifted beach deposits at Eldon and Cummings Point. The deposits consist of outwash gravels modified by wave action below an elevation of 290 ft; unmodified eskers (unit Qge) lie above the highest gravels. We did not find evidence in the field to support these sites being uplifted or being shorelines (Polenz and others, 2010a,b; see Fig. F3 in Appendix F for additional details). We mapped unit Qob between 135 and 85 ft in elevation primarily because of Bretz's work, the break in slope, the topography of Eldon, and terraces at similar elevations in Johns Creek and on the Kitsap Peninsula (Contreras and others, 2012a).

Qoa **Older alluvium**—Sand and silt with lesser gravelly sand, sandy pebble gravel, peat, and organic detritus; gray to brown-gray and blue-gray; loose; clasts subrounded to rounded; well sorted; well stratified. This alluvium underlies terraces above modern channels in Johns, Jorsted, and Waketickeh Creeks and the Hamma Hamma River that may record land-level changes, landslides, and earthquakes. These deposits commonly have wood and organic material at their base, which is near modern stream level. Radiocarbon dates indicate that these deposits filled outwash channels at various times throughout the Holocene. Samples obtained from these deposits in Johns Creek likely record an earthquake that drowned a forest between 827 to 1017 cal yr AD, about the time of the Seattle fault rupture, 900 to 930 cal yr AD (Atwater, 1999). This event may have dammed the drainage and covered the forest floor with sediment, thereby

preserving it. Additional radiocarbon age estimates from samples taken above and below a paleosol in the Hamma Hamma River valley floor (significant site HH1) provide limiting ages of a land-level change between 1290 ±30 and 1890 ±30 yr BP. While no diagnostic diatoms were found to confirm a land-level change (Brian Sherrod, USGS, written commun., 2012), two additional dates in the nearby Holly and Brinnon quadrangles (Contreras and others, 2012b; Lindstrum, 2002) are similar, and Lindstrum (2002) suggests a drop in land level at this time. Evidence for this event (or events) may be widespread because additional terrace deposits approximately 5 mi to the east in Anderson Creek also contain organic materials that have similar ages. Alluvial terrace deposits in Waketickeh Creek might be the result of Holocene faulting. See Appendix B for radiocarbon dates and columnar sections within the Hamma Hamma valley.

PLEISTOCENE GLACIAL AND NONGLACIAL DEPOSITS

Vashon Stade of the Fraser Glaciation

While Porter and Swanson (1998) suggested that deglaciation was accomplished prior to 16,420 cal yr BP at Lake Carpenter (approximately 30 mi to the northeast), recent work by Polenz and others (2012b) suggests that Vashon-age ice entered the Hoodsport quadrangle between 17,000 and 15,700 cal yr ago. The extent of the Vashon Stade Puget lobe glacial deposits is indicated by various blue dashed lines on the map. These lines are only inferred and are approximately located between 2200 and 1500 ft elevation ; they are similar to, but often lower than, the glacial limits previous mapping suggested (Todd, 1939; Frisken, 1965; Long, 1975a,b; Carson, 1980). We refined this limit by analyzing slopes on digital elevation models (Fig. D2) and from field evidence that included absence of Cordilleran-sourced deposits at high elevations, a major break in slope, and an ice-marginal channel noted by Todd (1939) at approximately 2100 ft on the north side of the Hamma Hamma River (Fig. D1). On the whole, evidence suggests a maximum ice thickness between 1500 and 900 ft above the glacially scoured and fluted topography on the west side of Hood Canal, between the canal and the dashed blue lines. The Vashon till in the map area is an unweathered, discontinuous, poorly developed, thin layer of subglacial melt-out till or stagnant-ice deposits. While there are tills containing exotic clasts above our ice limit, we contend they are relatively more weathered and were emplaced by earlier, more extensive glaciations.

Where our Olympic ice limit crosses the Hamma Hamma River there is a moraine deposited by Olympic ice. This location coincides with a lack of northern-sourced glacial deposits upstream. However, we did not estimate the extent of incursions of the Puget lobe into the Hamma Hamma drainage during the Vashon Stade. We agree with Carson (1980) that Olympic-sourced Fraser ice in the Hamma Hamma valley was likely confined to the mountain front and did not cross to the east side of the canal; the Olympic drift found east of this line is likely pre-Fraser in age. (See additional information about significant site 3 in Appendix F.)

Recessional Deposits of the Fraser Glaciation

Mapped recessional deposits of the Fraser Glaciation are units Qao, Qgo, Qgog and Qgic. Unit Qao is included in the recessional deposits because it overlies Vashon Stade glacial deposits of northern source, but it is the result of glacial, and likely nonglacial, transport of material from the Olympic Mountains. Haugerud (2009a,b), Porter and Carson (1971), and Porter and Swanson (1998) noted that deglaciation following the Vashon Stade in the southern Puget Lowland probably began with stagnation of the ice sheet: ice thinned, stopped moving, and melted in place, leaving behind subglacial drainage and other ice-contact features. We find consistent evidence of this in the Eldon quadrangle; Polenz and others (2009a,b), Derkey and others (2009), and Contreras and others (2010, 2012a) depict stagnant-ice features throughout the area. Previous mapping assumed that the area is covered with Vashon-age lodgment till; however, shaded relief on lidar images and field work show that stagnant-ice deposits are more extensive at the surface than previous mapping suggests. The apparent roughness in topography on and near drumlins coincides with locations of stagnant-ice deposits and the lack of lodgment till. These deposits are likely younger than 16,420 cal yr BP (see dates in Polenz and others, 2012b).

Qae **Esker deposits, Olympic-sourced**—Pebble to boulder gravel and sand; tan to brown; loose; clasts moderately to well rounded; typically well sorted; forms low, elongate, sinuous hills, typically less than 20 ft high. Unit Qae is mapped where field relations suggested deposition under Olympic-sourced ice.

Qao **Recessional outwash, Olympic-sourced**—Cobble to pebble gravel and pebbly sand and minor silt beds; brown-gray, weathering to red-brown; loose; clasts typically subrounded; moderately to well sorted; typically crudely stratified. Clasts are predominantly basalt; sandstone clasts are a minor component. This alluvial unit is present in drainages on the west side of Hood Canal, where we found few granitic clasts and could identify a local source.

Qgo **Vashon recessional outwash**—Cobble to pebble gravel, pebbly sand, and minor silt; gray, weathering to tan; loose; clasts subangular to rounded; moderately to well sorted; typically crudely stratified; derived from both northern and local sources; a few to tens of feet thick. Unit Qgo was deposited by glacial meltwater in sub- or superglacial outwash channels, in isolated basins on the fluted upland surface, and in areas in the Hamma Hamma valley where the deposits appear to have been surrounded by Cordilleran ice, but may have had an Olympic source. Some deposits are ice-proximal, suggesting a late Pleistocene age, and are difficult to separate from units Qgic and Qgik, resulting in gradational boundaries between units Qgic and Qgo.

Qgic **Vashon ice-contact deposits**—Diamicton, cobbly pebble gravel, silty sandy till, silty pebble gravel, and pebbly sand, with minor sand and silt; yellow-tan to gray; loose to very dense; clasts subangular to subrounded; variously sorted; massive to well stratified; accompanied by stagnant-ice features, such as kettles, hummocky topography, eskers (separately mapped as unit Qge where distinct), and subglacial or subaerial outwash channels. Unit Qgic ranges in thickness from a few to tens of feet and is mapped over a large part of the fluted upland surface on both sides of Hood Canal and against the Olympic Mountains below a break in slope at approximately 1250 ft elevation. Where lacking more recognizable stagnant-ice features, unit Qgic is commonly a friable, but compact, subglacial melt-out till that appears permeable. Typically distinguished from lodgment till by its apparent roughness in lidar shaded-relief and its association with other stagnant-ice features. It crudely corresponds with areas mapped by Haugerud (2009b) as a rippled, fluted glaciated surface (his unit gfr) on the Kitsap Peninsula. Unit Qgic lies directly on top of older material or basalt and may include more oxidized, locally derived deposits. It rarely is found on recognizable Fraser-age advance glacial deposits, and in this quadrangle does not appear to have a Vashon-age lodgment till beneath as found on Bainbridge Island (Haugerud, 2005). Though it can be found in fluted drumlins (indicating subglacial emplacement) as a diamict, it lacks subhorizontal foliation, is permeable, and is less competent than a 'typical' subglacial lodgment till. It may be related to tills found by Laprade (2003) in the Seattle area. See additional discussion in Contreras and others (2012a,b). Locally divided into:

Qge **Vashon esker deposits**—Pebble to cobble gravel and sand; tan to brown; loose; clasts moderately to well rounded; typically well sorted; forms low, elongate, sinuous hills; mapped in areas occupied by stagnant ice and may include Olympic Mountains–sourced outwash under Cordilleran ice.

Qgik **Vashon kame delta deposits**—Sandy pebble to cobble gravel with scattered lenses of diamicton and sand; gray to tan; loose to dense; clasts moderately to well rounded; moderately to well stratified, typically well sorted. These elevated fluvial-deltaic deposits were mapped where sedimentary structures, geomorphology, and (or) geological setting imply lateral ice-buttressing and are widespread in the drainages of Johns and Jorsted Creeks and the Hamma Hamma River. In Jorsted Creek, unit Qgik is the source of alluvium and is unstable in the upper drainage. This unit may include Olympic-sourced outwash deposited against Puget lobe ice. It is a local source of aggregate.

Proglacial and Subglacial Deposits of the Fraser Glaciation

Qgt **Vashon lodgment till**—Sand, pebbles, cobbles, silt, and clay (diamicton); gray, weathering to yellow-orange; very compact; clasts subangular to rounded; northern- and Olympic-sourced; unsorted and unstratified; contains angular clasts of basalt where directly overlying local bedrock. Lodgment till clasts are typically supported by a sandy-silty matrix and are unweathered, but near the surface the unit is

slightly oxidized and jointed as a result of weathering and desiccation. Some exposures include beds and lenses of sand and gravel that locally have an ice-shear foliation. Unit Qgt thickness ranges from 1 to 20 ft, but it is commonly less than 5 ft thick. Till is typically found on fluted upland surfaces where drumlins are smooth, wide, and well defined. Unit Qgt is typically covered by 1 to 6 ft of loose ablation till or rounded outwash gravel and is generally in sharp, unconformable contact with underlying units, which are most commonly older glacial deposits or may be unrecognized advance deposits.

Qad **Alpine drift, Olympic-sourced**—Diamicton and outwash; gray to red-brown; loose to very compact; clasts typically subangular to subrounded; moderately sorted to unsorted and unstratified; outwash generally level-bedded or crossbedded. Unit Qad is composed of locally derived basalt and minor sandstone clasts and includes alpine till, diamicton, and outwash deposits in the Hamma Hamma River valley. Unit Qad appears to be Fraser in age and includes a terminal moraine east of where Jefferson Creek enters the Hamma Hamma valley. It likely contains unrecognized Olympic drift of Possession and (or) early Fraser ages and may continue to the east, where Cordilleran ice deposits are dominant.

Pre-Fraser Glacial and Nonglacial Deposits

Prior to the Vashon Stade of the Fraser Glaciation, both Cordilleran and Olympic-sourced glaciers deposited sediment in the map area. Previous mapping suggests that stratigraphic relations are important because it is difficult to determine age by weathering alone (Bretz, 1913; Todd, 1939; Frisken, 1965; Deeter, 1979; Carson, 1980). We relied on the age suggested by one optically stimulated luminescence (OSL) sample and one infinite radiocarbon age estimate in the extensive nonglacial deposit of interbedded silt, sand, and clay (unit Qc_w) to interpret much of the stratigraphy. The OSL age estimate implies a correlation with MIS 5 with an age range equivalent to that of the Whidbey Formation (Easterbrook and others, 1967). This age estimate supported our assertion that overlying, poorly exposed drift that appears more oxidized than Fraser-age deposits is of Possession Glaciation age or early Fraser age—coeval with the Evans Creek Stade (Crandell, 1965). We also utilized oxidation, weathering, paleosols, and rind thickness to support mapping deposits as pre-Fraser.

Unit Qc_w is generally absent or unrecognized on the southeast side of Hood Canal in the map area; however, it is found in nearly all drainages along the west side as far south as Ayock Point. We correlated it with the post-Hoodsport nonglacial unit of Carson (1980). Commonly this unit is found directly on basalt or an older diamict, suggesting deposition on drift of Double Bluff Glaciation (MIS 6) age.

At significant site 3, a weathered Olympic-sourced drift and northern-sourced drift underlie Vashon ice-contact deposits, suggesting deposition by a Possession, early Fraser, or Evans Creek glacial lobe. Because these deposits are found stratigraphically above nonglacial deposits we map as Whidbey Interglaciation (MIS 5) age, we assert that both Olympic and Cordilleran ice advanced as far south as the Hamma Hamma River during MIS 4 (Possession time). This finding supports Carson's (1980) assertion that pre-Fraser, post-Hoodsport (Double Bluff) Olympic drift can be identified and mapped in the southeast Olympic Mountains.

Weathering was useful in mapping pre-Vashon deposits in the study area; however, the degree of weathering varies. Some older northern-sourced tills appear fresh, even where significant paleosols and deposits of multiple glacial successions occur above them. Elsewhere, tills are deeply weathered at the surface but can be mapped throughout the quadrangle. We attribute this variation to the amount of time the unit was exposed at the surface. We found extensive areas of weathered northern-sourced till in valleys and isolated outcrops above the limit of Vashon glacial deposits. These Vashon deposits are largely fresh, but where they display significant weathering at the surface, we attributed this to the ice incorporating older, weathered glacial and nonglacial deposits (unit $Qguc_2$) that are not easily distinguishable. These units were mapped in the adjacent Holly quadrangle between Fulton Creek and Triton Cove on the glacially fluted area between the canal and the basalt uplands (Contreras and others, 2012b). We mapped this unit in the northeast corner of the Eldon quadrangle where deposits appear to be older than Fraser, but are likely to have been covered by Vashon ice. Where we could discern stratigraphic relations, we mapped Possession-age drift and Whidbey-age deposits under the Vashon stagnant-ice deposits. Todd (1939) distinguished the age of drifts on the basis of surface smoothness and the abundance of surface boulders; she inferred that older drifts appear smoother and have fewer surficial boulders

Like Frisken (1965) and Todd (1939), we found the break in slope to be helpful in determining the extent of glaciations. A prominent terrace at about 1600 ft appears to mark the upper limit of Cordilleran ice during the Fraser glaciation. Below this terrace, there is a thin layer of Vashon deposits on top of older drift. Above this terrace, more

deeply oxidized till and drift appear at the surface. Todd noted northern-sourced till up to 1700 ft and a prominent break in slope at 1900 ft. She suggested that Vashon ice extended up to an ice-marginal drainage at 2100 ft. We found only older, dominantly northern-sourced drift above these elevations. We also mapped older deposits below this line because the dominant drift at these locations is older, typically northern-sourced drift mantled by a layer of Vashon-age stagnant-ice deposits too thin to show at map scale.

Our analysis of thin sections of selected samples led us to combine older units on the east side of Hood Canal into "pre-Fraser glacial and nonglacial deposits, undivided" because both glacial and nonglacial deposits of various source areas are present. These deposits also contain multiple well-developed paleosols and deeply weathered horizons, suggesting significant time between depositional events. Where we were able to consistently differentiate northern-sourced material, we did so for unit Qgd_d, which was likely deposited by Double Bluff glaciers. We correlate the oldest deposits of unit $Qguc_1$ with the Annas Bay and Clark Creek Drifts (Easterbrook and others, 1988; Birdseye and Carson, 1989) found at Capstan Rock. We provide eight composite stratigraphic sections on the east side of Hood Canal (Appendix B).

Deposits of the Possession Glaciation (MIS 4)

Qapd **Possession(?) drift, Olympic-sourced—**Till and diamict outwash consisting of cobble and pebble gravel with sparse boulders and sandy to clayey matrix; red-brown to gray; medium to very dense; subangular to subrounded; moderately sorted to unsorted. Outwash facies are bedded and stratified. Till is a chaotic mixture of locally derived basalt and minor sandstone in a sandy clay matrix. This drift is present in the Hamma Hamma River drainage and in Waketickeh Creek. Isolated deposits of unit Qapd on the east side of the upper Waketickeh Creek valley are not shown in favor of the dominant northern-sourced drift. Unit Qapd overlies laminated silts of Whidbey age along an erosional contact, best exposed in Waketickeh Creek south of significant site 1; a vesicular volcanic clast there may be similar to volcanic clasts noted by Polenz and others (2012c) in unit Qpu in the Brinnon quadrangle. Unit Qapd includes rare northern-sourced Possession drift in exposures too small to show at map scale. Weathering and a stratigraphic position above Whidbey-age deposits suggest a Possession age; however, it could be younger. Deposits on the west side of Waketickeh Creek could be older.

Qgd_p **Possession Drift**—Sand, sandy pebble gravel, and diamicton; brown to gray; coarsens upward from sand to pebble gravel and diamicton; compact; clasts subrounded to rounded; moderately to well sorted; moderately stratified and medium to thickly bedded. Deposits include metamorphic and granitic clasts. The maximum observed thickness of unit Qgd_p is about 150 ft. The unit is exposed in drainages on the west side of Hood Canal, stratigraphically above the nonglacial unit Qc_w, where it may be prone to landslides and liquefaction and may fail in large lateral spreads during earthquakes. The coarse sands and gravels are local aquifers. Northern-sourced Possession Drift is included in unit Qapd, where it appears to be a minor component of a dominantly Olympic-sourced drift. Exposures of Possession till are rare and typically found directly under Vashon till, which it closely resembles. Possession Drift may have been mapped as units Qpd or $Qguc_2$ where stratigraphic relations are unclear. Between the mouth of the Hamma Hamma River and Waketickeh Creek, unit Qgd_p may lie directly under or be mixed with Olympic-sourced drift we map as of Possession or early Fraser age.

Deposits of the Whidbey Interglaciation

Qc_w **Whidbey Formation**—Silt, clay, and sand (containing rare manganese nodules); light-gray to light-brown; dense and stiff; clasts typically subangular to subrounded; well stratified and well sorted; thinly laminated to very thickly bedded. Some portions of the unit contain preserved organic materials (see significant site 2 in Waketickeh Creek). Unit Qc_w appears to have an average thickness of about 100 ft, and a maximum of 300 to 325 ft; it extends to approximately 100 ft below sea level in the adjacent Holly quadrangle. This unit is found along the western shores of Hood Canal and in the bottom of drainages north of Ayock Point. It appears to represent prodelta deposits that received sand, silt and clay from deltas to the north, including clasts from Glacier Peak (Contreras and others, 2011). These exposures are 30 to 35 mi farther southwest than any previously mapped Whidbey Formation (Peterson, 2007). Rare basaltic sands from adjacent drainages can be found near the Hamma Hamma River, indicating local derivation.

Well reports and rare exposures suggest that thin, discontinuous oxidized glacial till and drift (predominantly advance sand) are present above this unit; we assume these are of MIS 4 (Possession) age. The base of this unit is not well exposed in the map area. Exposures in Waketickeh and Johns Creeks suggest deposition directly on basalt. However, two well reports, one south and one north of Waketickeh Creek suggest this unit lies on drift of MIS 6 (Double Bluff Glaciation) age or even older. Laminated clay in unit Qc_w appears to make it a hydrologic barrier, causing springs to appear at the top of the unit; it seems to be responsible for the majority of landslides along U.S. Highway 101. It is probably a poor aquifer; water wells typically are drilled through it and developed in drift or fractured basalt below. Luminescence dates of 132 ±7.19 ka (quartz) and 134 ±9.74 ka (feldspar) fall within the range of Berger and Easterbrook's (1993) ages in the Whidbey Formation of Easterbrook and others (1967); a luminescence age estimate from this unit in the adjacent Holly quadrangle, taken at a similar elevation, provided a date of 82.5 ±3.89 ka and may suggest differential uplift across the canal.

Pre-Fraser deposits, undivided

$Qguc_2$ **Pre-Fraser glacial and nonglacial deposits**—Predominantly sandy pebble to cobble gravel, but includes diamicton and silt; brown-gray and red-brown; dense and stiff; clasts subrounded to rounded; stratified; Olympic and northern glacial provenance; includes minor nonglacial silt and sand. Unit $Qguc_2$ is mapped on the west side of Hood Canal, southeast of Webb Mountain, and in the upper Waketickeh Creek drainage. Near Hood Canal it has been scoured and fluted by Vashon ice, but it appears unmodified in the upper Waketickeh drainage, where it is difficult to correlate with other deposits but appears to represent pre-Vashon Olympic-sourced and Cordillerian drift, silts that may be as young as MIS 5 (Whidbey age), and unidentified exposures of unit Qgd_d (below). This unit closely resembles unit Qpd, extensively weathered northern-sourced drift in the higher elevations of the Waketickeh Creek drainage. The Waketickeh Creek valley appears to have been covered by the Puget lobe during the Vashon Stade, but we found few discernible Vashon deposits. Instead, the basin's subdued topography (without fluting) suggests it was protected from the Puget lobe by snow, ice, or water. Unit $Qguc_2$ is typically stratigraphically above unit Qgd_d to the east in the Holly quadrangle and is tentatively mapped as younger than MIS 6 but without age control.

Qpd **Pre-Fraser glacial drift—**Till and minor sandy pebble to cobble gravel; red-brown to gray; compact; clasts subangular to subrounded; moderately sorted and stratified to unsorted and unstratified; coarsens upward from sand to pebble gravel to diamicton. Deposits include metamorphic and granitic clasts, indicating a northern source. The unit may reflect multiple glacial advances; weathering, specifically in Eagle Creek, suggests long periods of exposure. Unit Qpd is found on the on the eastern front of the Olympic Mountains and in discontinuous exposures in the higher elevations in this quadrangle, where it is commonly a well-developed, weathered lodgment till. In the drainages below the inferred Vashon ice limit, it is a less oxidized compact till and diamict and grades into advance outwash deposits above a weathered interval. We infer it to be MIS 6 (Double Bluff age) or significantly older (Birdseye and Carson, 1989), but have no age control. This unit closely resembles unit Qgd_d (below) and may be the same age in some locations, but exposures did not did not allow us to confidently differentiate it from Possession, Double Bluff, or older glacial deposits.

Deposits of the Double Bluff Glaciation

Qgd_d **Double Bluff Drift**—Sand, pebbles, cobbles, silt, and clay (diamicton); brown-gray to gray; very dense; clasts subangular to subrounded; unsorted to moderately sorted and stratified; medium to thickly bedded; coarsens upward from sand to pebble gravel and diamicton. Deposits include metamorphic and granitic clasts, indicating a northern source. Unit Qgd_d is approximately 300 to 400 ft thick and is exposed mainly on the east side of the canal; it is inferred from well logs and rare exposures on the west side. It is found stratigraphically above unit $Qguc_1$ where a paleosol suggests a hiatus before deposition of Double Bluff Drift. On the west side of Hood Canal, unit Qgd_d lies directly on basalt, with rare exposures of unit Qc_w above. Due to the areal extent of this unit at high elevations and the thickness of well-developed

lodgment till, this unit appears to represent a more extensive glaciation than the more recent Vashon Stade. Unit Qgd$_d$ is inferred to have been deposited during MIS 6 but without age control.

Pre–Double Bluff deposits, undivided

Qguc$_1$ **Pre-Double Bluff glacial and nonglacial deposits**—Sandy pebble gravel and cobble gravel with interstitial clay and minor beds of diamicton, sand, silt, and peat and paleosols; gray to orange-brown with buff interstitial clay; dense and very stiff; clasts mostly subrounded; poorly to moderately sorted; poorly to well stratified and massive to planar and crossbedded; predominantly glacial deposits (outwash and diamicts) of both Olympic and northern sources and minor nonglacial deposits. This unit includes at least two Olympic- and northern-sourced tills and four or more deeply weathered paleosols, suggesting long periods of exposure without deposition. Unit Qguc$_1$ has a thickness of more than 460 ft on the Kitsap Peninsula, but its total thickness is unknown. (For detailed composite stratigraphic sections, see Appendix B.) The Clark Creek and Annas Bay Drifts, which are magnetically reversed, occur low in this unit (see the Capstan Rock section of Easterbrook and others, 1988). Locally divided into:

Qapo **Pre-Double Bluff outwash, Olympic-sourced**—Sandy pebble to cobble gravel; orange-brown to gray; clasts subrounded to subangular; dense; poorly to moderately sorted; predominantly poorly stratified to massive. Clasts are dominantly basalt and sandstone that contain minor polycrystalline quartz and are moderately to very weathered. Unit Qapo is 260 ft thick near Ayock Point and is likely deposited on saprolitized basalt of the Crescent Formation as inferred from observations in Fulton and Eagle Creeks in the Holly and Lilliwaup quadrangles (Contreras and others, 2012b, 2010). On the east side of Hood Canal and in the adjacent Lilliwaup quadrangle (Contreras and others, 2010), this unit is as thick as 375 ft and has an Olympic-sourced till at its base. We suspect that unit represents multiple glaciations in the Olympic Mountains because of the widespread presence of weathered intervals and paleosols and association with underlying Olympic-sourced tills. This unit is likely older than MIS 6; Polenz and others (2010) report OSL age estimates of more than 245 ka for this unit in the Union and Skokomish Valley quadrangles, but we have no age estimates in this map area.

Qc$_R$ **Pre-Double Bluff nonglacial deposits**—Sand, sandy pebble gravel, silt, clay containing minor organic materials, and volcanic ash; tan to dark gray; very stiff to hard; well bedded; well stratified; typically laminated. This unit is found near the lower exposures of unit Qguc$_1$ along the eastern shore of Hood Canal east of Eldon, within a mile north and south of the Kitsap–Mason county boundary. Plant material and tephra support a nonglacial depositional environment for this unit. A tephra in the deposit, noted on the map as significant site 10 where it is easily accessible, was not analyzed because it is too weathered. Unit Qc$_R$ and the tephra are shown in stratigraphic column 4 of Birdseye and Carson (1989, p. 16). Stratigraphic correlation (see Figs. B5–13, Appendix B) suggests that unit Qc$_R$ is older than the Clark Creek Drift (Easterbrook and others, 1988) and is magnetically reversed (>780 ka).

Tertiary Sedimentary and Volcanic Rocks

The Crescent Formation (Arnold, 1906; Brown and others, 1960; Tabor and Cady, 1978) includes volcanic, volcaniclastic, and sedimentary rocks of the Olympic Mountains. (See Table C1 for geochemical data pertaining to this formation.) The five Crescent samples analyzed for this study are tholeiitic basalts (Fig. C2) that have within-plate (hot spot) chemical affinities (Fig. C3). These lavas have limited chemical variation (46.4–48.2 wt% SiO_2; 5.1–6.2 wt% MgO) but are notably more differentiated than lavas from the adjacent Brinnon quadrangle (Polenz and others, 2012c), as indicated by their lower Cr contents (averaging 56 ppm vs. 203 ppm) and lower Mg-numbers (34–45 vs. 44–58 (100*molar Mg/(Mg+Fe)). Samples from the Eldon quadrangle are also distinguished from those of the Brinnon quadrangle by higher concentrations of incompatible elements including TiO_2 (2.8–4.3 wt% vs. 1.6–2.4 wt%) and Zr (199–319 ppm vs. 93–117 ppm). Elevated incompatible element contents indicate derivation of the Eldon samples from a more enriched mantle source.

Em_{1c} **Siltstone and sandstone (early to middle Eocene)**—Marine siltstone and feldspathic sandstone and rare pebble conglomerate; dark gray to green-gray; fine- to coarse-grained; grains angular to subrounded; moderately to well sorted and well bedded; thinly bedded to massive. Grains are dominantly quartz. Feldspars are minor and are altered to chlorite and clay minerals. The unit is 600 to 800 ft thick and is exposed in the drainages of Waketickeh and Jorsted Creeks. Unit Em_{1c} appears to be interbeds of the Crescent Formation (unit Ev_c) and is under- and overlain by basalt. This unit locally displays primary sedimentary structures, including flame structures. Some siltstones are highly deformed and locally in fault contact with basalt; this unit dips approximately 65 degrees or is overturned to the southeast where it is faulted against basalt. Beds appear offset right-laterally across the Hamma Hamma fault zone. The unit is locally fossiliferous; the fauna includes serpulids and echinoids that are not age-diagnostic.

Ev_c **Crescent Formation (early to middle Eocene)**—Basalt; black to greenish black where fresh, weathers gray and medium yellow-brown; commonly occurs as fine-grained sills and, locally, pillows; commonly includes amygdules of zeolite and chlorite-group minerals. Flows include palagonitized breccias and rare columns. This unit typically includes plagioclase with intergrowths of pyroxenes and disseminated opaque minerals, is locally metamorphosed to prehnite-pumpellyite facies, and displays quartz and pyrite hydrothermal alteration. Replacement of interstitial glass by chlorite and oxidation products is also common. Unit Ev_c is exposed on the west side of Hood Canal, where it is not covered with glacial deposits. Most of the exposures are likely part of the upper Crescent Formation (Kenneth Clark, Univ. of Puget Sound, oral commun., 2011); we were unable to confidently distinguish between upper and lower Crescent. The rare, discontinuous exposures of altered greenstone (indicative of the lower Crescent) are near the western edge of the quadrangle, and other outcrops are too small to show at map scale. Cady and others (1972) included areas that we mapped as tectonic zone (unit tz) as lower Crescent. Some unit Ev_c contains rare thin sedimentary interbeds (unit Em_{1c}). Unit Ev_c may include small areas of discontinuous weathered northern-sourced and Olympic drifts (units Qpd and Qapd). Locally divided into:

tz **Tectonic zone**—Cataclasite, fault breccia, clay-rich fault gouge, basalt, and strongly slickensided and fractured basalt in fault zones; variously colored, mottled, and veined as a result of local hydrothermal alteration or strong weathering. The extent of this unit is not well constrained. Unit tz is probably under-represented in the northwest corner of the map where the remote and rugged terrain was difficult to access. Unit tz may be correlated with lower Crescent Formation (Cady and others, 1972) or may be highly deformed basalt of the upper Crescent in the Saddle Mountain fault zone (Wilson, 1975; Lamb and others, 2012).

POSTGLACIAL LANDFORMS

Stagnant-ice Features and Landslides

Glacial drift dominates the deposits surrounding Hood Canal. Some of these deposits are unstable, others are stable. Making this map, we consulted lidar-derived shaded relief with a vertical sun angle and 6X vertical exaggeration to more easily discern un-eroded glacial landforms. The shaded relief suggests that the area's topography has not changed dramatically since the glaciers melted at the end of the Vashon Stade of the Fraser Glaciation (Armstrong and others, 1965). Additionally, radiocarbon estimates from the Holly quadrangle indicate that alluvial terraces preserved in drainages date from the past 5000 years (Contreras and others, 2012a,b). Examples of this preservation exist at Johns and Waketickeh Creeks, where eskers are preserved right up to the former outwash channels, and terraces contain organics approximately 1100 years old.

Gryta (1975), Carson (1975, 1976a), and Serdar and Powell (2007) have identified numerous landforms as landslides. These parallel Hood Canal on the west side and ring each moderately sized drainage between Lilliwaup and Holly. We agree with Gryta (1975), who suggested these features formed as the ice melted, and we interpret many of these landslides as slumped stagnant-ice deposits. Many have headscarps and parallel ridges that mimic landslides, but they are likely stable. These landforms appear where a moderate thickness of ice-contact stratified drift was deposited as kames against stagnant ice. In the lower parts of each fairly large drainage, stagnant-ice deposits and kames indicate that ice persisted there while melting likely progressed on the uplands. Carson (1980) suggested a possible sequence: Olympic valley glacier ice could have remained in protected drainages as the Puget lobe advanced and overrode this ice. Then, as the Puget lobe stagnated, this protected ice might have remained under

a cover of Cordilleran drift. Finally, as the last of the ice melted, ice-marginal drainage and kames would have slumped into the spaces formerly occupied by older ice.

Additional modification of the topography likely occurred during earthquakes, given proximity to active faults and stratigraphy conducive to liquefaction. However, we interpret landslides as earthquake-induced only where stratigraphy suggests this. Determining the true nature of these landforms is beyond the scope of this mapping. Site-specific analysis is required to adequately assess slope stability.

The slumped landform at the mouth of the Hamma Hamma River has been mapped as an older landslide, but this too we interpret as a stagnant-ice deposit, as did Todd (1939), Thorson (1981), and Carson (1976a), on the basis of the elevations of terraces supplying the deposit and the ice-slump features between the terraces. In order for there to be this kind of deposition, ice would have to provide a "bridge" from the upper reaches of the Hamma Hamma to the river-mouth deposit. Lidar elevation models, paleoflow indicators, and other kames and ice-contact deposits along Johns Creek support this interpretation. Multiple kame elevations in the map area and adjacent Fulton Creek deltas suggest these kames were deposited at various elevations controlled by ice in the canal and may not necessarily be related to postglacial lakes.

ACTIVE AND POSTGLACIAL LANDSLIDES

Landslides into Jorsted Creek appear to be the result of two different mechanisms: active shallow debris slides and inactive slump-earthflows. Shallow debris slides originating in kame deposits in SW¼ sec. 33 provide large volumes of gravel to the drainage. Additionally, two deep-seated slides appear morphologically distinct in the lidar shaded-relief. Gryta (1975) recognized these earthflows and, from a radiocarbon age estimate, suggested movement at about 9000 years ago. These two slides appear to have initiated on silts and clays and could have been seismically induced.

In general, active landslides in the map area appear to be the result of collapse of steep slopes created by glacial and wave erosion and the construction of U.S. Highway 101. However, south of the Hamma Hamma River, the contact between Vashon-age kame gravel deposits (and possibly Possession-age drift) and underlying, relatively impermeable Whidbey-age silts (unit Qc_W) seems to be a plane of failure. Pore-water pressure increased by long or heavy precipitation events causes the younger units to slip along the silts.

SHORELINES

Few exposures in the map area appear related to shorelines of recessional lakes. We mapped the beach deposits at Eldon (unit Qob) primarily because Bretz mentioned them in his 1913 work; they seem too low to be attributed to glacial Lakes Russell or Leland. There are Holocene terraces in most major drainages in the area that appear to be graded to lake levels and are too young to be attributed to recessional lakes (Contreras and others, 2012a,b).

We have mapped few strandlines, which we suggest could be related to recessional lake shorelines. Our hesitation is due to a likely tectonic influence of active faults in the area and the likelihood of these deposits being deposited against melting ice. Near Eldon, we mapped shorelines between 315 to 290 ft and 135 and 85 ft because (1) eskers are truncated below an elevation of 290 ft, and (2) terraces to the west and to the northeast (at Waketickeh Creek) approximately correspond to elevations between 290 and 315 ft. This upper elevation is likely the upper limit for lake levels in the area because gravels in the eskers would quickly be reworked by wave action. The break in slope and bench below 250 ft along the west shore of the canal between Jorsted Creek and Ayock Point may approximate a shoreline, but we chose not to map it as such because we weren't sure.

Thorson (1981) suggested the Eldon delta was deposited into glacial Lake Hood, but he appears to have inconsistent arguments for using this delta to reconstruct the lake elevations. He noted the delta was built against ice, is channelized, and lacks a textural change at the topset–foreset contact, yet still attributed it to glacial Lake Hood. Thorson described the lower Fulton Creek delta (between Triton Cove and the Duckabush River in the Holly quadrangle) as being unlike any other deltas he described. It is composed of locally derived material and contains a few granitic clasts. It has a topset–foreset contact at about 95 ft, approximately the elevation of the bench Bretz (1913) noted and that we have shown on the map near Eldon.

Mapping to the north in the Brinnon quadrangle by Polenz and others (2012c) revealed additional shorelines between about 315 and 380 ft and 95 to 135 ft, and mapping to the south by Polenz and others (2010; 2012a) suggests an outlet from Hood Canal to Lake Russell at Purdy Canyon at an elevation of 240 ft. This elevation may roughly correspond with the previously mentioned bench between Jorsted Creek and Ayock Point.

STRUCTURE

Seattle, Hood Canal, Saddle Mountain, and Dow Mountain Fault Zones

It is difficult to model the interaction of the Seattle, Tacoma, Hood Canal, and Dow Mountain fault zones in the quadrangle due to the structural complexity and relatively minor changes in geophysical anomalies. Our map provides additional field evidence for extending the Seattle fault zone west from its suggested location near Holly and connecting it with the Saddle Mountain fault zone. (Blakely and others, 2009; Lamb and others, 2012; Contreras and others, 2012a). In this quadrangle, we continue the Seattle fault zone across Hood Canal via a zone of high-angle strike-slip faults near the Hamma Hamma River and reverse faults to the north, and merge it with the Saddle Mountain fault zone to the southwest as Blakely and others (2009) and Lamb and others (2012) suggest.

We give the name Hamma Hamma fault zone to a group of high-angle, west-trending strike-slip faults that cross part of the map area. They appear to be responsible for the east–west portion of the deep canyon occupied by the Hamma Hamma River and are exposed in the canyon and along Waketickeh Creek. The fault zone coincides with the right-lateral offset of a northeast-trending magnetic anomaly. These faults appear to exhibit both right- and left-lateral movement at outcrop scale, but likely are dominantly right-lateral. This movement is inferred from (1) the magnetic anomaly and (2) the right-lateral offset of two sedimentary interbeds in the Crescent basalts (unit Em_{1c}) between exposures in Johns and Wacketickeh Creeks by approximately the same amount across the fault zone as the magnetic anomaly. We concede these beds might be incorrectly correlated because there are few exposures of sedimentary rocks in the area and many are faulted; however, explaining the offset of these beds by normal or reverse faulting is inconsistent with the high-angle nature of the faults.

Our mapping does not favor either of the models proposed by Johnson and others (2004), but it appears to fit with various elements of the two. Additionally, the models proposed by Blakely and others (2009) and Lamb and others (2012) simplify the Saddle Mountain deformation zone into a left-lateral thrust system. While this may be an adequate model in the larger sense, it does not fit the numerous styles of faulting found in trenches and exposures in the area (Walsh and Logan, 2007; Witter and others, 2008; Barnett and others, 2009). As with previous studies, we also found a complex system of faults that does not easily conform to any one model, that is, north- to northeast-trending faults display both right- and left-lateral oblique movement. Future lidar-assisted field mapping to the west and north of the map area and re-analysis of work by Haug (1998) may clarify this complex system.

On our map, faults are shown with varying levels of confidence, but we tend to be conservative. Where confidently constrained in outcrop, faults are shown as solid lines; they are extended with lower levels of confidence. Some faults are shown as questioned and concealed where we are less sure or where we have depicted faults on the basis of magnetic anomalies (Richard Blakely, USGS, written commun., 2011) and the seismic profiles of Haug (1998) and Lamb and others (2012).

ANALYSIS OF FAULT PLANES AND SLICKENLINES

Fault orientations were collected using a Brunton pocket transit; strike and dip were recorded as an azimuth (0–360°) using “the right hand rule”, with dip direction to the right. The rakes of slickenlines were recorded independent of the direction of the perceived movement and as dipping down; the trend and plunge were calculated from the orientation of the fault plane. The data were modeled in the programs *Stereonet* and *Faultkin* (Allmendinger and others, 2012; Marrett and Allmendinger, 1990). We used *Stereonet* to generate stereonet projections of fault planes and poles to planes. We contoured the poles to planes using the 1 percent method where E = (100)/N, and E is the expected density and N is the total number of data points. We also used rose diagrams to visualize the distribution of fault orientations. (See Fig. A1 for a plot of poles to planes of these fault planes and additional data pertaining to faulting in the map area.)

We attempted to measure only faults that were not effectively healed by mineralization: a total of 133 fault planes. We are confident about the orientation and offset direction of slickenlines on only 21 of these. We used this small sample set to generalize about the additional faults where we did not have good indications of slip direction and to correlate these faults to known faults in the area (for example, the Dow Mountain, Frigid Creek, and Saddle Mountain fault zones). The entire set of fault planes, poles to planes, poles to planes contours, and rose diagrams is shown in Figure 1A. Additionally, we do not assume all of these faults have been recently active, as some movement likely represents reactivation of older faults or older movement.

STYLE OF FAULTING

We placed faults in four broad categories: (1) northeast-trending bedding-plane faults; (2) east-trending faults, both near-vertical and less steeply dipping; (3) northwest-striking faults; and (4) southwest-striking faults. Six of the northeast-trending faults show left-lateral oblique normal movement. The seven right- and two left-lateral east-trending faults appear to be high-angle oblique strike-slip faults. The two northwest-trending faults show northeast-verging reverse and northeast-side-down, right-lateral oblique movement. Of the four southwest-trending faults, one has had pure reverse movement, two are right-lateral, and one is left-lateral. (See Fig. A2 for plots of the slickenlines that helped us distinguished these categories of faults.)

LOCATION OF FAULTING

We partitioned the map into overlapping thirds in order to analyze faulting style based on position within the quadrangle. From north to south within this quadrangle, there is a decrease in west-trending faults and an increase in southeast-trending faults. The northern faults (Seattle fault zone) are a small sample set, but they appear to represent west-trending reverse, normal, and strike-slip faulting connected to folding and thrusting in the adjacent Holly quadrangle and shown by Lamb and others (2012). These faults merge into northeast-trending oblique-reverse deformation similar to that in the Saddle Mountain deformation zone in the middle of the map, near the Hamma Hamma River. Throughout the entire quadrangle, there are north- and northeast-trending bedding-plane faults, their greatest abundance in the middle third. The middle third also contains a high density of west-trending, high-angle strike-slip faults. The number of southeast-oriented faults increases to the south near the Dow Mountain fault, which has a similar trend (Wilson, 1975).

Southern Portion of the Quadrangle

Connecting the Saddle Mountain fault zone to the Seattle fault zone

The Saddle Mountain East fault was the first fault in Washington State on which post-glacial ground rupture was demonstrated (Carson, 1973). Since then, various studies have concluded that the faults were last active about 1000 to 1300 cal yr BP (Hughes, 2005; Blakely and others, 2008, 2009). Snook (2011) used dendrochronology to demonstrate that the most recent earthquake at Price Lake (~3 mi southwest of the southwest corner of the quadrangle) occurred about AD 811. (See the compilation of work on these faults in Polenz and others, 2012b.)

The northeast-trending Saddle Mountain fault zone (Blakely and others, 2009) extends from the Hoodsport quadrangle to the Eldon quadrangle. Blakely integrates various geophysical data and fault studies to delineate the Saddle Mountain fault zone and characterizes it as a zone of deformation extending 45 km from the Canyon River fault, northeast to Hood Canal, where it connects with strands of the Seattle fault zone. Our mapping supports this model, but the kinematic indicators do not always show left-lateral reverse movement along the Saddle Mountain fault zone.

The northeast-trending faulting that enters the southwest map corner near Eagle Creek appears to mimic the complex and often contradictory styles of movement observed in paleoseismic trench studies to the southwest (Witter and others, 2008; Barnett and others, 2009). Kinematic indicators from the trench studies argue for a component of right-lateral movement and provide additional indications of left-lateral movement. The faults observed in this quadrangle suggest both styles of movement along northeast-trending faults. However, in the map area, the dominant movement along these northeast-trending faults appears to have been right-lateral oblique. This right-lateral movement is indicated at two locations in the north branch of Johns Creek and at one between Jorsted Creek and South Fork Johns Creek (significant sites 4 and 6). Additional right-lateral oblique movement is suggested from slickenlines on faults near Jefferson Creek along the western edge of the map and in the Waketickeh Creek valley. However, at one location in an eastern gorge between Jorsted Creek and South Fork Johns Creek, left-lateral oblique movement is indicated along a fault surface with a northeast trend (significant site 8). These northeast-trending faults continue along a magnetic anomaly that changes character at the Hamma Hamma River and appear to be offset to the east.

Examples of these northeast-trending faults exist in the southwest corner of the map between Eagle Creek and North Fork Johns Creek, as a pair of conspicuous parallel gorges cut into basalt. They start in the NW¼ sec. 6, T23N R3W, and extend northeast to the NE¼ sec. 29, T24N R3. The gorges are interrupted by high-angle, east-trending strike-slip faults, making drainages between. Todd (1939) described them as ice-marginal drainage channels, and detailed maps by Carson (unpub. maps) also show these gorges. The gorges are typically about 200 ft deep, but in

places are deeper than 400 ft and as narrow as 400 ft. We agree that they were cut by meltwater, but they appear strangely unique to the area. Exposures of fault gouge in these gorges exhibit both right- and left-lateral oblique movement. In one location in the west gorge, right-lateral northwest-side-down movement is recorded, whereas the gorge to the east has indications of left-lateral down-to-the-southeast movement.

If the dominant movement along this fault zone is right-lateral oblique, then it could explain the strange orientation of the Waketickeh Creek valley—perpendicular to major valleys of the area. A right step-over in a right-lateral fault system could produce a pull-apart basin. This idea is substantiated by the rare fault exposures in the Waketickeh Creek valley that demonstrate normal movement along both north-northeast- and south-southeast-trending faults. Further work is needed to resolve how this apparent right-lateral component of slip fits into a tectonic model of the area.

Quaternary faulting in Eagle Creek

Faulting in the southwestern portion of the map, specifically in the drainage of Eagle Creek, is important because it provides exposures of faulted Quaternary pre-Vashon deposits that may be analogous to faulting in the Saddle Mountain and Dow Mountain area and likely represents the northern extension of this fault zone. North of this area, the orientations appear to become more north–south and east–west. These faults exhibit both northeast- and northwest-striking fault planes.

We found three locations along Eagle Creek where Quaternary pre-Vashon deposits appear to be faulted against basalt. These locations are indicated on the map by orange diamonds (significant sites 11, 12, and 13). The faults appear to extend from the area of Dow Mountain and follow a magnetic anomaly to the northeast; the faults change character at the significant sites and becomes less pronounced northward.

At significant site 11, multiple sets of slickenlines were found on multiple fault planes in exposures of what appears to be oxidized pre-Vashon drift in contact with broken and altered basalt. The dominant slickenlines suggest reverse movement on a southeast-trending fault that dips 71 degrees SW. Additional movement along a fault trending north-northeast and dipping 84 degrees SE appears on trend with the gorges mentioned previously. (See Fig. F9, Appendix F, for photos of this site.)

Faulting in the lower reach of Eagle Creek (significant sites 12 and 13) places basalt over sand along a high-angle reverse fault striking southwest. Slickenlines in mineralized faulted material record primarily reverse movement. The faulting may continue to the southwest as it appears to be on trend with a magnetic anomaly that extends through upper Lilliwaup Falls and possibly on to Miller Creek, where Polenz and others (2012a) found deformation in the Hoodsport quadrangle.

Hood Canal fault

Recent work by Blakely and others (2009) suggests the Hood Canal fault is not a continuous fault as Gower and others (1985) previously postulated. Our map shows a portion of the Hood Canal fault, but its location is based on filtered magnetic anomalies (Richard Blakely, USGS, written commun., 2011) and seismic profiles from Haug (1998) and Dadisman and others (1997). It is depicted with a low level of confidence as “identity or existence questionable, location concealed”, and the sense of movement is shown only where seismic profiles suggest reverse movement.

Field measurements from this mapping suggest there are faults that parallel Hood Canal and thus it is likely that there are discontinuous faults under portions of Hood Canal. Faults observed on the west side of the canal near the mouth of the Hamma Hamma River are shown dipping approximately 45 to 65 degrees to the southeast and northwest. We could not confidently measure kinematic indicators on these faults, but interpret these faults as dominantly bedding-parallel reverse faults. Recent mapping in adjacent quadrangles that depicts the Hood Canal fault as one distinct continuous structure (Contreras and others, 2010, 2012a; Polenz and others 2012a) is based on the work of Lidke and others (2003), but magnetic anomalies do not support a continuous structure (Richard Blakely, USGS, oral commun., 2011).

Central Portion of the Quadrangle

The gorges in the southwest corner of the map can be traced to the North Fork Johns Creek, where the magnetic field anomaly is offset to the east by about 2500 ft before it continues to the northeast corner of the map. The offset of the anomaly coincides with the downstream end of the Hamma Hamma River canyon. Several east–west high-angle strike-slip faults are centered on the Hamma Hamma River and appear to be responsible for the east–west

portion of the canyon in the SE¼NE¼ sec. 21, T24N R3W. Where the canyon bends to the south, we suggest the river intersects the northeast-oriented faults and the east–west Hamma Hamma River faults, which provide a link between the Saddle Mountain fault zone and the Seattle fault zone.

In the central portion of the quadrangle, most faults appear to be east–west high-angle strike-slip faults and northeast-trending bedding-parallel reverse faults. In the few exposures measured, we found evidence for both right- and left-lateral and reverse movement. Seismic profiles by Haug (1998) and Lamb (2012) suggest the faults may continue east across Hood Canal to Holly, where a monocline fits between the Seattle uplift and Seattle basin to the north (Contreras and others, 2011).

Wilson and others (1979) suggested extension of the Saddle Mountain fault zone north of its known location on the basis of a zone of fractured basalt to the west of the southwest corner of the quadrangle. We also observed highly fractured basalt outside the map area to the west and suggest that the Saddle Mountain fault zone continues northeast along trend and enters the central portion of the Eldon quadrangle along its western margin near Quitter Creek. There, we mapped a large area of unit tz and inferred, questioned faults because we could not pick out distinct faults in this highly fractured fault zone.

Near Jefferson Creek, in parallel north-aligned drainages, we found east-dipping oblique reverse faults that place metamorphosed basalt in contact with less-altered basalt. The faulting is complex, but in one exposure, right-lateral movement appears to have dominated. We speculate that this could be an extension of the Saddle Mountain fault zone. The faults align with magnetic anomalies but display right-lateral movement. We did not trace this zone across the Hamma Hamma River, but based on magnetic anomalies, we think it likely continues into the drainage of Watson Creek.

In Waketickeh Creek (NE¼NE¼ sec. 22, T24N R3W), we observed a fault with an orientation of N89ºW, dipping 64 degrees N, that has two sets of slickenlines—one having a normal-right lateral sense of motion (rake of 20°), the other reverse right-lateral movement (rake of 25°).

Indications of a land-level change at Eldon

A paleosol in the lower Hamma Hamma valley is bracketed by two radiocarbon age estimates and suggests that a land-level change likely occurred between about 1900 and 1300 years ago. No diatoms were found (Brian Sherrod, USGS, written commun., 2012); we rely on sedimentary facies and a soil layer to suggest a land-level change. This timing may correspond with other age estimates (Lindstrum, 2002; Contreras and other, 2012a; Polenz and others, 2012c) associated with changes in base level due to earthquakes (Sherrod and others, 2000; Martin, 2011). Lindstrum dated a buried soil in the Hamma Hamma and Duckabush River deltas that suggested subsidence in the past 1400 to 1000 years.

Bretz (1913) suggested the presence of a terrace with shells just north of the Hamma Hamma River. We think his location is either the site of Eldon and or the bench between 135 and 85 ft (significant site 5). The eskers above Eldon appear intact above an elevation of 290 ft. Later reworking of the deposits by lower lake levels or tectonic uplift may be responsible for the bench at Eldon.

Johns Creek preserved forest

A radiocarbon age estimate obtained from a tree preserved in the banks of Johns Creek that might have been buried at the time the Seattle fault last ruptured, approximately AD 900 to 930 (Atwater, 1999). Three growth rings were taken 47 rings from the bark and provide a calibrated age of tree death between 827 and 1017 cal yr AD (GD7, Beta-318212, 1160 ±30 BP; 2-sigma calibrated results by Beta Analytic using the INTCAL09 database [Heaton and others, 2009; Reimer and others, 2009; Stuiver and others, 1993; Oeschger and others, 1975]). An earthquake-triggered landslide or another mechanism may have blocked the drainage, causing the alluvium to be deposited on and preserve the tree stumps (see Fig. F5, Appendix F).

Quaternary faulting in Johns Creek

Along North Fork Johns Creek, at significant site 4, is an area of multiple, diversely oriented faults. One fault appears to incorporate pre-Vashon alluvium. It is unclear if the alluvium is of glacial or nonglacial origin. The fault strikes N10°E and dips east at 56 degrees. Slickenlines indicate both normal right-lateral movement with a rake of 23 degrees and reverse right-lateral oblique movement with a rake of 30 degrees. The faulting in the surrounding area appears complex, but both sets of slickenlines could be the result of one event—overall right-lateral reverse movement followed by a relaxation of stress, resulting in the normal movement.

Quaternary faulting along Waketickeh Creek

In Waketickeh Creek, pre-Vashon glacial deposits of both Olympic and northern sources are placed against marine sedimentary rocks by a fault that trends northeast. Additionally, MIS 5 (Whidbey age) silts are deformed and faulted in this area; this deformation could be glaciotectonic in nature. We have mapped east-trending faults with varying levels of confidence throughout the area; we have termed faults in this area the Hamma Hamma fault zone.

Northern Portion of the Quadrangle

The northern portion of the quadrangle is rugged and has few access roads. We measured several faults in this area, but faulting is likely under-represented on the map. While we suspect that faulting similar to the Saddle Mountain fault zone continues on the north side of the Hamma Hamma River, based on magnetic anomalies and previous mapping of folds in the lower Crescent Formation by Cady and others (1972), we do not show faults in this area because it is remote with few access roads and is densely vegetated.

In the northeast corner of the quadrangle, in the drainages between Fulton and Waketickeh Creeks, and in the adjacent Holly quadrangle (Contreras and others, 2012b), we found west-oriented faults displaying indicators of both reverse and normal movement. Kinematic analysis suggests reverse left-lateral movement, but measurements in the adjacent Holly quadrangle, taken along the trend of these faults, suggests right- and left-lateral reverse and normal movement, all testament to the complexity of the faulting. The Holly and Brinnon quadrangles are where Lamb and others (2012) depict complex folding and thrusting in their seismic and magnetic profiles of the Seattle fault zone.

ACKNOWLEDGMENTS

This report was funded in part by the U.S. Geological Survey National Cooperative Geologic Mapping Program under award no. G11AC20236. Special thanks to the Robbins family and the Hamma Hamma Company, without whose cooperation this map could not have been made. Additional thanks to Hank Bloomfield for his interest in the project and for cutting the subfossil wood; Andy Lamb (Boise State Univ.) for sharing seismic data and drafts of his work; Rick Blakely (USGS) and Megan Anderson (Colorado College) for magnetic and gravity data; Brian Sherrod (USGS) for suggestions and diatom analysis. Thanks also to Wash. Div. of Geology and Earth Resources staff (now or formerly) Tim Walsh, Joe Dragovich, Michael Polenz, Jessica Czajkowski, and Jeff Bowman for constructive discussions of the geology; Lee Walkling for library support; Eric Schuster and Anne Olson for cartographic expertise; and Jari Roloff, Kitty Reed, and Meredith Payne for editing the map and pamphlet.

REFERENCES CITED

Allmendinger, R. W.; Cardozo, Nestor; Fisher, D. M., 2012, Structural geology algorithms—Vectors and tensors: Cambridge University Press, 302 p.

American Association of State Highway and Transportation Officials, 1988, Manual on subsurface investigations, 1988: American Association of State Highway and Transportation Officials, Inc., 391 p. [http://www.sil.ucdavis.edu/downloads/NHI_SI_Manual.pdf]

Armstrong, J. E.; Crandell, D. R.; Easterbrook, D. J.; Noble, J. B., 1965, Late Pleistocene stratigraphy and chronology in southwestern British Columbia and northwestern Washington: Geological Society of America Bulletin, v. 76, no. 3, p. 321-330.

Arnold, Ralph, 1906, Geological reconnaissance of the coast of the Olympic Peninsula, Washington: Geological Society of America Bulletin, v. 17, p. 451-468.

Atwater, B. F., 1999, Radiocarbon dating of a Seattle earthquake to A.D. 900-930 [abstract]: Seismological Research Letters, v. 70, no. 2, p. 232.

Barnett, E. A.; Sherrod, B. L.; Kelsey, H. M.; Czajkowski, J. L.; Walsh, T. J.; Contreras, T. A.; Davis-Staunton, K.; Schermer, E. R.; Carson, R. J., 2009, Active faulting along the Saddle Mountain fault zone, southeast Olympic Mountains, WA [abstract]: Eos (American Geophysical Union Transactions), v. 90, no. 52, Suppl., S51B-1404.

Berger, G. W.; Easterbrook, D. J., 1993, Thermoluminescence dating tests for lacustrine, glaciomarine, and floodplain sediments from western Washington and British Columbia: Canadian Journal of Earth Sciences, v. 30, no. 9, p. 1815-1828.

Birdseye, R. U.; Carson, R. J., 1989, Tephra of Salmon Springs age from the southeastern Olympic Peninsula, Washington: Washington Division of Geology and Earth Resources Open File Report 74-1 (revised), 23 p. [http://www.dnr.wa.gov/publications/ger_ofr74-1_tephra_olympic_peninsula.pdf]

Blakely, R. J.; Sherrod, B. L.; Hughes, J. F.; Anderson, M. L.; Wells, R. E.; Weaver, C. S., 2008, Western boundary of the Seattle uplift, Washington [abstract]: Eos (American Geophysical Union Transactions), v. 89, no. 53, Suppl., p. F2481.

Blakely, R. J.; Sherrod, B. L.; Hughes, J. F.; Anderson, M. L.; Wells, R. E.; Weaver, C. S., 2009, Saddle Mountain fault deformation zone, Olympic Peninsula, Washington—Western boundary of the Seattle uplift: Geosphere, v. 5, no. 2, p. 105-125.

Bretz, J H., 1913, Glaciation of the Puget Sound region: Washington Geological Survey Bulletin 8, 244 p., 3 plates. [http://www.dnr.wa.gov/publications/ger_b8_glaciation_pugetsound.pdf]

Brocher, T. M.; Blakely, R. J.; Wells, R. E., 2004, Interpretation of the Seattle uplift, Washington, as a passive-roof duplex: Seismological Society of America Bulletin, v. 94, no. 4, p. 1379-1401.

Brown, R. D., Jr.; Gower, H. D.; Snavely, P. D., Jr., 1960, Geology of the Port Angeles–Lake Crescent area, Clallam County, Washington: U.S. Geological Survey Oil and Gas Investigations Map OM-203, 1 sheet, scale 1:62,500. [http://ngmdb.usgs.gov/Prodesc/proddesc_5357.htm]

Cady, W. M.; Sorensen, M. L.; MacLeod, N. S., 1972, Geologic map of the Brothers quadrangle, Jefferson, Mason and Kitsap Counties, Washington: U.S. Geological Survey Geologic Quadrangle Map GQ-969, 1 sheet, scale 1:62,500. [http://ngmdb.usgs.gov/Prodesc/proddesc_2268.htm]

Carson, R. J., 1973, First known active fault in Washington: Washington Geologic Newsletter, v. 1, no. 3, p. 1-2. [http://www.dnr.wa.gov/Publications/ger_washington_geology_1973_v1_no3.pdf]

Carson, R. J., 1975, Slope stability map of north-central Mason County, Washington: Washington Division of Geology and Earth Resources Open File Report 75-4, 1 sheet, scale 1:62,500. [http://www.dnr.wa.gov/publications/ger_ofr75-4_slope_mason_co_62k.pdf]

Carson, R. J., 1976a, Geologic map of north-central Mason County, Washington: Washington Division of Geology and Earth Resources Open File Report 76-2, 1 sheet, scale 1:62,500. [http://www.dnr.wa.gov/publications/ger_ofr76-2_geol_map_mason_co_62k.pdf]

Carson, R. J., 1976b, Preliminary geologic map of the Brinnon area, Jefferson County, Washington: Washington Division of Geology and Earth Resources Open File Report 76-3, 1 sheet, scale 1:24,000. [http://www.dnr.wa.gov/publications/ger_ofr76-3_geol_map_ brinnon_24k.pdf]

Carson, R. J., 1980, Quaternary, environmental, and economic geology of the eastern Olympic Peninsula, Washington: [unpublished report], 275 p.

Contreras, T. A.; Legorreta Paulin, Gabriel; Czajkowski, J. L.; Polenz, Michael; Logan, R. L.; Carson, R. J.; Mahan, S. A.; Walsh, T. J.; Johnson, C. N.; Skov, R. H., 2010, Geologic map of the Lilliwaup 7.5-minute quadrangle, Mason County, Washington: Washington Division of Geology and Earth Resources Open File Report 2010-4, 13 p., 1 plate, scale 1:24,000. [http://www.dnr.wa.gov/ Publications/ger_ofr2010-4_geol_map_lilliwaup_24k.zip]

Contreras, T. A.; Weeks, S. A.; Perry, B. B., 2012a, Analytical data from the Holly 7.5-minute quadrangle, Jefferson, Kitsap, and Mason Counties, Washington—Supplement to Open File Report 2011-5: Washington Division of Geology and Earth Resources Open File Report 2011-6, 16 p. [http://www.dnr.wa.gov/Publications/ger_ofr2011-6_holly_supplement.pdf]

Contreras, T. A.; Weeks, S. A.; Stanton, K. M. D.; Stanton, B. W.; Perry, B. B.; Walsh, T. J.; Carson, R. J.; Clark, K. P.; Mahan, S. A., 2012b, Geologic map of the Holly 7.5-minute quadrangle, Jefferson, Kitsap, and Mason Counties, Washington: Washington Division of Geology and Earth Resources Open File Report 2011-5, 1 sheet, scale 1:24,000, 13 p. text.

Crandell, D. R., 1965, The glacial history of western Washington and Oregon. *In* Wright, H. E., Jr.; Frey, D. G., editors, The Quaternary of the United States: Princeton University Press, p. 341-353.

Dadisman, S. V.; Johnson, S. Y.; Childs, J. R., 1997, Marine, high-resolution, multichannel, seismic-reflection data collected during Cruise G3-95-PS, northwestern Washington: U.S. Geological Survey Open-File Report 97-735, 3 CD-ROM disks. [http://pubs.er.usgs.gov/pubs/ofr/ofr97735]

Deeter, J. D., 1979, Quaternary geology and stratigraphy of Kitsap County, Washington: Western Washington University Master of Science thesis, 175 p., 2 plates.

Derkey, R. E.; Heheman, N. J.; Alldritt, Katelin, 2009, Geologic map of the Lake Wooten 7.5-minute quadrangle, Mason County, Washington: Washington Division of Geology and Earth Resources Open File Report 2009-5, 1 sheet, scale 1:24,000. [http://www.dnr.wa.gov/Publications/ger_ofr2009-5_geol_map_lakewooten_24k.pdf]

Dickinson, W. R., 1970, Interpreting detrital modes of greywacke and arkose: Journal of Sedimentary Petrology, v. 40, no. 2, p. 695-707.

Easterbrook, D. J.; Crandell, D. R.; Leopold, E. B., 1967, Pre-Olympia Pleistocene stratigraphy and chronology in the central Puget Lowland, Washington: Geological Society of America Bulletin, v. 78, no. 1, p. 13-20.

Easterbrook, D. J.; Roland, J. L.; Carson, R. J.; Naeser, N. D., 1988, Application of paleomagnetism, fission-track dating, and tephra correlation to lower Pleistocene sediments in the Puget Lowland, Washington. *In* Easterbrook, D. J., editor, Dating Quaternary sediments: Geological Society of America Special Paper 227, p. 139-165.

Elmendorf, W. W.; Kroeber, A. L.,1992, The structure of Twana culture—With comparative notes on the structure of Yurok culture: Washington State University Press, 576 p.

Frisken, J. G., 1965, Pleistocene glaciation of the Brinnon area, east-central Olympic Peninsula, Washington: University of Washington Master of Science thesis, 75 p., 3 plates.

Garling, M. E.; Molenaar, D.; and others, 1965, Water resources and geology of the Kitsap Peninsula and certain adjacent islands: Washington Division of Water Resources Water-Supply Bulletin 18, 309 p., 5 plates. [http://www.ecy.wa.gov/programs/eap/wsb/pdfs/WSB_18_Book.pdf (book) and http://www.ecy.wa.gov/programs/eap/wsb/pdfs/WSB_18_Plates.pdf (plates)]

Gerstel, W. J.; Lingley, W. S., Jr., 2003, Geologic map of the Mount Olympus 1:100,000 quadrangle, Washington: Washington Division of Geology and Earth Resources Open File Report 2003-4, 1 sheet, scale 1:100,000. [http://www.dnr.wa.gov/Publications/ger_ofr2003-4_geol_map_mountolympus_100k.pdf]

Gower, H. D.; Yount, J. C.; Crosson, R. S., 1985, Seismotectonic map of the Puget Sound region, Washington: U.S. Geological Survey Miscellaneous Investigations Series Map I-1613, 1 sheet, scale 1:250,000, with 15 p. text.

Gryta, J. J., 1975, Landslides along the western shore of Hood Canal, northern Mason County, Washington: North Carolina State University Master of Science thesis, 120 p., 3 plates.

Haug, B. J., 1998, High resolution seismic reflection interpretations of the Hood Canal–Discovery Bay fault zone; Puget Sound, Washington: Portland State University Master of Science thesis, 1 v.

Haugerud, R. A., 2005, Preliminary geologic map of Bainbridge Island, Washington: U.S. Geological Survey Open-File Report 2005-1387, version 1.0, 1 sheet, scale 1:24,000. [http://pubs.usgs.gov/of/2005/1387]

Haugerud, R. A., 2009a, Deglaciation of the southern Salish lowland [abstract]. *In* Northwest Scientific Association, The Pacific Northwest in a changing environment—Northwest Scientific Association 81st annual meeting; Program with abstracts: Northwest Scientific Association, p. 27-28.

Haugerud, R. A., 2009b, Preliminary geomorphic map of the Kitsap Peninsula, Washington; version 1.0: U.S. Geological Survey Open-File Report 2009-1033, 2 sheets, scale 1:36,000. [http://pubs.usgs.gov/of/2009/1033/]

Heaton, T. J.; Blackwell, P. G.; Buck, C. E., 2009, A Bayesian approach to the estimation of radiocarbon calibration curves—The IntCal09 methodology: Radiocarbon, v. 51, no. 4, p. 1151-1164.

Hughes, J. F., 2005, Meters of synchronous Holocene slip on two strands of a fault in the western Puget Sound Lowland, Washington [abstract]: Eos (American Geophysical Union Transactions), v. 86, no. 52, p. F1437.

Irvine, T. N.; Baragar, W. R. A., 1971, A guide to the chemical classification of the common volcanic rocks: Canadian Journal of Earth Sciences, p. 523-548.

Johnson, S. Y.; Blakely, R. J.; Stephenson, W. J.; Dadisman, S. V.; Fisher, M. A., 2004, Active shortening of the Cascadia forearc and implications for seismic hazards of the Puget Lowland: Tectonics, v. 23, TC1011, doi:10.1029/2003TC001507, 2004, 27 p.

Karel, Patrick; Liberty, L. M., 2008, The western extension of the Seattle fault—New insights from seismic reflection data [poster]: American Geophysical Union Fall Meeting 2008, poster T21B-1951.

Kramer, S. L., 1996, Geotechnical earthquake engineering: Prentice Hall, 653 p.

Lamb, A. P.; Liberty, L. M.; Blakely, R. J.; Pratt, T. L.; Sherrod, B. L.; van Wijk, K., 2012, Western limits of the Seattle fault zone and its interaction with the Olympic Peninsula, Washington: Geosphere, v. 8, no. 3, doi: 10.1130/GESoo780.1.

Lamb, A. P.; Liberty, L. M.; Blakely, R. J.; van Wijk, Kasper, 2009, The Tahuya lineament—Southwestern extension of the Seattle fault? [abstract]: Geological Society of America Abstracts with Programs, v. 41, no. 7, p. 479.

Laprade, W. T., 2003, Subglacially reworked till in the Puget Lowland [abstract]: Geological Society of America Abstracts with Programs, v. 35, no. 6, p. 216.

Le Bas, M. J.; Le Maitre, R. W.; Streckeisen, A. L.; Zanettin, Bruno, 1986, A chemical classification of volcanic rocks based on the total alkali-silica diagram: Journal of Petrology, v. 27, part 3, p. 745-750.

Le Maitre, R. W., editor; and others, 1989, A classification of igneous rocks and glossary of terms—Recommendations of the International Union of Geological Sciences Subcommission on the Systematics of Igneous Rocks: Blackwell Scientific Publications, 193 p., 1 plate.

Lidke, D. J.; Johnson, S. Y.; McCrory, P. A.; Personius, S. F.; Nelson, A. R.; Dart, R. L.; Bradley, Lee-Ann; Haller, K. M.; Machette, M. N., 2003, Map and data for Quaternary faults and folds in Washington State: U.S. Geological Survey Open-File Report 03-428, 1 sheet, scale 1:750,000, with 15 p. text. [http://pubs.usgs.gov/of/2003/428]

Lindstrum, E. F., 2002, Stratigraphic analysis of Holocene deltaic deposits on the western margin of the Puget Lowland, Hood Canal, Washington: University of Oregon Master of Science thesis, 77 p.

Long, W. A., 1975a, Glacial studies on the Olympic Peninsula: U.S. Forest Service, 1 v., 9 plates.

Long, W. A., 1975b, Salmon Springs and Vashon continental ice in the Olympic Mountains and relation of Vashon continental to Fraser Olympic ice. *In* Long, W. A., Glacial studies on the Olympic Peninsula: U.S. Forest Service, 1 v.

Marrett, R. A.; Allmendinger, R. W., 1990, Kinematic analysis of fault-slip data: Journal of Structural Geology, v. 12, no. 8, p. 973-986.

Martin, M. E., 2011, Coastal marsh stratigraphy as an indicator of past earthquakes, Puget Lowland, Washington State: University of Washington Doctor of Philosophy thesis, 186 p.

Morrison, R. B., editor, 1991, Quaternary nonglacial geology—Conterminous U.S.: Geological Society of America DNAG Geology of North America, v. K-2, 672 p., 8 plates in accompanying case.

Mullen, E. D., 1983, $MnO/TiO_2/P_2O_5$—A minor element discriminant for basaltic rocks of oceanic environments and its implications for petrogenesis: Earth and Planetary Science Letters, v. 62, p. 53-62.

Oeschger, H.; Siegenthaler, U.; Schotterer, U.; Gugelmann, A., 1975, A box diffusion model to study the carbon dioxide exchange in nature: Tellus, v. 27, p. 168–92.

Peterson, Jonathan, 2007, Petrographic signature for the Whidbey Formation: Western Washington University Master of Science thesis, 157 p.

Pettijohn, F. J., 1957, Sedimentary rocks; 2nd ed.: Harper & Brothers, 718 p.

Polenz, Michael; Alldritt, Katelin; Heheman, N. J.; Logan, R. L., 2009a, Geologic map of the Burley 7.5-minute quadrangle, Kitsap and Pierce Counties, Washington: Washington Division of Geology and Earth Resources Open File Report 2009-8, 1 sheet, scale 1:24,000. [http://www.dnr.wa.gov/Publications/ger_ofr2009-8_geol_map_burley_24k.pdf]

Polenz, Michael; Alldritt, Katelin; Heheman, N. J.; Sarikhan, I. Y.; Logan, R. L., 2009b, Geologic map of the Belfair 7.5-minute quadrangle, Mason, Kitsap, and Pierce Counties, Washington: Washington Division of Geology and Earth Resources Open File Report 2009-7, 1 sheet, scale 1:24,000. [http://www.dnr.wa.gov/Publications/ger_ofr2009-7_geol_map_belfair_24k.pdf]

Polenz, Michael; Czajkowski, J. L.; Legorreta Paulin, Gabriel; Contreras, T. A.; Miller, B. A.; Martin, M. E.; Walsh, T. J.; Logan, R. L.; Carson, R. J.; Johnson, C. N.; Skov, R. H.; Mahan, S. A.; Cohan, C. R., 2010a, Geologic map of the Skokomish Valley and Union 7.5-minute quadrangles, Mason County, Washington: Washington Division of Geology and Earth Resources Open File Report 2010-3, 1 sheet, scale 1:24,000, with 21 p. text. [http://www.dnr.wa.gov/Publications/ger_ofr2010-3_geol_map_skokomish_valley_union_ 24k.zip]

Polenz, Michael; Miller, B. A.; Contreras, T. A.; Czajkowski, J. L.; Legorreta Paulin, Gabriel; Martin, M. E.; Logan, R. L.; Carson, R. J.; Johnson, C. N.; Skov, R. H.; Mahan, S. A.; Cohan, C. R., 2010b, Supplement to the geologic maps of the Lilliwaup, Skokomish Valley, and Union 7.5-minute quadrangles, Mason County, Washington—Geologic setting and development around the Great Bend of Hood Canal: Washington Division of Geology and Earth Resources Open File Report 2010-5, 27 p. [http://www.dnr.wa.gov/Publications/ ger_ofr2010-5_lilliwaup_skokomish_valley_union_suppl_24k.pdf]

Polenz, Michael; Miller, B. A.; Davies, Nigel; Perry, B. B.; Clark, K. P.; Walsh, T. J.; Carson, R. J.; Hughes, J. F., 2012a, Geologic map of the Hoodsport 7.5-minute quadrangle, Mason County, Washington: Washington Division of Geology and Earth Resources Open File Report 2011-3, 1 sheet, scale 1:24,000, 18 p. text. [http://www.dnr.wa.gov/Publications/ger_ofr2011-3_geol_map_hoodsport_24k.zip]

Polenz, Michael; Miller, B. A.; Davies, Nigel; Perry, B. B.; Hughes, J. F.; Clark, K. P.; Walsh, T. J.; Tepper, J. H.; Carson, R. J., 2012b, Analytical data from the Hoodsport 7.5-minute quadrangle, Mason County, Washington—Supplement to Open File Report 2011-3: Washington Division of Geology and Earth Resources Open File Report 2011-4, 42 p. [http://www.dnr.wa.gov/Publications/ger_ofr2011-4_hoodsport_supplement.pdf]

Polenz, Michael; Spangler, Eleanor; Fusso, L. A.; Reioux, D. A.; Cole, R. A.; Walsh, T. J.; Cakir, Recep; Clark, K. P.; Tepper, J. H.; Carson, R. J.; Pileggi, Domenico; Mahan, S. A., 2012c, Geologic map of the Brinnon 7.5-minute quadrangle, Jefferson and Kitsap Counties, Washington: Washington Division of Geology and Earth Resources Map Series 2012-02, 1 sheet, scale 1:24,000, with 47 p. text. [http://www.dnr.wa.gov/Publications/ger_ms2012-02_geol_map_brinnon_24k.zip]

Porter, S. C.; Carson, R. J., 1971, Problems of interpreting radiocarbon dates from dead-ice terrain, with an example from the Puget Lowland of Washington: Quaternary Research, v. 1, no. 3, p. 410-414.

Porter, S. C.; Swanson, T. W., 1998, Radiocarbon age constraints on rates of advance and retreat of the Puget lobe of the Cordilleran ice sheet during the last glaciation: Quaternary Research, v. 50, no. 3, p. 205-213.

Reimer, P. J.; Baillie, M. G. L.; Bard, E.; Bayliss, A.; Beck, J. W.; Blackwell, P. G.; Bronk Ramsey, C.; Buck, C. E.; Burr, G. S.; Edwards, R. L.; Friedrich, M.; Grootes, P. M.; Guilderson, T. P.; Hajdas, I.; Heaton, T. J.; Hogg, A. G.; Hughen, K. A.; Kaiser, K. F.; Kromer, B.; McCormac, F. G.; Manning, S. W.; Reimer, R. W.; Richards, D. A.; Southon, J. R.; Talamo, S.; M Turney, C. S.; van der Plicht, J.; Weyhenmeyer, C. E., 2009 IntCal09 and Marine09 radiocarbon age calibration curves, 0–50,000 years cal BP: Radiocarbon, v. 51, no. 4, p. 1111-1150. [http://www.google.com/search?sourceid=navclient&ie=UTF-8&rlz=1T4SNCA_enUS247US247&q=INTCAL09]

Serdar, Carol; Powell, Lorraine, 2007, Landslide hazard zonation project—Mass wasting assessment—Great Bend watershed, Kitsap and Mason Counties, Washington: Washington Department of Natural Resources, Forest Practices, 36 p., 2 plates, scale 1:24,000. [http://www.dnr.wa.gov/BusinessPermits/Topics/LandslideHazardZonation/Pages/fp_lhz_completed.aspx]

Sherrod, B. L.; Bucknam, R. C.; Leopold, E. B., 2000, Holocene relative sea level changes along the Seattle fault at Restoration Point, Washington: Quaternary Research, v. 54, no. 3, p. 384-393.

Snook, Roxanne, 2011, The use of dendrochronology to establish climate-growth relationships and date a prehistoric earthquake: University of the Fraser Valley Bachelor of Science thesis, 23 p.

Stuiver, M.; Braziunas, T. F., 1993, Modeling atmospheric ^{14}C influences and ^{14}C ages of marine samples to 10,000 BC: Radiocarbon, v. 35, no. 1, p. 137-189.

Tabor, R. W.; Cady, W. M., 1978, Geologic map of the Olympic Peninsula, Washington: U.S. Geological Survey Miscellaneous Investigations Series Map I-994, 2 sheets, scale 1:125,000.

Thorson, R. M., 1981, Isostatic effects of the last glaciation in the Puget Lowland, Washington: U.S. Geological Survey Open-File Report 81-370, 100 p., 1 plate. [http://pubs.er.usgs.gov/djvu/OFR/1981/ofr_81_370.djvu (text) and http://pubs.er.usgs.gov/djvu/OFR/1981/ofr_81_370_plt.djvu (plate)]

Todd, M. R., 1939, The glacial geology of the Hamma Hamma Valley and its relation to the glacial history of the Puget Sound basin: University of Washington Master of Science thesis, 48 p., 1 plate.

U.S. Geological Survey Geologic Names Committee, 2010, Divisions of geologic time—Major chronostratigraphic and geochronologic units: U.S. Geological Survey Fact Sheet 2010-3059, 2 p. [http://pubs.usgs.gov/fs/2010/3059/]

Walsh, T. J.; Logan, R. L., 2007, Field data for a trench on the Canyon River fault, southeast Olympic Mountains, Washington: Washington Division of Geology and Earth Resources Open File Report 2007-1, 1 plate. [http://www.dnr.wa.gov/Publications/ger_ofr2007-1_canyon_river_fault_trench.pdf]

Walsh, T. J.; Logan, R. L.; Neal, K. G., 1997, The Canyon River fault, an active fault in the southern Olympic Range, Washington: Washington Geology, v. 25, no. 4, p. 21-24. [http://www.dnr.wa.gov/Publications/ger_washington_geology_1997_v25_no4.pdf]

Washington Department of Ecology, 1979, Coastal zone atlas of Washington; volume 10, Kitsap County: Washington Department of Ecology, 1 v., maps, scale 1:24,000.

Washington Department of Ecology, 1980, Coastal zone atlas of Washington; volume 9, Mason County: Washington Department of Ecology, 1 v., maps, scale 1:24,000.

Wilson, J. R., 1975, Geology of the Price Lake area, Mason County, Washington: North Carolina State University Master of Science thesis, 79 p., 2 plates.

Wilson, J. R.; Bartholomew, M. J.; Carson, R. J., 1979, Late Quaternary faults and their relationship to tectonism in the Olympic Peninsula, Washington: Geology, v. 7, no. 5, p. 235-239.

Witter, R. C.; Givler, R. W.; Carson, R.J., 2008, Two post-glacial earthquakes on the Saddle Mountain west fault, southeastern Olympic Peninsula, Washington: Bulletin of the Seismological Society of America, v. 98, no. 6, p. 2894-2917.

Appendix A. Fault-related Measurements

Fault orientations were measured using a Brunton pocket transit; strike and dip were recorded as an azimuth (0-360°) using "the right hand rule", wherein dip direction is to the right. Rakes of slickenlines were recorded independent of the direction of perceived movement, and most of the trends and plunges were calculated from the orientation of the fault planes and rakes. Trends and plunges of slickenlines are directed into the ground (or lower hemisphere), regardless of fault movement.

The data were plotted in the programs *Stereonet* and *Faultkin* (Allmendinger and others, 2012; Marrett and Allmendinger, 1990). We used *Stereonet* to generate stereonet projections of fault planes and poles to planes. We contoured the poles to planes using the 1% method where E = (100)/N, E is the expected density and N is the total number of data points. We also used rose diagrams to depict the distribution of fault orientations.

The structural data used in Figure A1 are in the DGER ArcGIS files in the *gattud* feature data set associated with the map files. The locations of the *gattud* feature data set are correct. They were recorded with a Garmin 76CSx GPS and may differ from those on the map plate. Locations on the map plate may have been moved or omitted in complex areas to more clearly show selected details.

We attempted to measure only faults that were not completely healed by mineralization; however, many slickensided surfaces were mineralized. We do not assume that all the faults measured have been recently active. Fault movement could, and likely does, represent reactivation of older faults or older movement. Additionally, some oblique fault surfaces have produced two sets of distinct slickensides that in many places recorded reverse and normal movement having the same strike-slip direction.

We measured 133 fault planes; the entire set of fault planes, poles to planes, poles-to-planes contours, and rose diagram is shown in Figure A1. We are confident about the orientation and offset direction of slickenlines on only 21 of these faults; Figure A2 is a depiction of those faults. The point along the fault plane depicts the trend and plunge of the slickenline. The arrow from each point indicates the slip direction of the hanging wall.

Additional photos pertaining to faults at significant sites are in Appendix F.

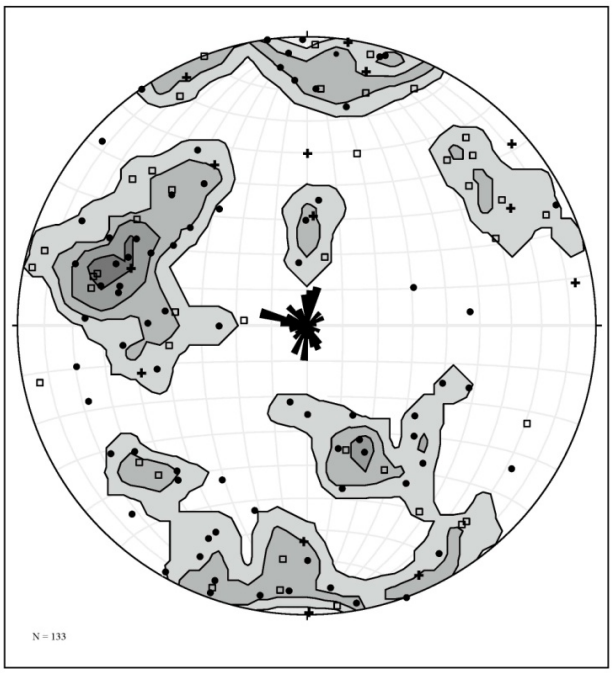

Figure A1. Stereonet projection plot of poles to fault planes with 1% area contoured and a rose diagram for fault strikes. Plus signs represent poles to fault planes in the northern third of the map area, circles represent poles to fault planes in the middle third, and hollow squares denote poles to fault planes in the southern third. The rose diagram indicates that most faults strike east-northeast.

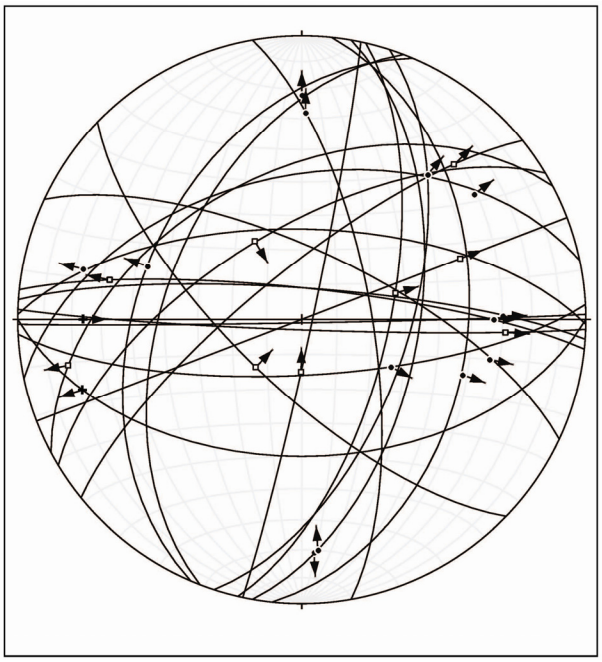

Figure A2. *Faultkin* projection of fault planes for faults in the Eldon quadrangle for which slickenlines were recorded. Shown here are fault planes for 21 of the 133 faults on which 23 observed sets of slickenlines gave a clear indication of orientation and offset direction. The black arrow on each plane shows the direction of slip and offset on the hanging wall, plus signs indicate faults in the northern third of the quadrangle, circles those in the central third, and squares those in the southern third.

Appendix B. Composite Stratigraphic Sections

We measured 12 composite stratigraphic sections within the map area. They are indicated on the map by purple diamonds. Four sections are near the mouth of the Hamma Hamma River and eight are on the east side of Hood Canal. The Hamma Hamma sections, HH1 to HH4, are in Holocene deposits and often are sample locations of radiocarbon samples. The sections from the east side of Hood Canal, SS1 to SS8, are composite sections measured along roads and drainages, and their locations are approximate. Figure B13 depicts our interpretation of the correlation of units along the eastern shoreline, but we lack age control. To estimate age, we made correlations on the basis of weathered soil layers (paleosols) and stratigraphic successions. We relied primarily on the reversed magnetic polarity of nonglacial silts at Capstan Rock (near SS8) (Easterbrook and others, 1988) to determine the age of the oldest deposits. Additionally, we used unpublished data from the adjacent Lilliwaup and Holly quadrangles (Contreras and others, 2010, 2012b) south and east of the map area, respectively, to help constrain our correlations. The elevation data in the sections were calculated or approximated from lidar elevations provided by the Puget Sound Lidar Consortium; a handheld Garmin 76CSx GPS located the exposures along the transect.

Key for Stratigraphic Sections Measured at the Mouth of the Hamma Hamma River

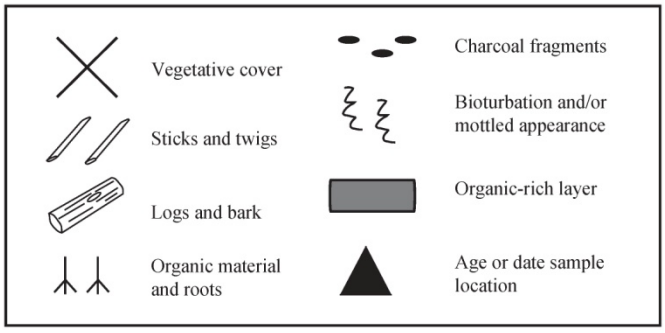

Key for Stratigraphic Sections on the East Side of Hood Canal

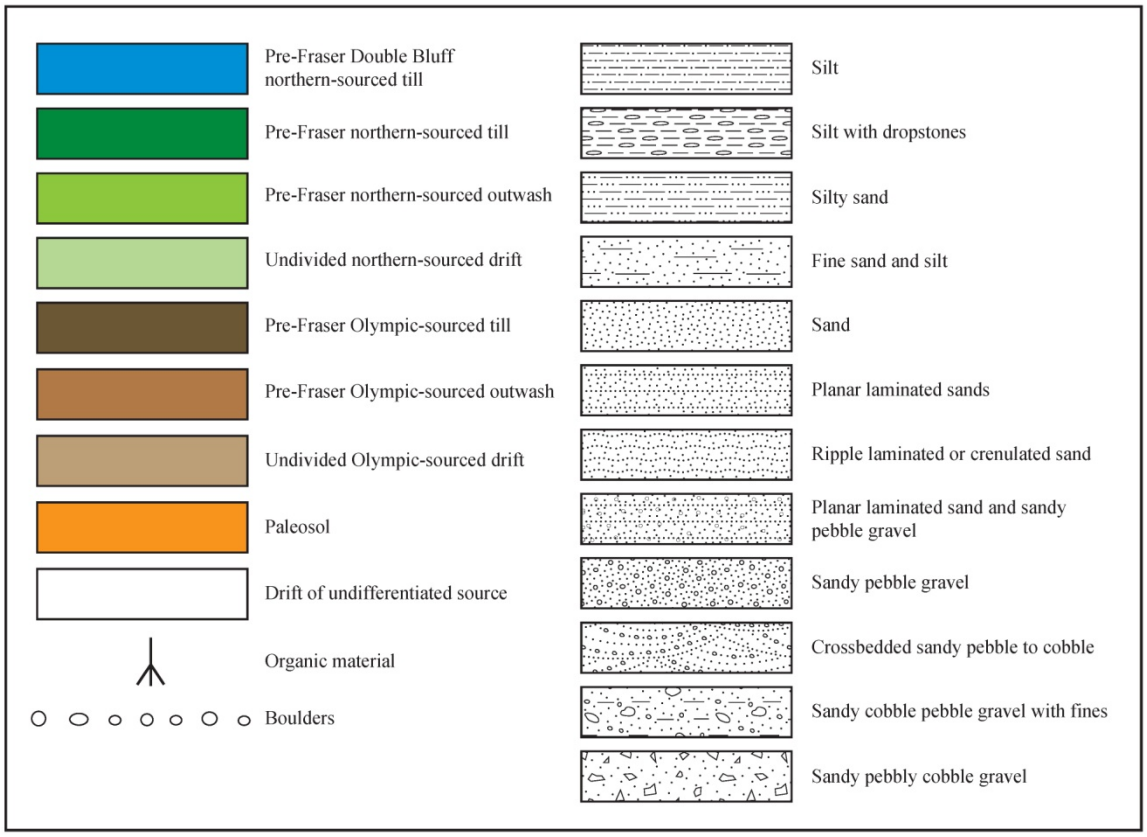

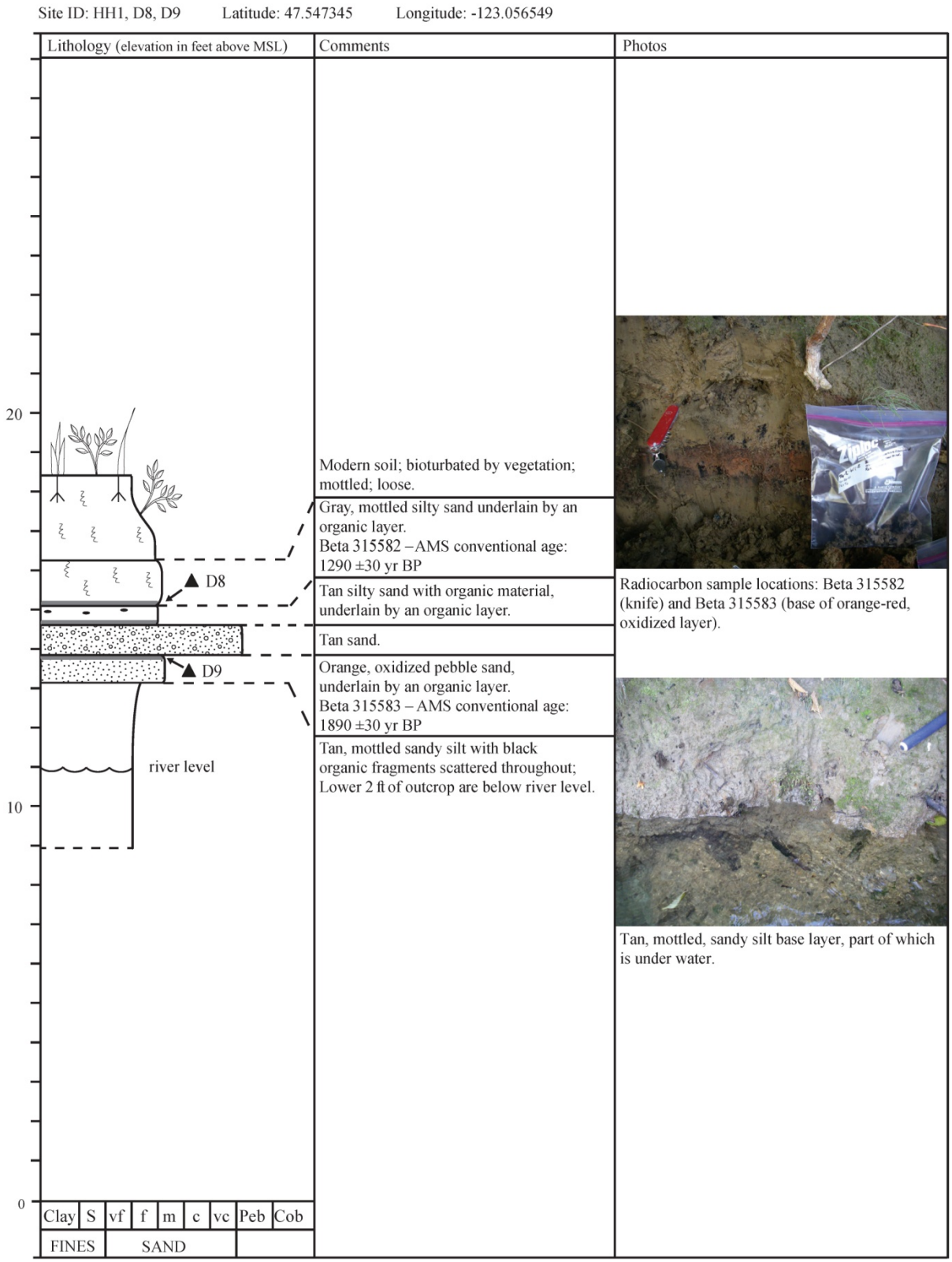

Figure B1. Columnar section through unit Qoa at location HH1 near the mouth of the Hamma Hamma River. Radiocarbon samples are listed in Table 1 on the map plate.

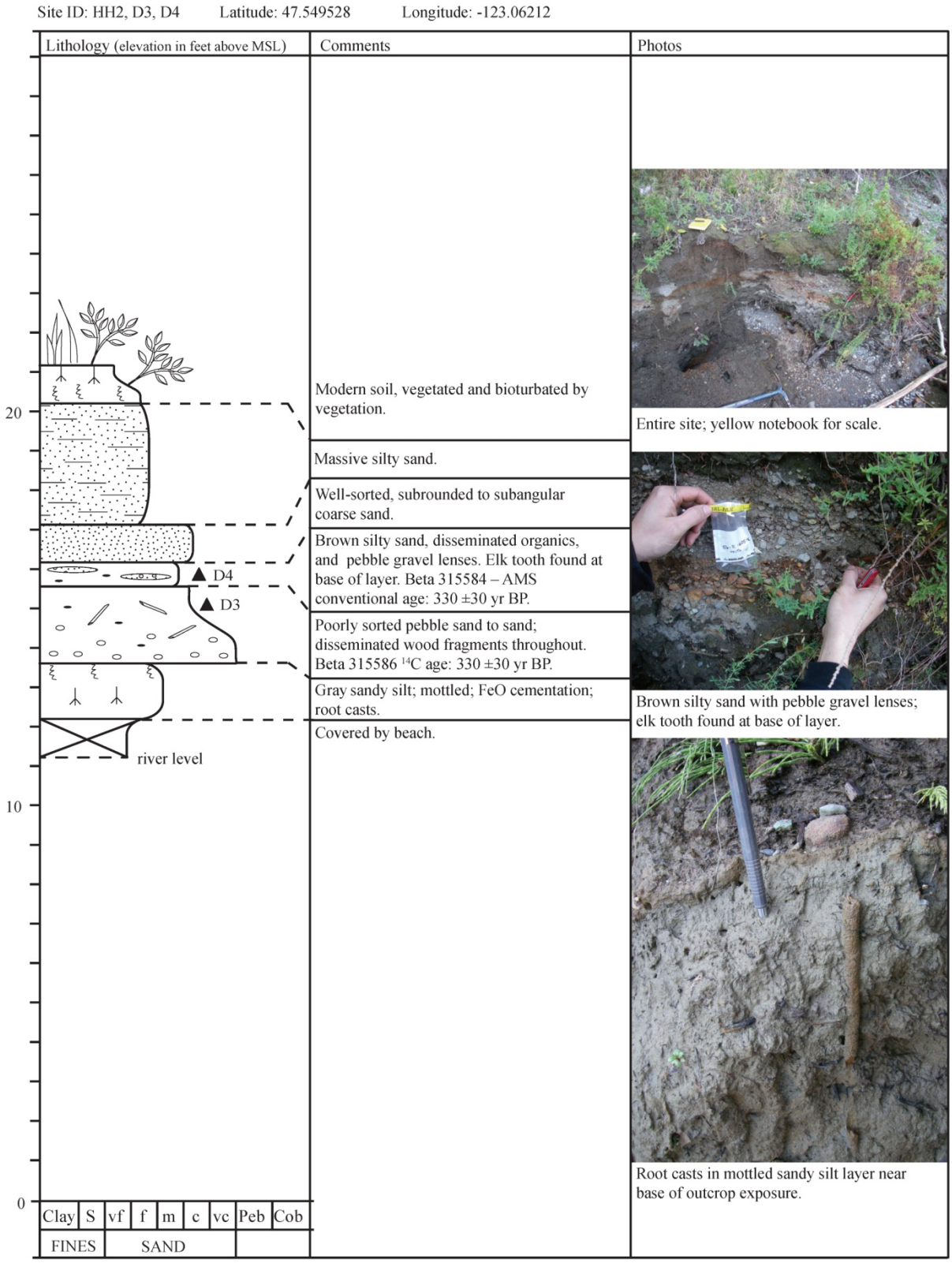

Figure B2. Columnar section through unit Qoa at location HH2 near the mouth of the Hamma Hamma River. Radiocarbon samples are listed in Table 1 on the map plate.

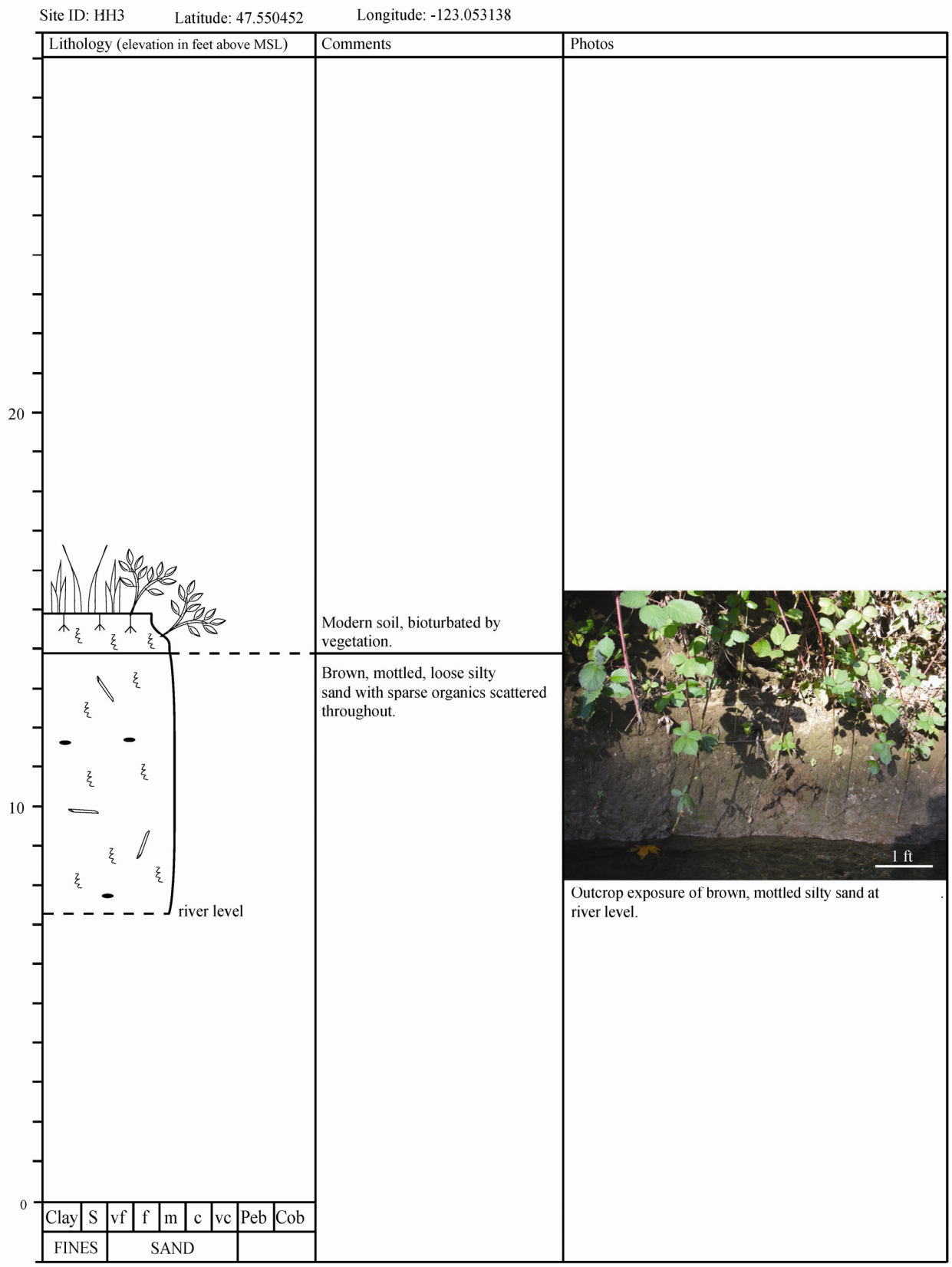

Figure B3. Columnar section through unit Qoa at location HH3 near the mouth of the Hamma Hamma River.

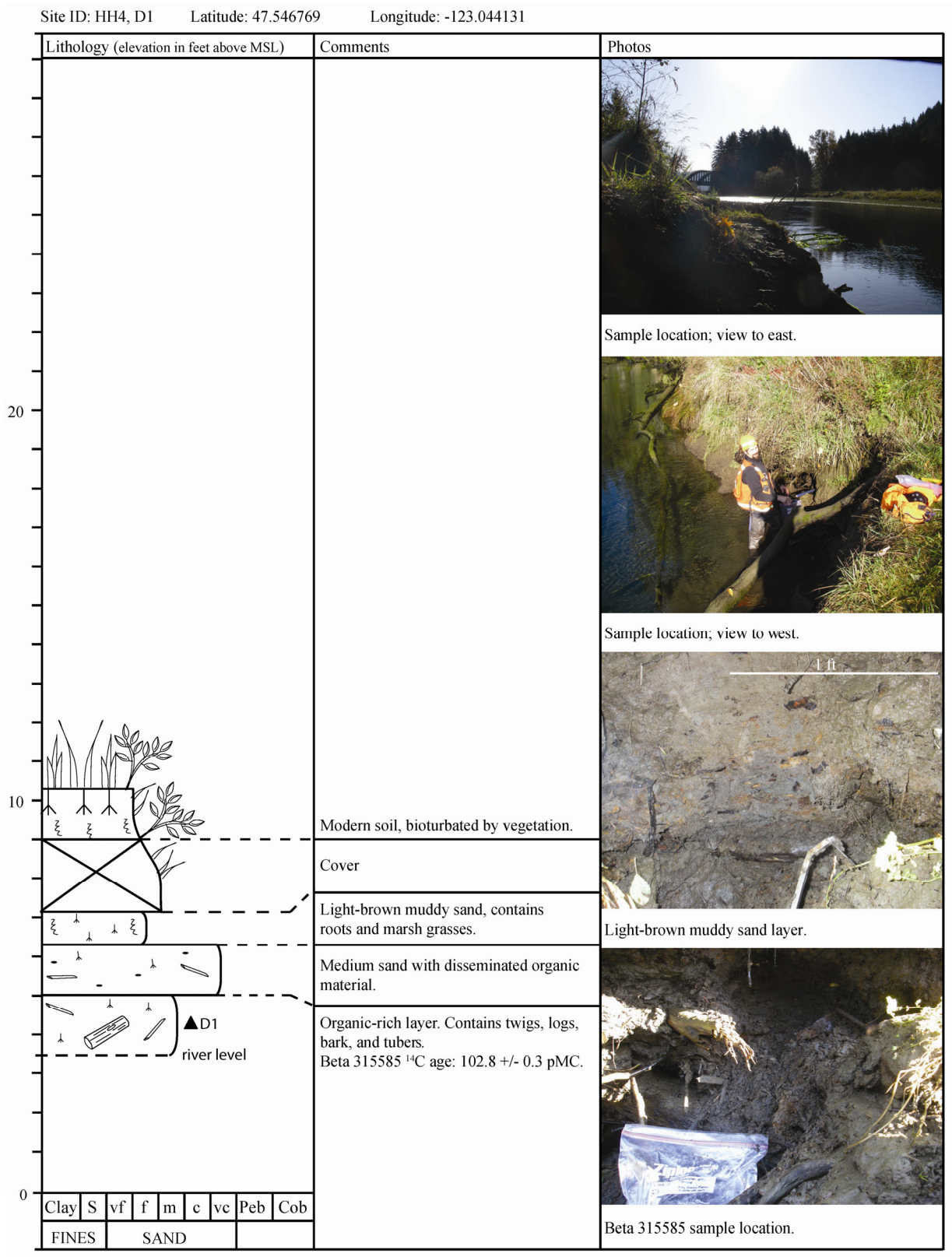

Figure B4. Columnar section through unit Qoa at location HH4 near the mouth of the Hamma Hamma River. Radiocarbon samples are listed in Table 1 on the map plate.

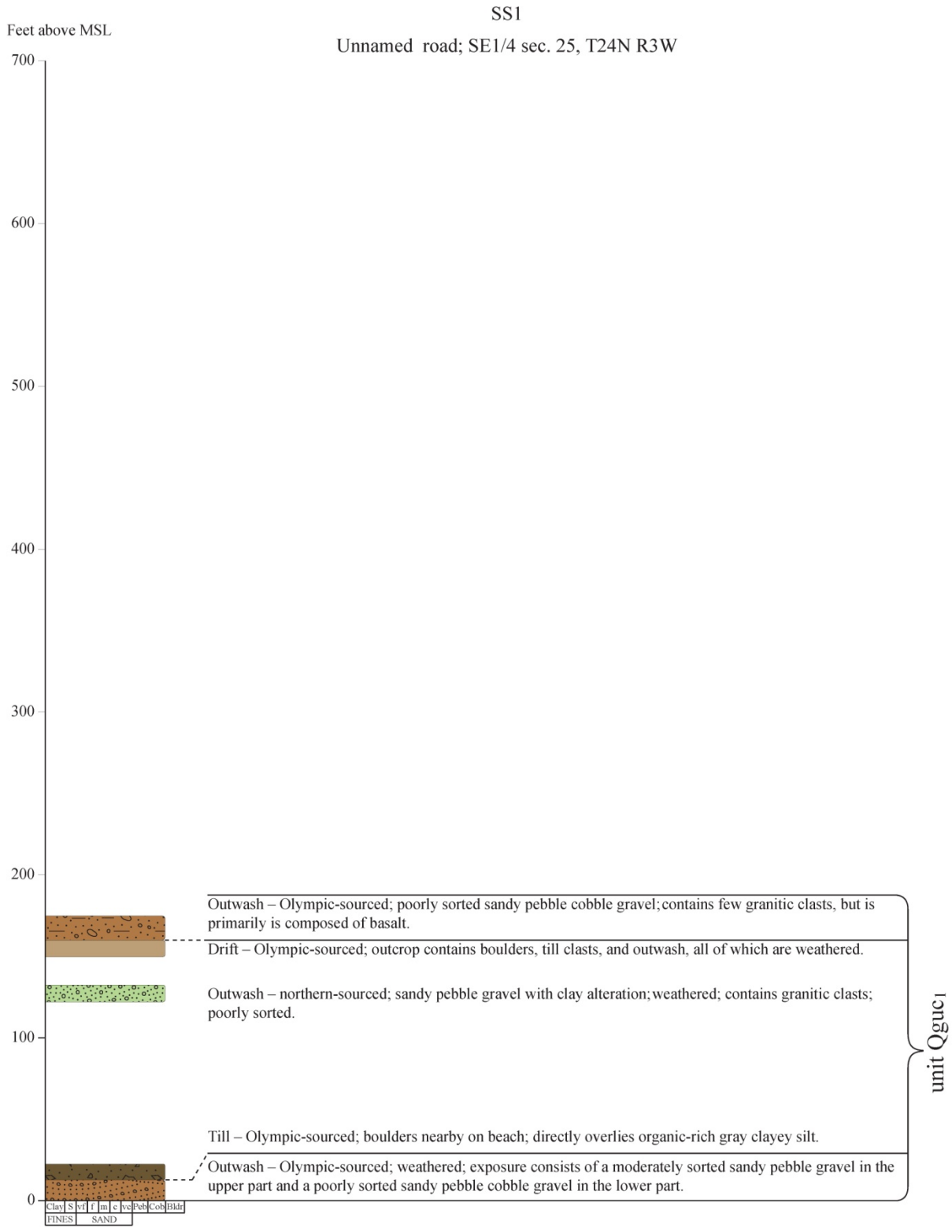

Figure B5. Composite stratigraphic section at location SS1 on the east side of Hood Canal.

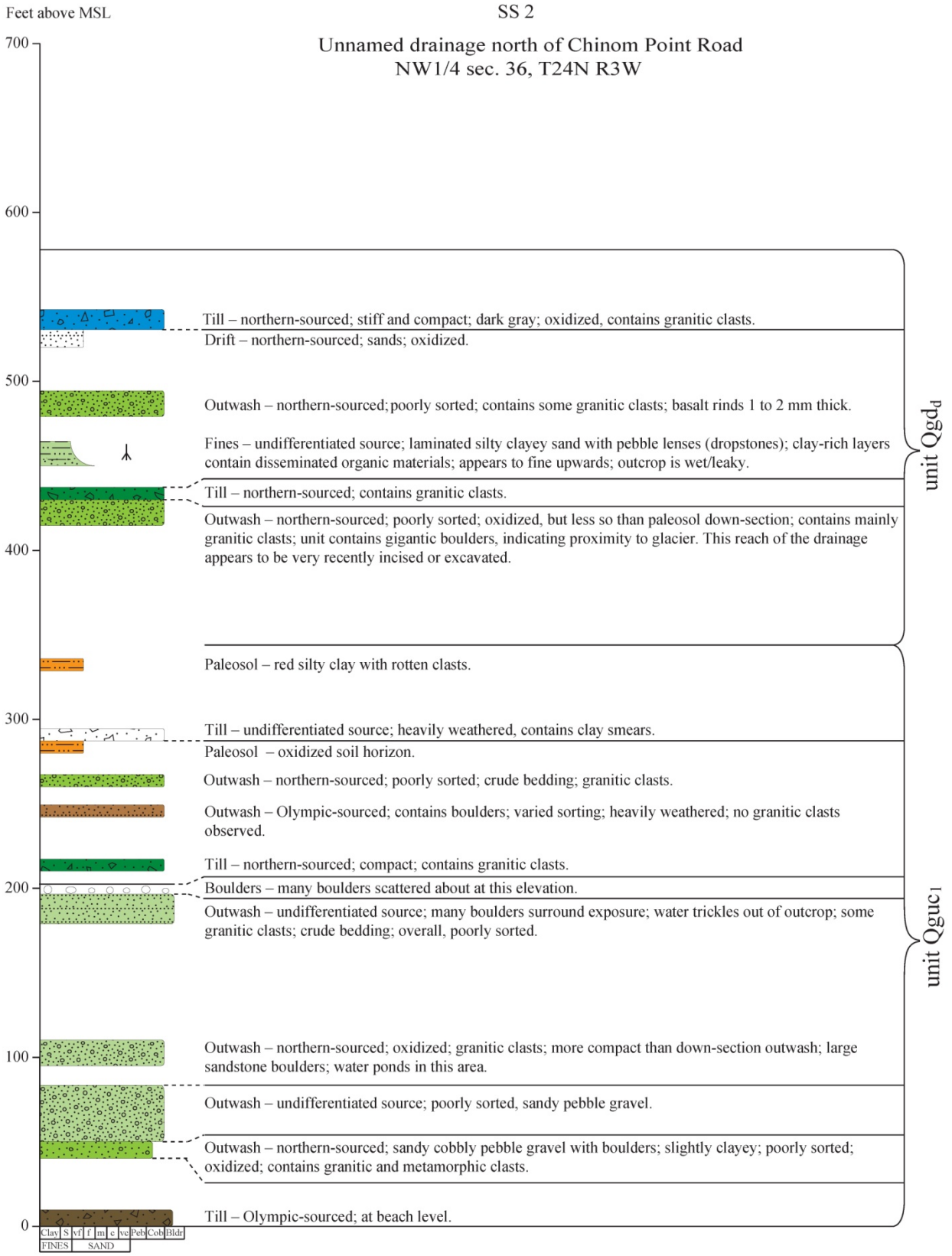

Figure B6. Composite stratigraphic section at location SS2 on the east side of Hood Canal.

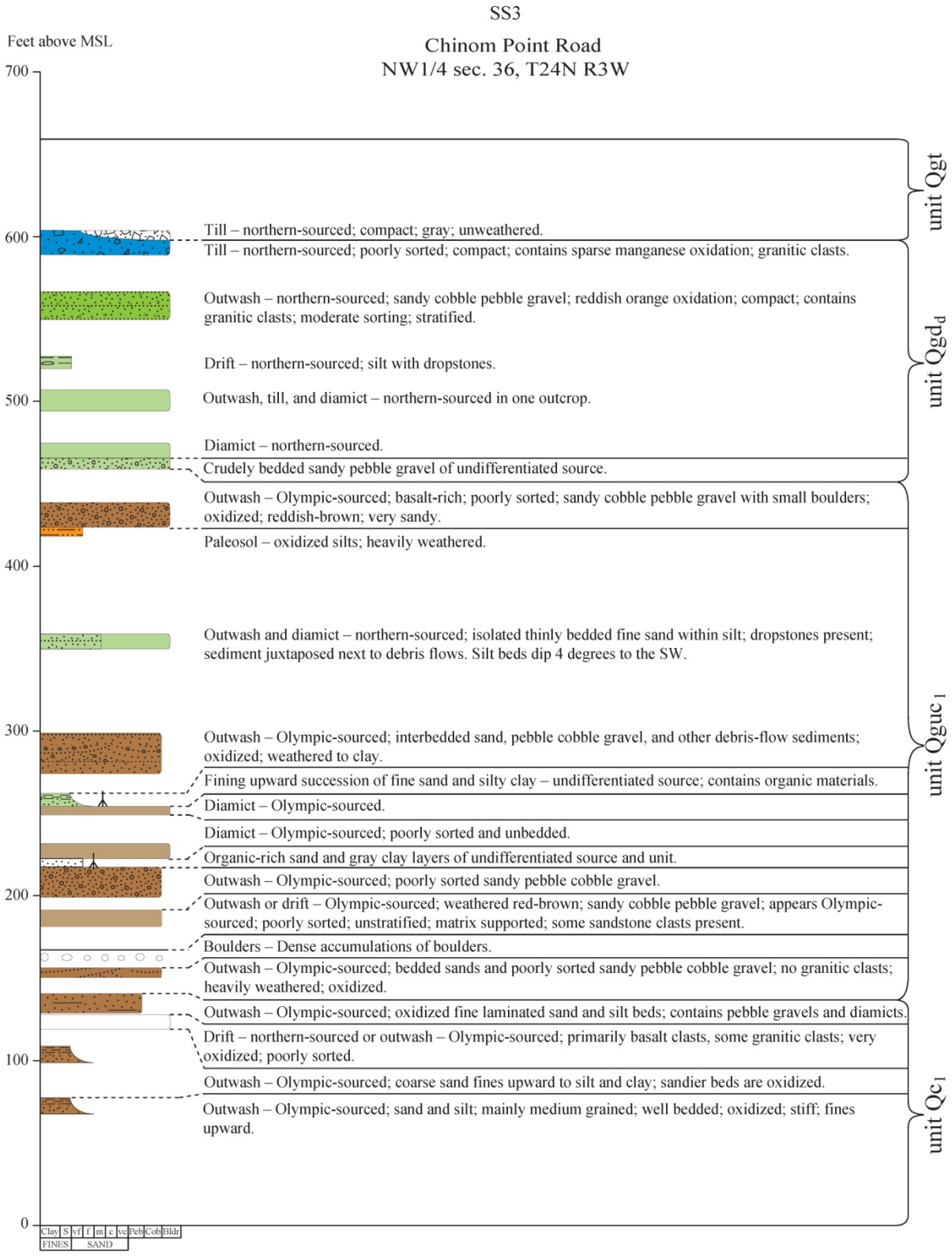

Figure B7. Composite stratigraphic section at location SS3 on the east side of Hood Canal.

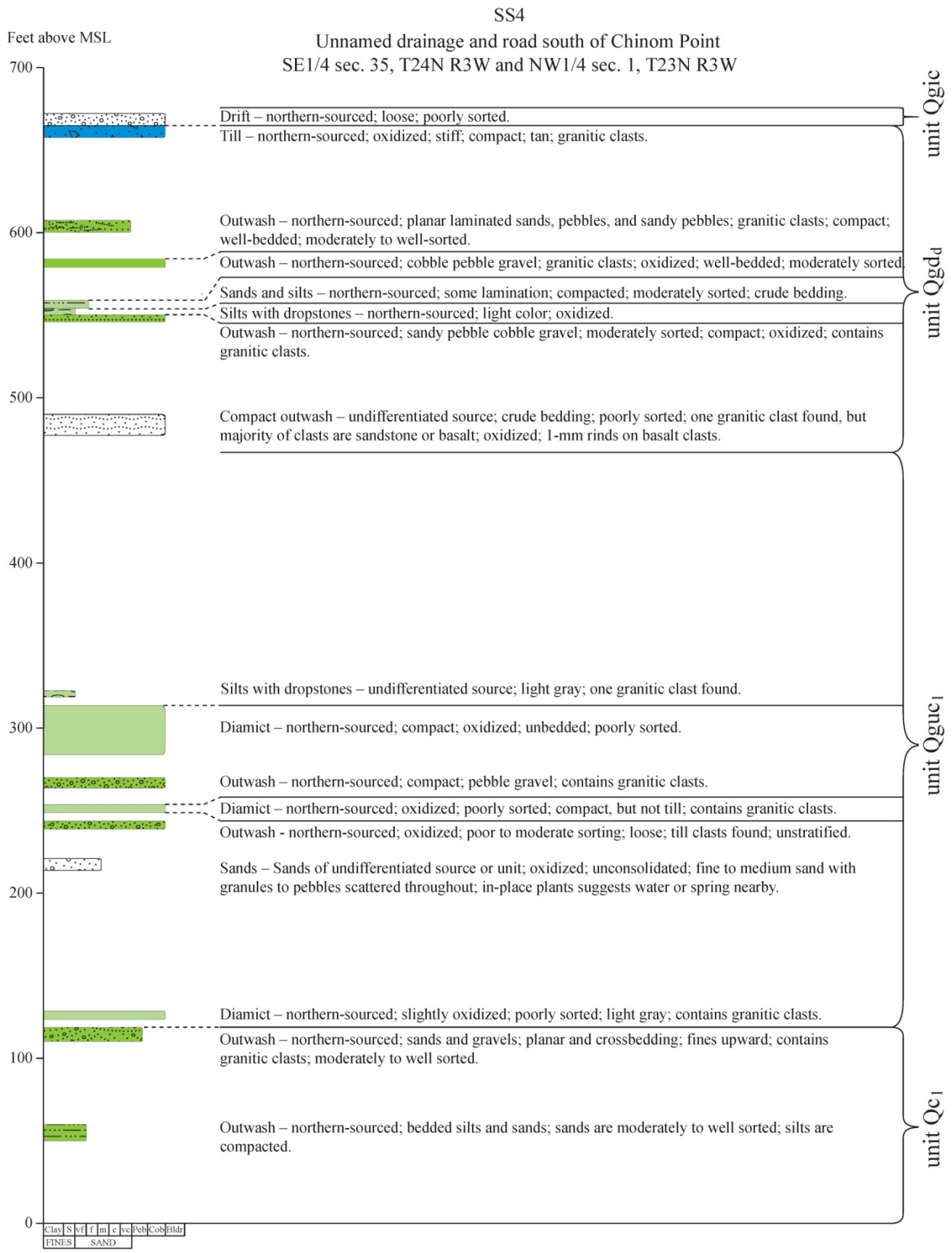

Figure B8. Composite stratigraphic section at location SS4 on the east side of Hood Canal.

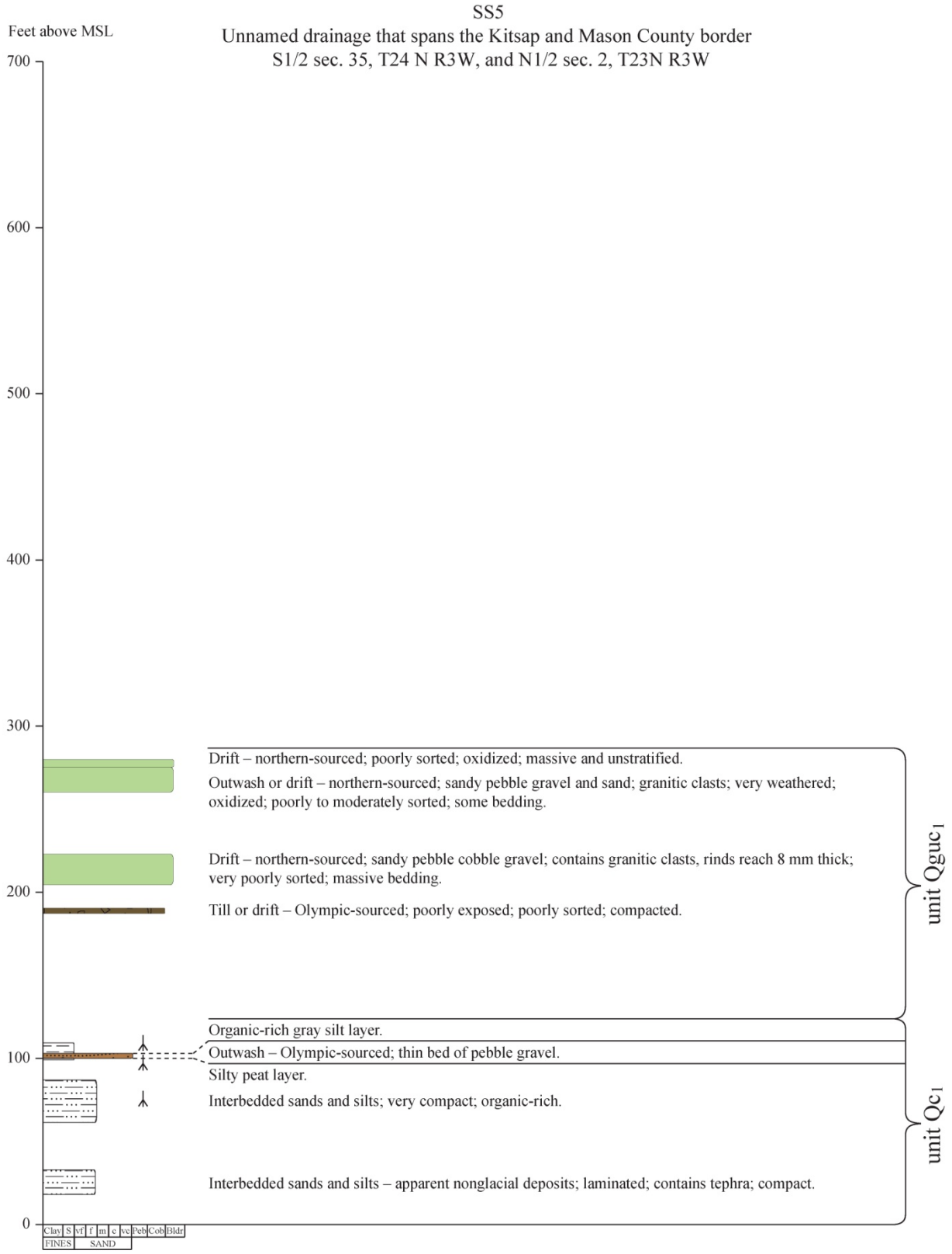

Figure B9. Composite stratigraphic section at location SS5 on the east side of Hood Canal.

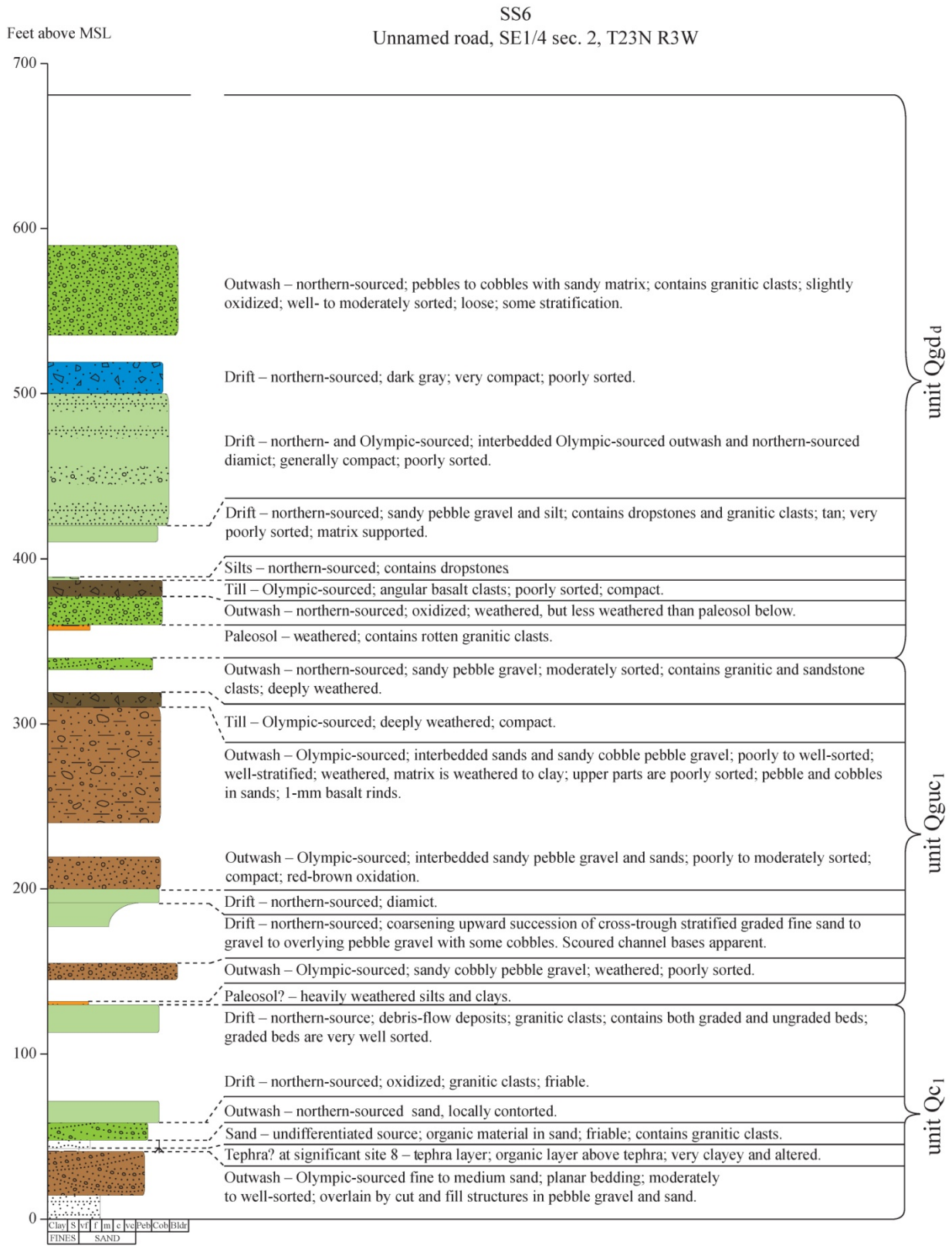

Figure B10. Composite stratigraphic section at location SS6 on the east side of Hood Canal.

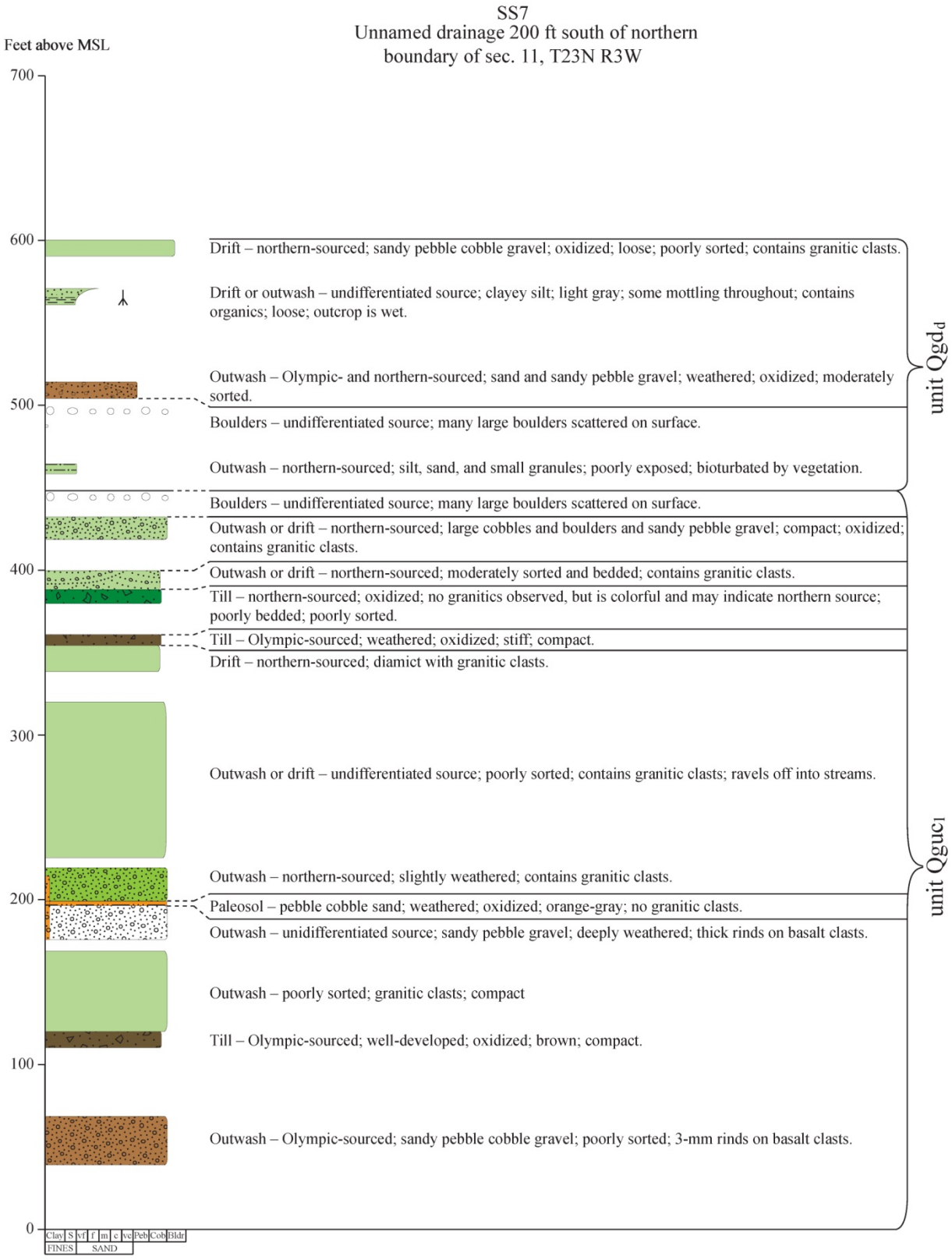

Figure B11. Composite stratigraphic section at location SS7 on the east side of Hood Canal.

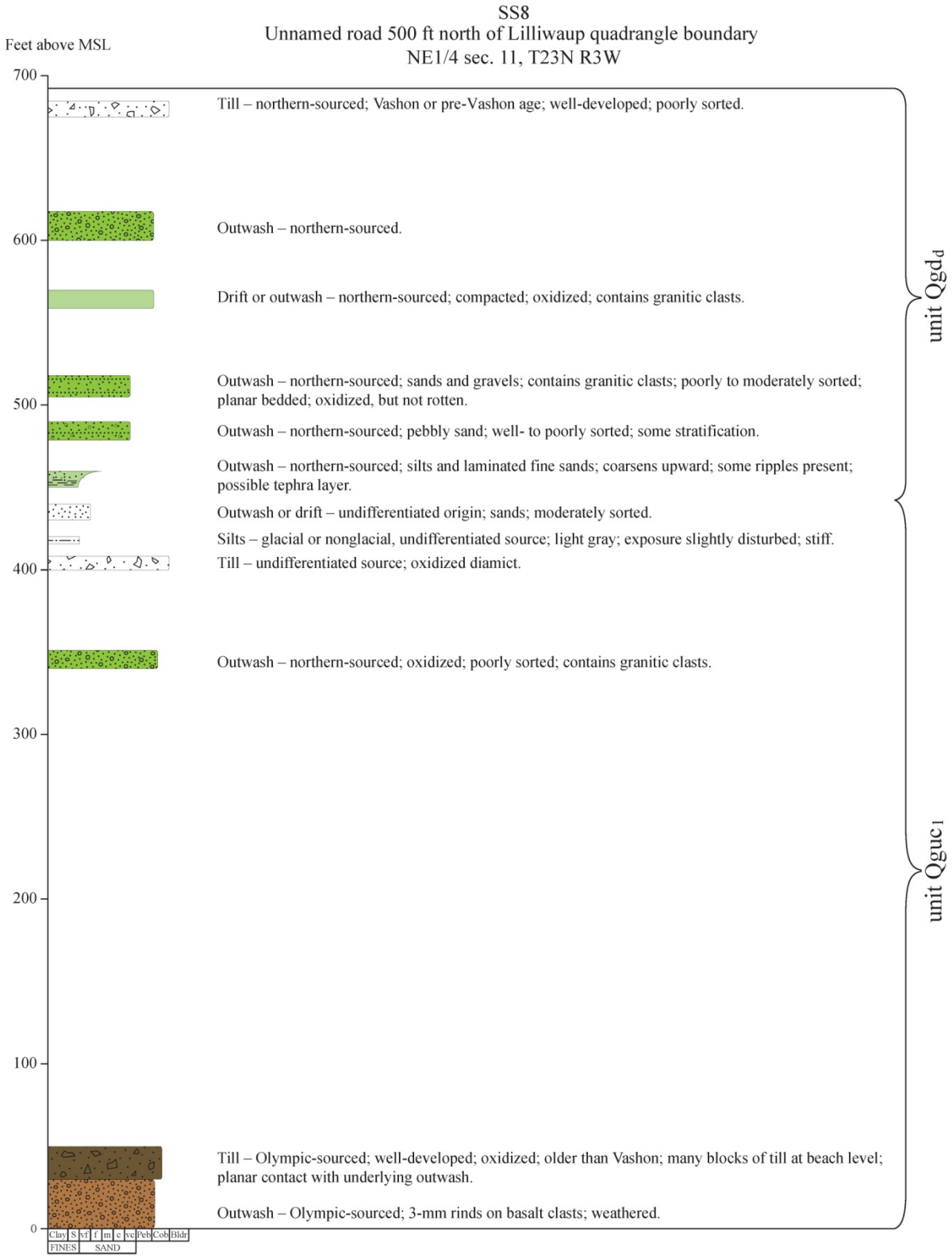

Figure B12. Composite stratigraphic section at location SS8 on the east side of Hood Canal.

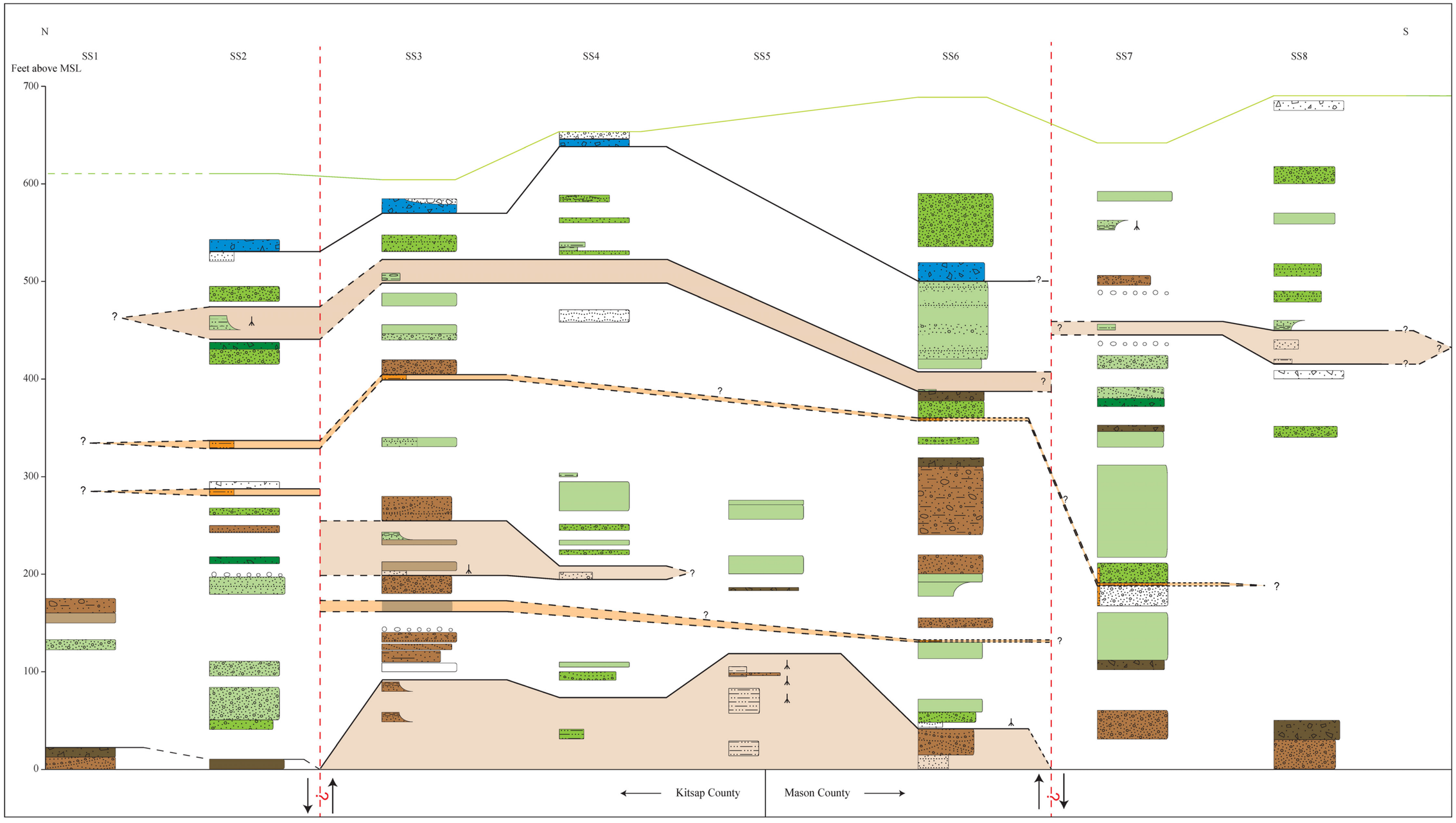

Figure B13. Correlation diagram of stratigraphic sections SS1–8 along the east side of Hood Canal. Black lines (dashed and solid) represent correlations of individual units. The green line denotes surface topography; red dashed lines are inferred faults. Light brown areas denote nonglacial intervals; and orange-shaded areas denote paleosol horizons.

THIS PAGE LEFT INTENTIONALLY BLANK.

Appendix C. Geochemical Data for Basalt Samples

Five basalt whole-rock chemical samples were analyzed for this study by ALS Chemex, North Vancouver, BC, Canada. The sample locations are indicated by green diamonds on the geologic map and a number prefaced by G. Major oxides were determined by x-ray fluorescence (XRF) and trace elements by inductively coupled plasma mass spectrometry (ICP-MS). The samples plot as basalts in a total alkali versus silica plot of Le Bas and others (1986) (Fig. C1) and as tholeiitic basalts on an AFM diagram after Irvine and Baragar (1971)(Fig. C2); they have within-plate (hot spot) chemical affinities (Fig. C3). These lavas have limited chemical variation (46.4–48.2 wt% SiO_2; 5.1–6.2 wt% MgO) but are notably more differentiated than lavas from the adjacent Brinnon quadrangle (Polenz and others, 2012c), as indicated by their lower Cr content (averaging 56 ppm vs. 203 ppm for Brinnon) and lower Mg content (100*molar Mg/(Mg+Fe) 34–45 vs. 44–58). Samples from the Eldon quadrangle are also distinguished from those of the Brinnon quadrangle by higher concentrations of incompatible elements, including TiO_2 (2.8–4.3 wt% vs. 1.6–2.4 wt%) and Zr (199–319 ppm vs. 93–117 ppm). Elevated incompatible element contents indicate derivation of the Eldon samples from a more enriched mantle source than that in the Brinnon quadrangle.

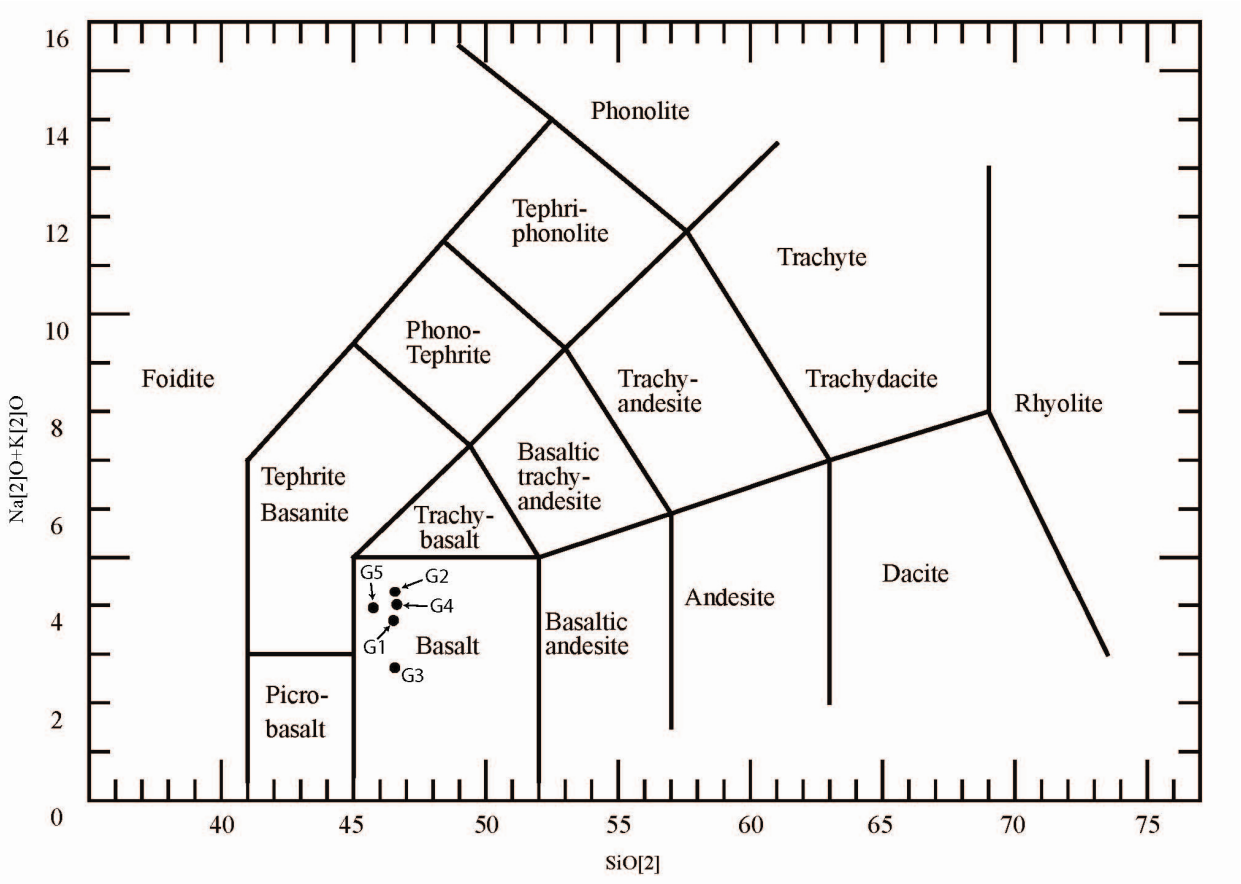

Figure C1. Total alkali vs. silica plot (Le Bas and others, 1986). All bedrock samples for the Eldon quadrangle project plot as basalt. See Table C1 for analytical data.

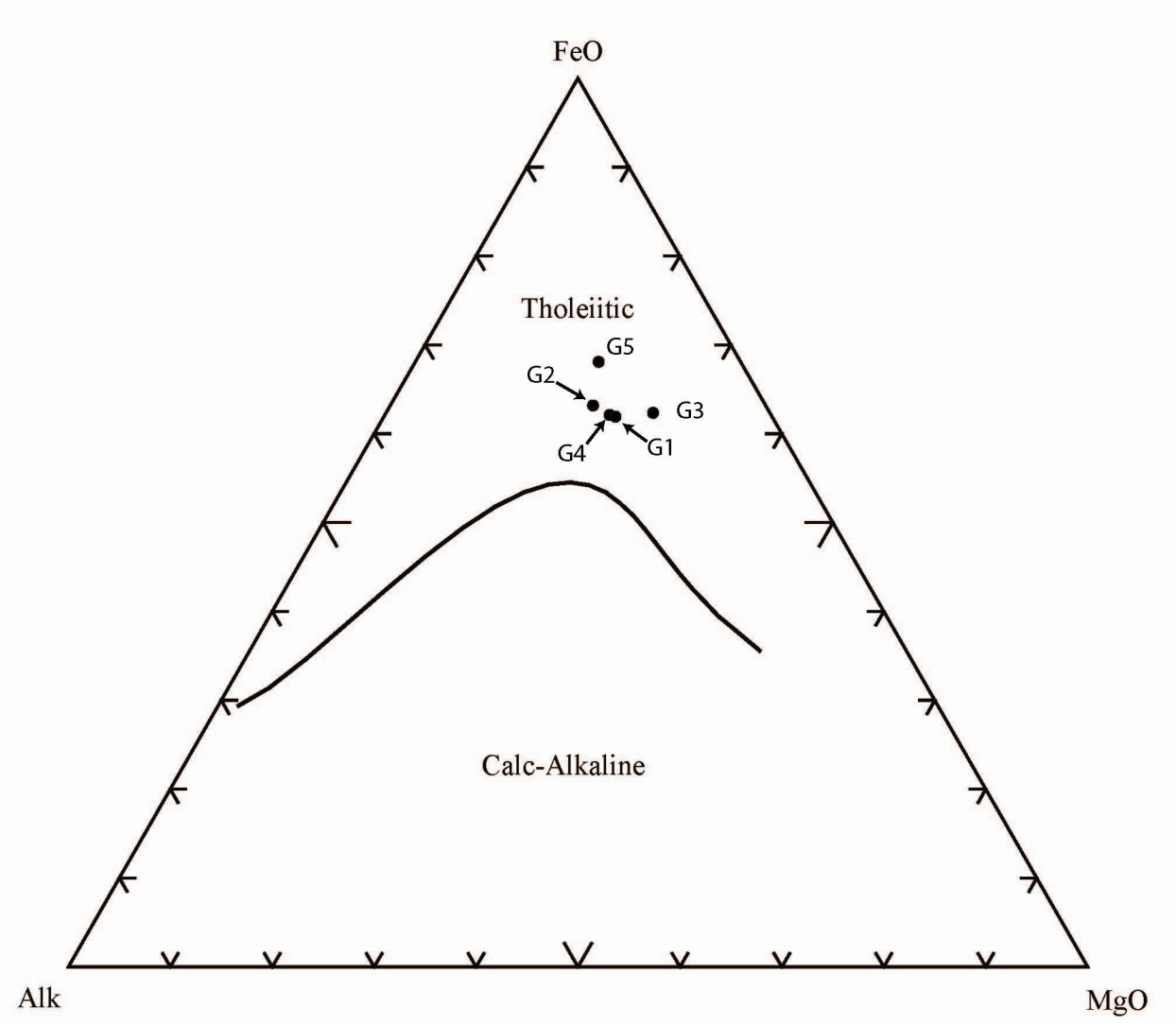

Figure C2. AFM ternary diagram between alkali and iron and magnesium oxides after Irvine and Baragar (1971). All bedrock samples from the Eldon quadrangle are tholeiitic basalt. See Table C1 for analytical data.

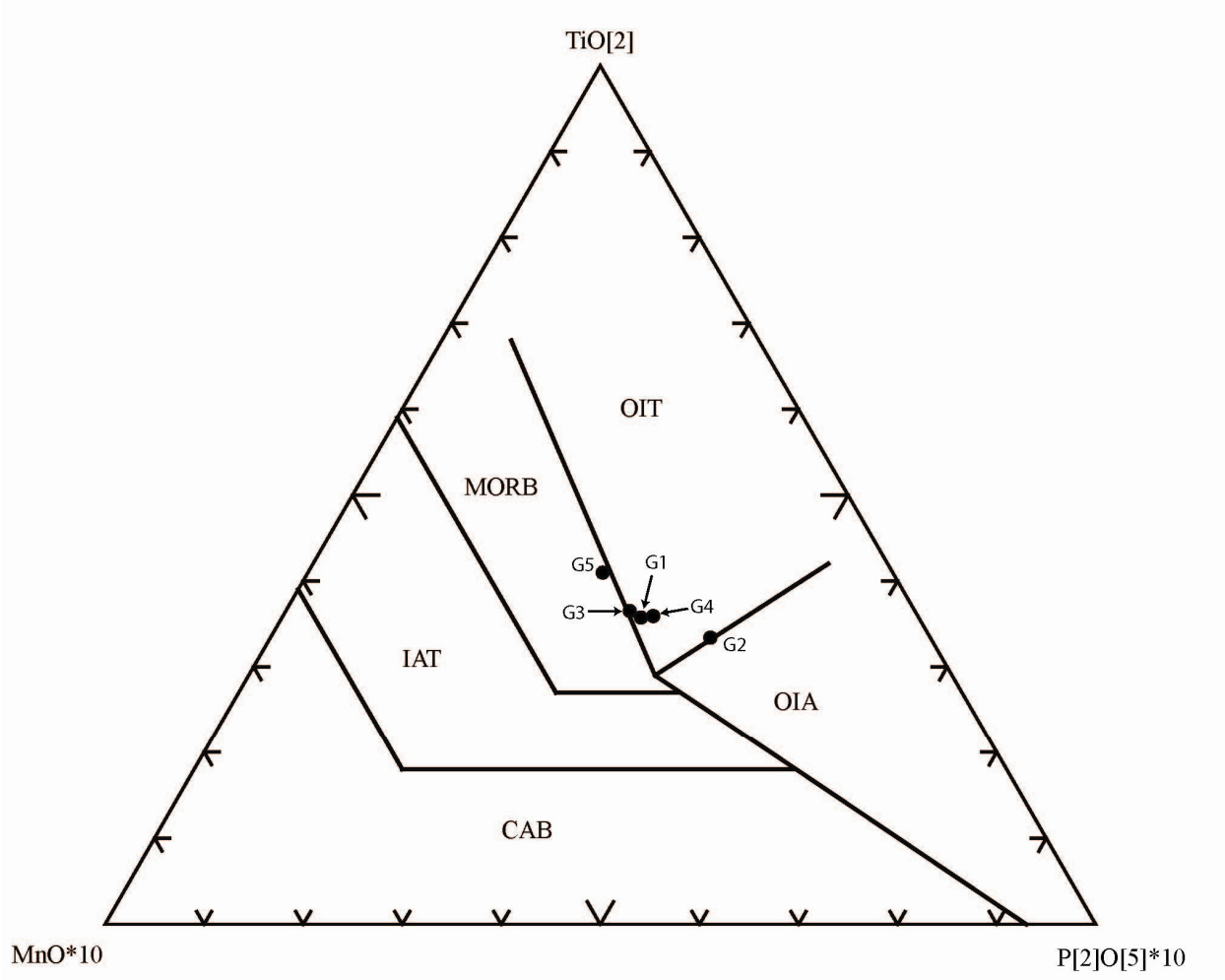

Figure C3. Tectonic discrimination diagram (Mullen, 1983) showing that Crescent Formation basalt from the Eldon quadrangle displays both MORB (mid-ocean ridge basalt) and OIT (ocean island tholeiite) affinities. See Table C1 for analytical data.

Table C1. Whole-rock chemical analyses for basalt samples from the Eldon quadrangle. Sample sites are shown on the plate as green diamonds labeled G1 through G5. Major oxides were determined by x-ray fluorescence methods and trace elements by inductively coupled plasma mass spectrometry (ICP-MS). Analyses were done by ALS Chemex, N. Vancouver, BC, Canada. The lab states that accuracy is 5% for major element oxides (unnormalized) and 10% for trace elements. Fe_2O_3 represents total iron; LOI, loss on ignition.

				Trace elements																														
Site ID	Latitude	Longitude	Geologic unit	Ba	Ce	Co	Cr	Cs	Dy	Er	Eu	Ga	Gd	Hf	Ho	La	Lu	Mo	Nb	Nd	Pr	Rb	Sm	Sn	Sr	Ta	Tb	Th	Tl	Tm	U	V	W	Y	Yb	Zr
G1	47.619635	-123.01051	Ev_C	147	40.5	48.6	50	0.02	7.2	3.78	2.28	20.2	7.41	5.5	1.2	17.7	0.51	2	19.8	26	5.91	3.8	6.51	2	261	1.4	1.18	1.44	<0.5	0.54	0.47	478	1	36.9	3.16	199
G2	47.60591	-123.00355	Ev_C	62.7	57.3	44.3	30	0.02	9.6	5.06	3.11	21.6	9.97	8.3	1.64	24.6	0.68	2	31.1	36.4	8.33	5.3	8.9	2	208	2.1	1.63	2.56	<0.5	0.73	0.8	419	1	48.7	4.24	319
G3	47.53855	-123.05668	Ev_C	94.9	40	52	160	0.08	7.1	3.86	2.17	23	7.13	5.1	1.34	15.9	0.49	<2	17.7	26.9	5.63	7.7	6.55	2	242	1.1	1.11	1.25	<0.5	0.53	0.37	471	1	38.5	3.25	210
G4	47.53532	-123.04326	Ev_C	47.5	50.3	49.7	30	0.02	8.21	4.1	2.63	22.9	8.54	6.3	1.36	21.5	0.56	2	23.3	32	7.41	4.8	7.82	2	124	1.6	1.35	1.93	<0.5	0.58	0.62	521	1	40.9	3.41	242
G5	47.53532	-123.06305	Ev_C	102	41.8	52.8	10	0.01	7.89	4.11	2.61	22.5	8.05	5.7	1.33	18.3	0.55	2	19	27.1	6.18	7.7	7.01	2	169	1.3	1.3	1.39	<0.5	0.58	0.46	733	1	40.6	3.5	209

				Major oxides (%)—unnormalized										
Site ID	Latitude	Longitude	Geologic unit	SiO_2	TiO_2	Al_2O_3	Fe_2O_3	CaO	MgO	Na_2O	K_2O	MnO	P_2O_5	LOI	Total
G1	47.619635	-123.01051	Ev_C	46.51	2.93	13.00	14.86	9.61	5.45	0.23	3.29	0.40	0.30	3.01	99.59
G2	47.60591	-123.00355	Ev_C	46.57	3.31	13.32	16.01	7.47	5.04	0.22	3.91	0.38	0.44	3.14	99.81
G3	47.53855	-123.05668	Ev_C	46.56	2.79	13.45	14.78	10.86	6.21	0.22	2.31	0.41	0.27	1.44	99.30
G4	47.53532	-123.04326	Ev_C	46.63	3.28	11.77	15.78	9.60	5.60	0.25	3.63	0.39	0.37	2.58	99.88
G5	47.53532	-123.06305	Ev_C	45.74	4.34	10.57	19.30	8.97	5.10	0.31	3.50	0.45	0.32	1.19	99.79

				Major oxides (%)—normalized to 100% anhydrous										
Site ID	Latitude	Longitude	Geologic unit	SiO_2	TiO_2	Al_2O_3	Fe_2O_3	CaO	MgO	Na_2O	K_2O	MnO	P_2O_5	LOI	Total
G1	47.619635	-123.01051	Ev_C	48.16	3.03	13.46	15.39	9.95	5.64	0.24	3.41	0.41	0.31	3.01	99.59
G2	47.60591	-123.00355	Ev_C	48.17	3.42	13.78	16.56	7.73	5.21	0.23	4.04	0.39	0.46	3.14	99.81
G3	47.53855	-123.05668	Ev_C	47.58	2.85	13.74	15.10	11.10	6.35	0.22	2.36	0.42	0.27	1.44	99.30
G4	47.53532	-123.04326	Ev_C	47.93	3.37	12.10	16.22	9.87	5.76	0.26	3.73	0.40	0.38	2.58	99.88
G5	47.53532	-123.06305	Ev_C	46.39	4.40	10.72	19.58	9.10	5.17	0.31	3.55	0.46	0.32	1.19	99.79

Appendix D. Extent of Puget Lobe Ice During the Vashon Stade of the Fraser Glaciation

The areal extent of the Vashon Stade Puget lobe glacial deposits is indicated by various dashed blue lines on the map. To construct these lines, we consulted previous work, field relations, and technology not available to previous workers. Margaret Todd (1939) noted ice-marginal channels along the Olympic mountain front and in part used these to estimate glacial ice limits. These conspicuous breaks in slope are shown in Figure D1. Building on Todd's observations, we utilized maps showing the slope percentage derived from 10-m resolution digital elevation models, such as the one shown in Figure D2, to guide our interpretation of this limit. While our interpretation is similar to those of other workers (Frisken, 1965; Long, 1975a,b; Carson, 1980), we differ slightly from Todd's interpretation: our limit is at a lower elevation. Our different interpretation stems from mapping glacial drift at higher elevations as pre-Fraser in age. See the Pleistocene Glacial and Nonglacial Deposits section in the pamphlet for additional discussion.

Figure D1. Upper breaks in slope (~1500 and ~1600 ft) that coincide with Todd's (1939) ice-contact deposits near or at the maximum altitude of the Vashon Puget lobe ice on the west margin of Hood Canal. The lower benches represent ice marginal drainages. The Hamma Hamma River flows east (left) between the ridges. View is to the south-southwest; Hood Canal is in the left middle ground.

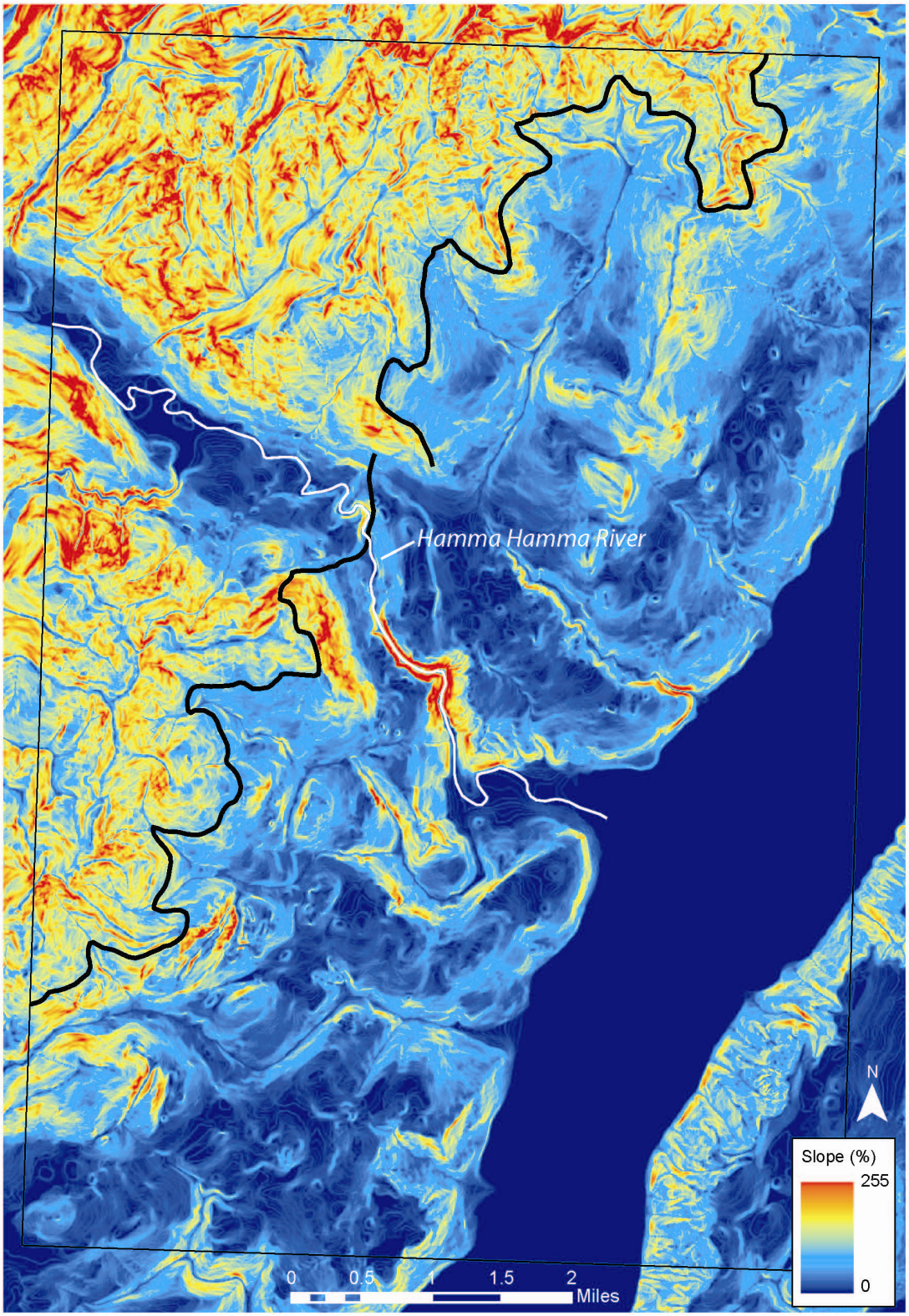

Figure D2. Slope percent map of the Eldon quadrangle and immediately surrounding areas. The map is based on a USGS 10-meter digital elevation model. Steeper slopes, shown by yellows and oranges, are generally in the higher terrain of the west and north part of the quadrangle. Areas shown in blue were overridden by Puget lobe ice. The exception is the lower Hamma Hamma River valley, where recent river incision resulted in extremely steep channel walls.

Appendix E. Geophysical data, Significant Sites HVSR1 to HVSR6

We interpreted horizontal–vertical spectral ratio (HVSR) passive seismic data from significant sites HVSR1 to HVSR6 to estimate the depth to bedrock at each location. At these HVSR stations, we used a formula from Kramer (1996; see also Lane and others, 2008) to infer overlying unit thicknesses from fr values (resonant frequencies corresponding to peak HVSRs). The depth to bedrock in meters is determined by this equation: depth = Vs/4*(fr), where Vs is the shear wave velocity through the units overlying bedrock. Shear wave velocities for HVSR sites were determined on the basis of the calibration of the fr value from site HVSR3 to known depth to bedrock at water well W1. We used the inferred similarity of lithologic substrate properties in HVSR3 and the remaining sites to arrive at a Vs of 620 m/s, thence to estimate the depth to bedrock at HVSR sites 1, 2, 4, 5, and 6. We conducted the HVSR surveys to aid in the construction of the cross section and to determine the depth to bedrock. The sites are plotted on the cross section at the suggested bedrock contact depths; the survey station locations on the surface are shown on the map.

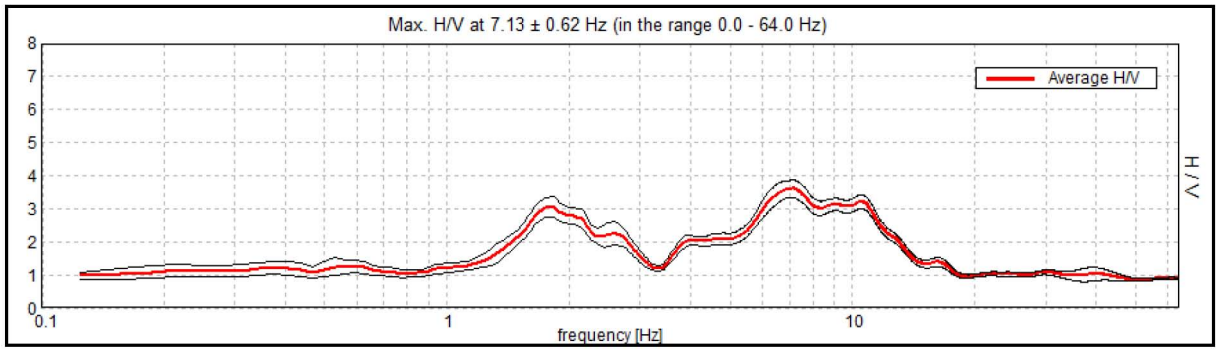

Figure E1. HVSR1 – The presence of multiple H/V peaks in HVSR1 represents velocity changes attributed to multiple lithologic boundaries. The first H/V peak at 7.13 Hz is interpreted to represent the contact between alluvium and underlying compact silts. The large trough that occurs at 3.3 Hz is interpreted to represent the transition from compact silts to loose drift below. The transition from the trough to the next peak at 1.8 Hz then represents the contact between the loose drift and hard bedrock. With an assumed Vs of 620 m/s and a fr value of 1.8 as obtained from the graph, the depth to bedrock at this location is 86.1 m.

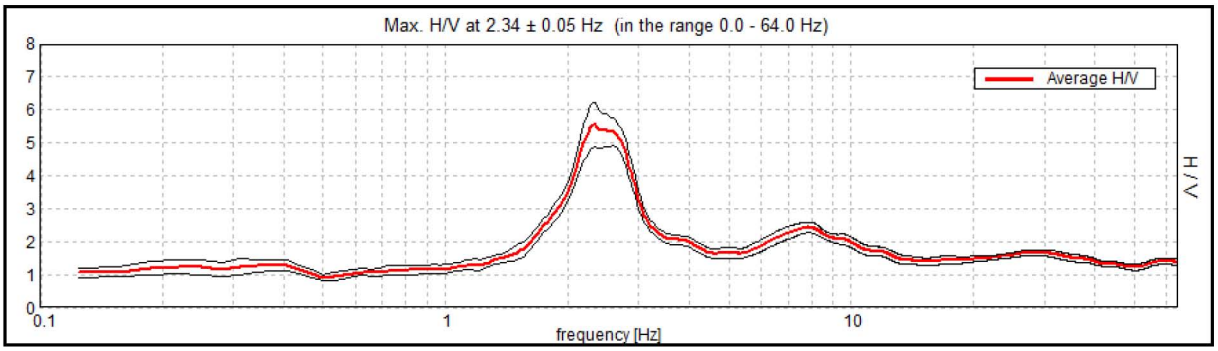

Figure E2. HVSR2 – The peak H/V value at 2.34 Hz is interpreted to represent the contact between bedrock and overlying unconsolidated sediments. With an fr value of 2.34 and an assumed Vs of 620 m/s, the depth to bedrock at this location is 66.2 m.

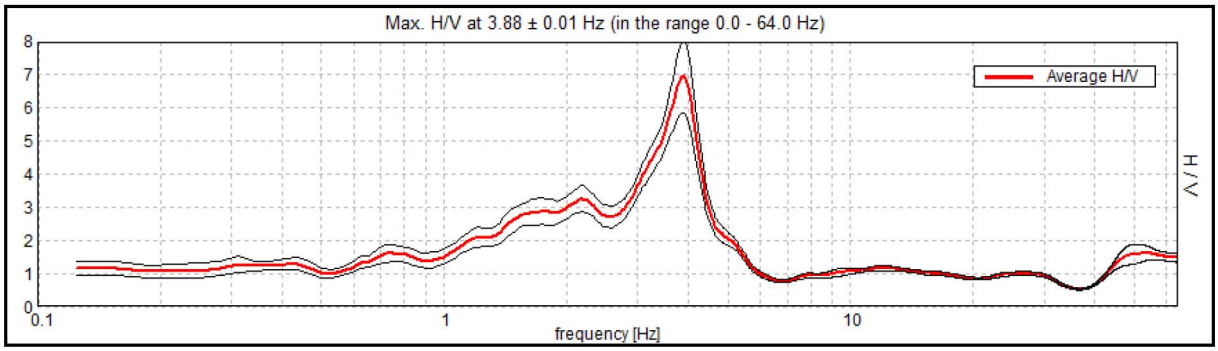

Figure E3. HVSR3 – Due to the proximity of HVSR3 to well W1 (90 ft due south of W1), the peak H/V ratio in this survey was calibrated from the depths of lithologic contacts in the well record in order to determine a Vs value for the sediments overlying bedrock. Utilizing the depth to bedrock in well W1, 40.23 m, in conjunction with the peak H/V ratio of 3.88 Hz, we calculated the Vs for the sediments overlying bedrock to be ~620 m/s.

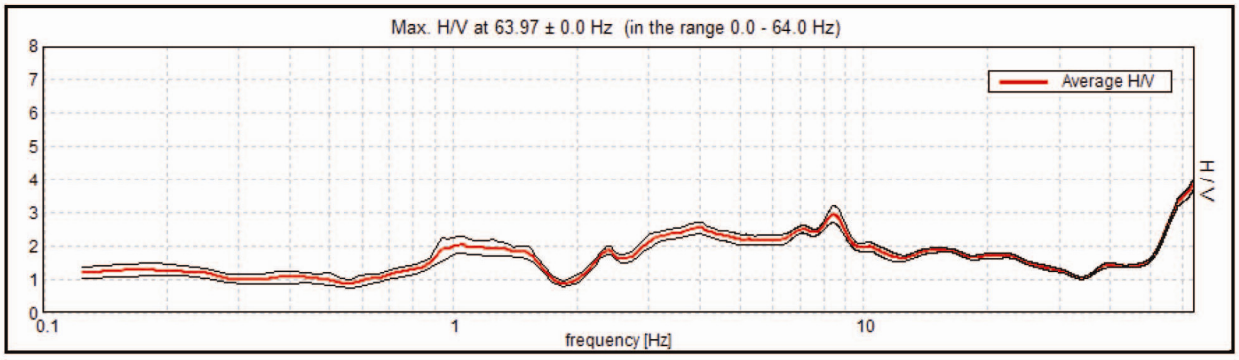

Figure E4. HVSR4 – The peak H/V value occurs at 63.97 Hz, which is a very shallow layer. Due to outcrop field relations in this area, we infer that this velocity contrast is not associated with bedrock and the overlying sediments, but rather a compacted or cemented horizon at a shallow depth, possibly a till. Based on the presence of a trough preceding a broad H/V peak between 0 and 1.7 Hz, we interpret the contact between basalt and overlying unconsolidated sediments to be at 1.2 Hz. With a fr value of 1.2 and a Vs of 620 m/s, the depth to bedrock at this location is 129 m.

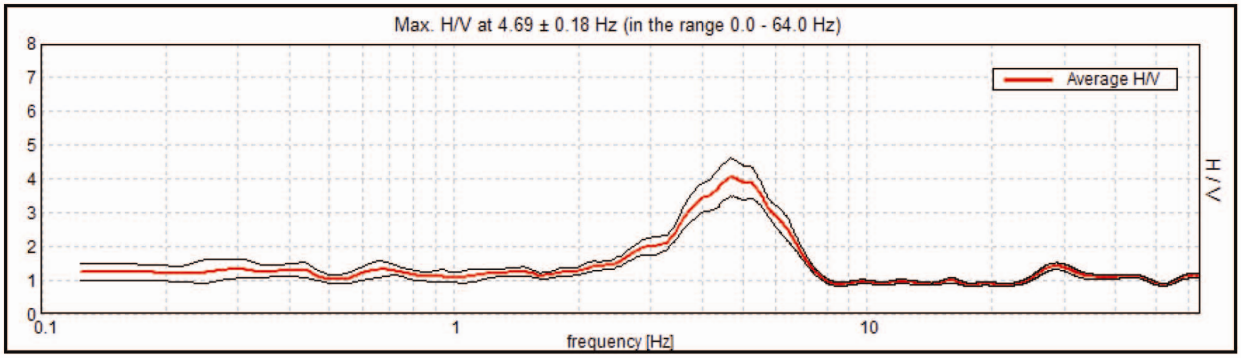

Figure E5. HVSR5 – The peak H/V ratio at 4.69 Hz is interpreted to represent the contact between bedrock and overlying unconsolidated sediments. With a fr value of 4.69 Hz, and an assumed Vs of 620 m/s the depth to bedrock at this location is 33 m.

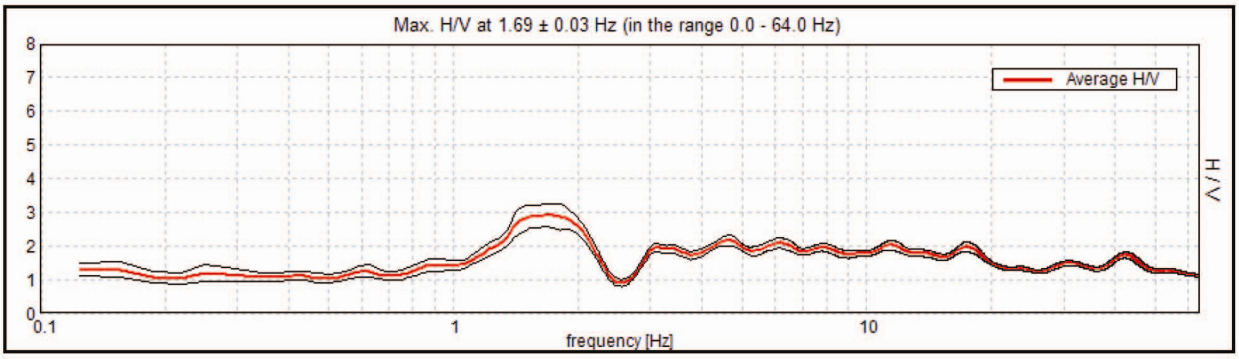

Figure E6. HVSR6 – The broad H/V peak at 1.69 Hz is interpreted to represent the contact between bedrock and overlying unconsolidated sediments. With a fr value of 1.69 Hz, and an assumed Vs of 620 m/s, the depth to bedrock at this location is 91.7 m.

Appendix F. Significant Sites

Site S1: Plant Fossils of Waketickeh Creek

Nonglacial silts containing well-preserved fossil wood fragments, reeds, and leaf imprints are exposed in Waketickeh Creek. An infinite (>43,500 yr BP) radiocarbon date estimate from compressed carbonized wood near the top of the unit suggests that these silts were deposited prior to the Vashon Glaciation. Correlation with silts with similar characteristics mapped in the Holly quadrangle (Contreras and others, 2012b) and a luminescence age estimate of 124.26 to 143.74 ka from this study suggest that these silts were deposited during the Whidbey interglacial period (MIS 5). In Waketickeh Creek, the silts extend up to an elevation of approximately 375 ft and are covered by Olympic-sourced drift that is likely MIS 4 (Possession Glaciation age) glacial diamict.

Site S2: Quaternary Faulting in Waketickeh Creek

A possible fault contact between drift that is likely Possession or early Fraser in age and a Crescent Formation marine sedimentary interbed is exposed on the north side of Waketickeh Creek (Fig. F1). The sedimentary rocks of the Crescent Formation, in turn, appear to be in fault contact with basalt. The fault surface strikes N24E and dips 69° east. There is 3 ft of siltstone cataclasite between the drift and the less fractured siltstone; however, we were not able to determine slip direction. While the contact between the drift and the siltstone may glacial tectonic, the fault appears to roughly follow bedding and is consistent with other bedding plane–parallel faults found in the map area, suggesting this site may also represent faulting in the Quaternary.

Waketickeh Creek is the site of a native story explaining why salmon no longer run up the creek and may record fault rupture in the drainage. In the story, Transformer slipped on the salmon while crossing the creek and cursed the creek; now the creek is full of boulders and lacks a gravel bottom (Elmendorf and Kroeber, 1992). The story may explain a debris flow of boulders found at the alluvial fan at the mouth of the creek or may indicate historic earthquakes.

Site S3: Pre-Vashon Olympic-sourced Till North of the Hamma Hamma River

We found pre-Vashon Olympic-sourced drift and till at this site north of the Hamma Hamma River. This drift is either early Fraser (Evans Creek Stade) or Possession (MIS 4) in age. Below this is a northern-sourced drift (exposed in an area too small to show at map scale) that we suggest is Possession in age on the basis of our correlation of the silt and sand deposit below and to the east, that we mapped as unit Qc_W, Whidbey-age nonglacial silts. This site is important because Possession age Olympic-sourced drift had not been positively identified in previous mapping of this area.

Site S4: A Quaternary Fault in Johns Creek

Quaternary faults exposed at significant site 4 are evidenced by a fault exposure that appears to fault oxidized pre-Vashon sediments (Fig. F2). This fault surface displays two sets of distinct slickensides; both are right-lateral oblique, but with reverse and normal movement evident. For additional discussion, see the Structure section, under the “Central portion of the quadrangle” subsection.

Site S5: Uplifted Beach Deposit at Eldon

Bretz (1913) noted the presence of an uplifted beach terrace containing shells just north of the Hamma Hamma River. We are uncertain of his location, but suggest it could be the site of Eldon and (or) the bench between 135 and 85 ft (Fig. F3). We are also unsure of what this apparent bench represents; it could be an uplifted shoreline from a postglacial lake or an ice-marginal drainage. We did not find any shells, but mapped the deposit as an uplifted beach, based on Bretz’ observations. The eskers above 300 ft elevation appear unmodified by post-glacial lakes or ice-marginal drainage. We mapped a shoreline at approximately this elevation at this location and to the northeast based on a distinct bench, but contend the apparent shoreline could be interpreted as kame deltas or ice-marginal drainage deposits instead of relict shoreline deposits.

Figure F1. Quaternary fault(s) in Waketickeh Creek, significant site S2. *Top.* A Crescent Formation sedimentary interbed on the left is in sharp contact with Crescent Formation basalt (unit Ev_c) on the right. *Bottom.* A possible fault zone separates pre-Vashon alpine drift (unit Qapd) to the left from a Crescent sedimentary interbed that is sheared to cataclasite on the right.

Figure F2. A Quaternary fault in North Fork Johns Creek at significant site S4 that appears to incorporate pre-Vashon alluvium (sand and pebble gravel – white arrow) into the fault zone (see photo on the right). The fault strikes N10ºE and dips east 56º; it exhibits both reverse right-lateral (rake of 30º) and normal right-lateral (rake of 23º) movement. Black arrows indicate slickenline trend direction.

Site S6: Fault in North Fork Johns Creek

We noted a gouge zone 18 to 24 in. wide in Crescent Formation basalt at this location in the North Fork Johns Creek (Fig. F4). Slickensides indicated reverse right-lateral movement with a rake of 40 degrees on a north-northeast-striking fault. This fault has a trend similar to other right-lateral faults in the area.

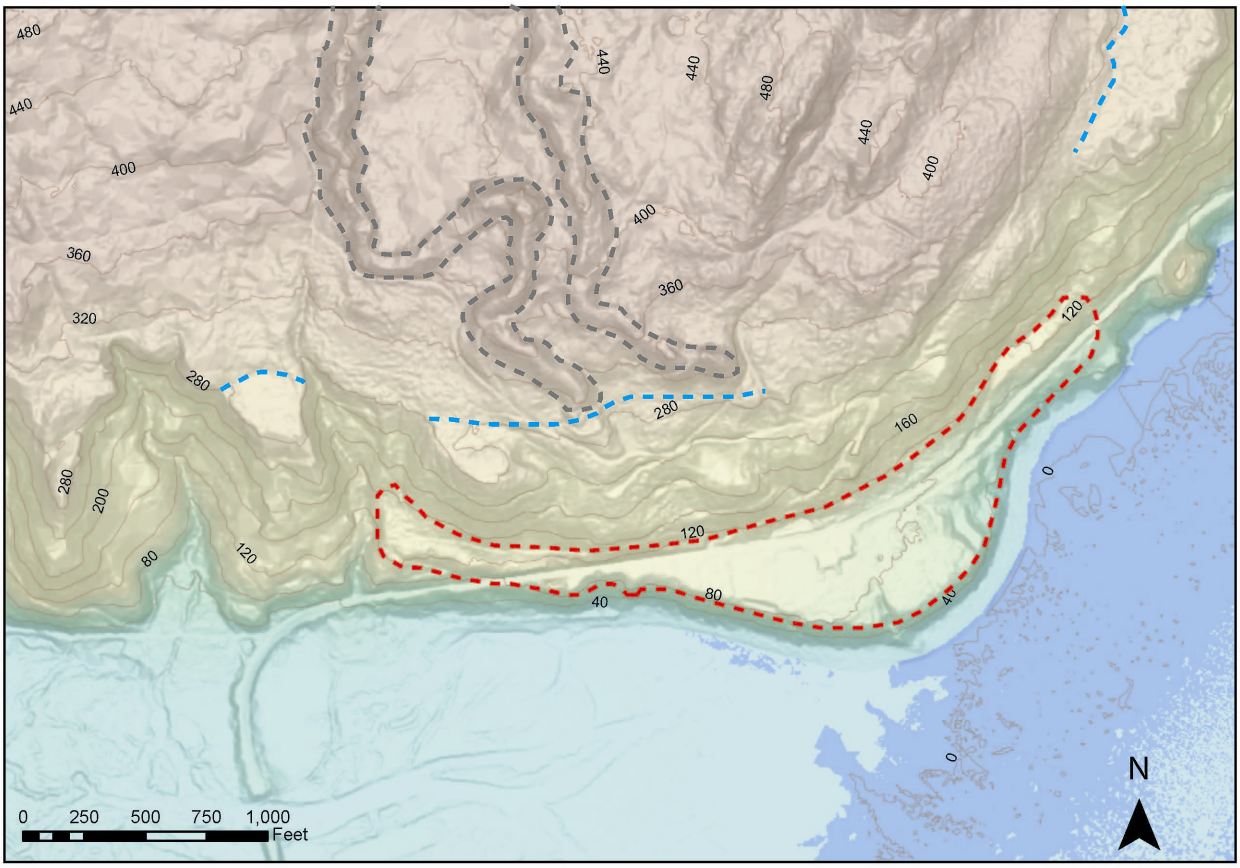

Figure F3. Lidar shaded relief image of the north side of the Hamma Hamma River near Eldon. Significant site S5 is represented by the uplifted beach deposits as identified by Bretz (1913), the approximate location of which is outlined in red. The mapped shoreline (blue dashed line) at approximately 315 to 290 ft elevation appears to coincide with the termination of eskers (gray dashed lines). For a more detailed discussion on the significance of the uplifted beach deposits, mapped shorelines, and the termination of eskers, see the Shorelines section of the Eldon quadrangle pamphlet.

Site S7: Preserved Forest in Johns Creek

We identified the remains of a forest floor in the banks of Johns Creek; a radiocarbon age estimate taken from the wood preserved in the deposit suggests the forest was killed and preserved between 827 to 1017 cal yr AD (GD7, Beta-318212, 1160 ± 30 BP, 2-sigma calibrated results by Beta Analytic using the INTCAL09 database [Heaton and others, 2009; Reimer and others, 2009; Stuiver and others, 1993; Oeschger and others, 1975]). The sample consisting of three growth rings was located 47 rings in from the bark. We added 47 years to the calibrated age to account for sample offset from outer bark (Fig. F5). Additional trees, in growth position and additional organics are preserved very well in unit Qoa. This sample and one additional date are presented in Table 1 on the map plate. For additional information on this site, see the description for unit Qoa and the Structure section, “Central Portion of the Quadrangle”.

Site S8: Left-lateral Normal Oblique Faulting in an Eastern Gorge

Few faults in the map area exhibit evidence of left-lateral faulting, but the fault at significant site S8 does (Fig. F6). The mineralized slickenlines in basalt have a rake of 70 degrees on the north-northeast-striking fault. The dominate component of movement appears to be down to the southeast.

Site S9: Faults in Basalt at the Southwest End of a Western Gorge

We found a rare and easily accessible exposure of faulted basalt and cataclasite in one of the conspicuous parallel gorges in the southwest corner of the map. In this exposure, faults both parallel and subparallel to the gorges can be observed. It is unique because the fault gouge is easily erodible and little remains to be observed (Fig. F7).

Figure F4. Fault in North Fork Johns Creek, significant site S6. The fault strikes N18°E and dips 59° east. Slickensides indicate reverse right-lateral movement; their rake is 40°. The gouge zone is from 18 to 24 in. wide.

Site S10: Tephra in an Unnamed Drainage on the West-Facing Shore of the Kitsap Peninsula, Mason County

A tephra identified and analyzed by Birdseye and Carson (1980) to correlate nonglacial deposits throughout the southern Puget Lowland, specifically the Lake Tapps and the Frigid Creek tephras is exposed at sec. 2, T23N R3W, within unit Qc_R, and is believed to be older than 780 ka (Fig. F8). This tephra is also exposed in the bluff north of the creek-bed exposure. The tephra is altered to clay, so while we sampled it, we did not submit it for electron

microprobe analysis. Tephras are rarely preserved in the Quaternary deposits of the Puget Lowland, making this location important enough to show on this geological map.

Figure F5. Johns Creek buried forest, significant site S7. *Top left.* Tree stump (outlined in white) in growth position within an alluvial terrace, suggesting burial of an older forest floor. *Top right.* Fallen tree protrudes from the alluvial terrace into the modern stream channel; bark is still preserved on the tree. *Bottom left.* Hank Bloomfield cutting a sample from the fallen tree for radiocarbon dating and dendrochronology. *Bottom right.* Wedge cut from fallen tree in alluvial terrace; radiocarbon sample GD7 consists of 3 rings taken 47 rings in from bark on tree. Death of tree is estimated to be between 827 to 1017 cal yr AD, which coincides with the timing of tectonic events on the Seattle, Tacoma, or Saddle Mountain fault zones.

Sites S11, S12, and S13: Multiple Sites of Quaternary Faulting along Eagle Creek

Three significant sites were designated along Eagle Creek in the southwest corner of the map area. At each of these sites, Quaternary faulting can be observed. Photos of the sites are shown here (Figs. F9–F11) with additional descriptions are in the pamphlet in the Structure section, “Southern Portion of the Quadrangle”. While we have no age control to suggest these locations are active faults, these sites are important because of their proximity to known active faults, and there are very few locations where Quaternary faulting can be observed.

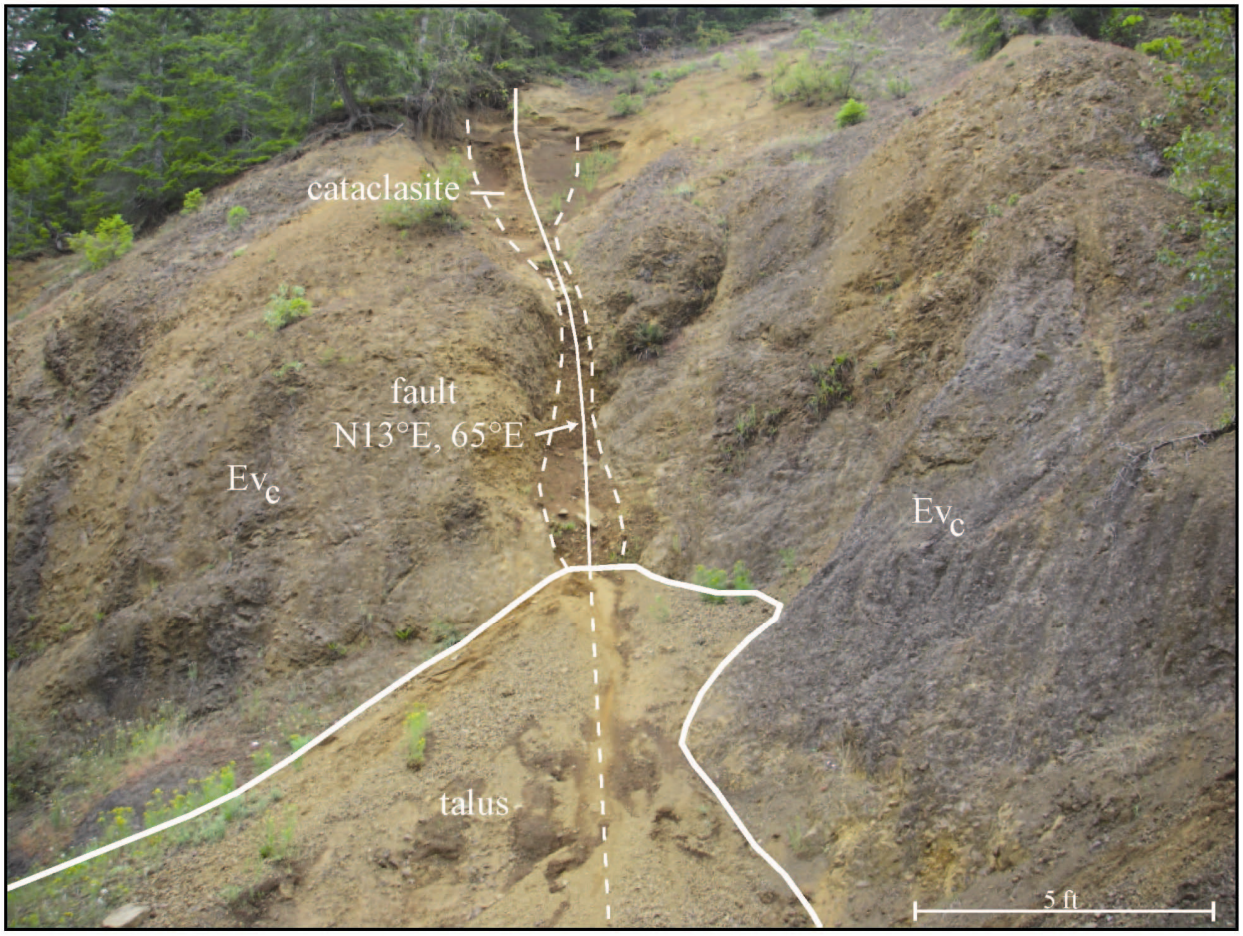

Figure F6. Faulting in the eastern gorge, between Jorsted Creek and South Fork Johns Creek at significant site S8. Slickenlines on the fault surface have a rake of 77° and exhibit left-lateral, down to the southeast movement.

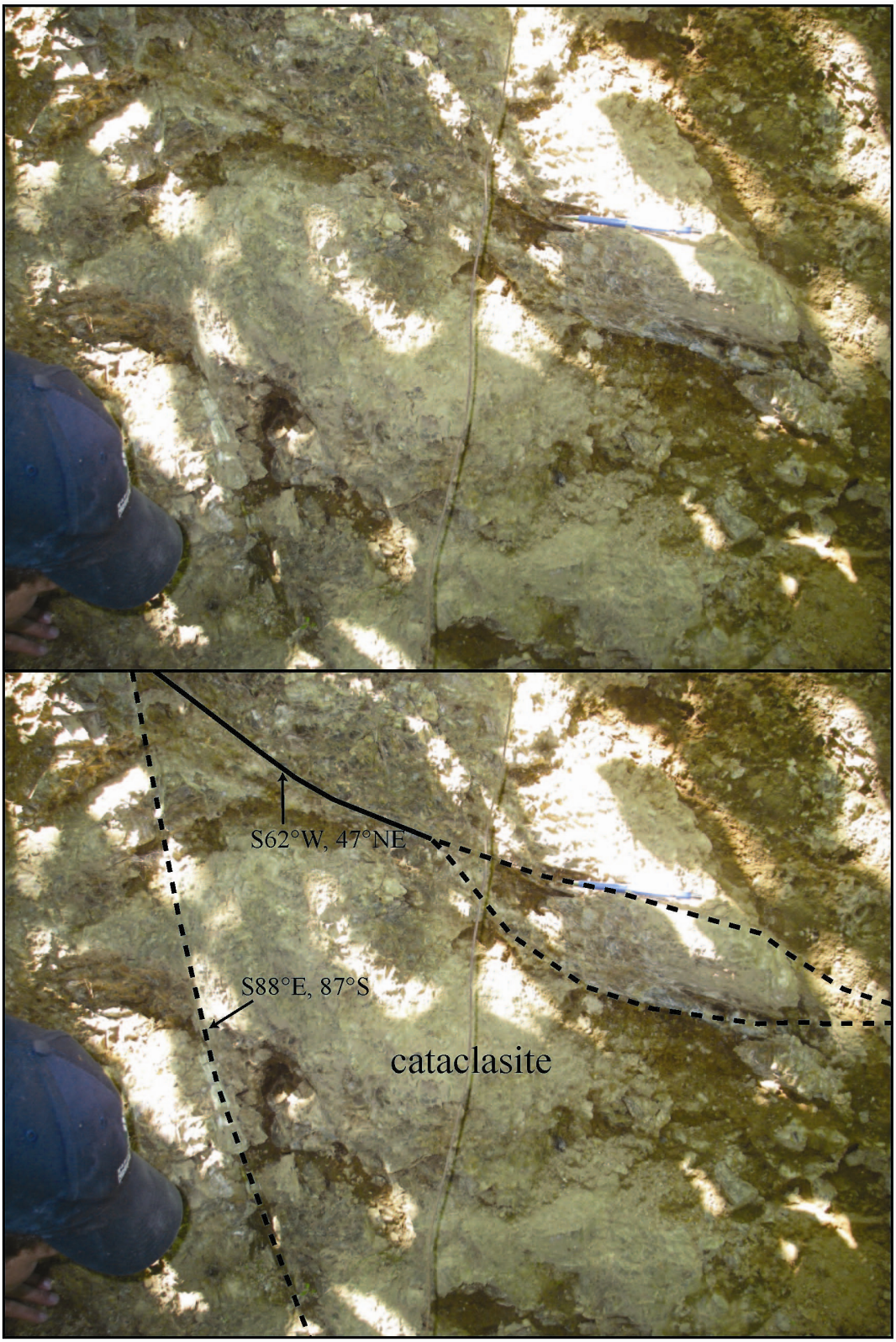

Figure F7. Quaternary faults at the southwest end of a western gorge at significant site S9. In this photo the upper fault strikes S62°W and dips 47°NE, slickenlines trend N36°E, plunge 24°SE, and exhibit right-lateral, northwest side down movement. Slickenlines on the fault that strikes S88°E and dips 87°S have a rake of 29°.

Figure F8. Tephra layer at significant site S10 along the shore on the east side of Hood Canal. This tephra layer (outlined in white) is exposed in unit Qc_R, near the lower exposures of unit $Qguc_1$. This tephra was originally identified and analyzed by Birdseye and Carson (1980).

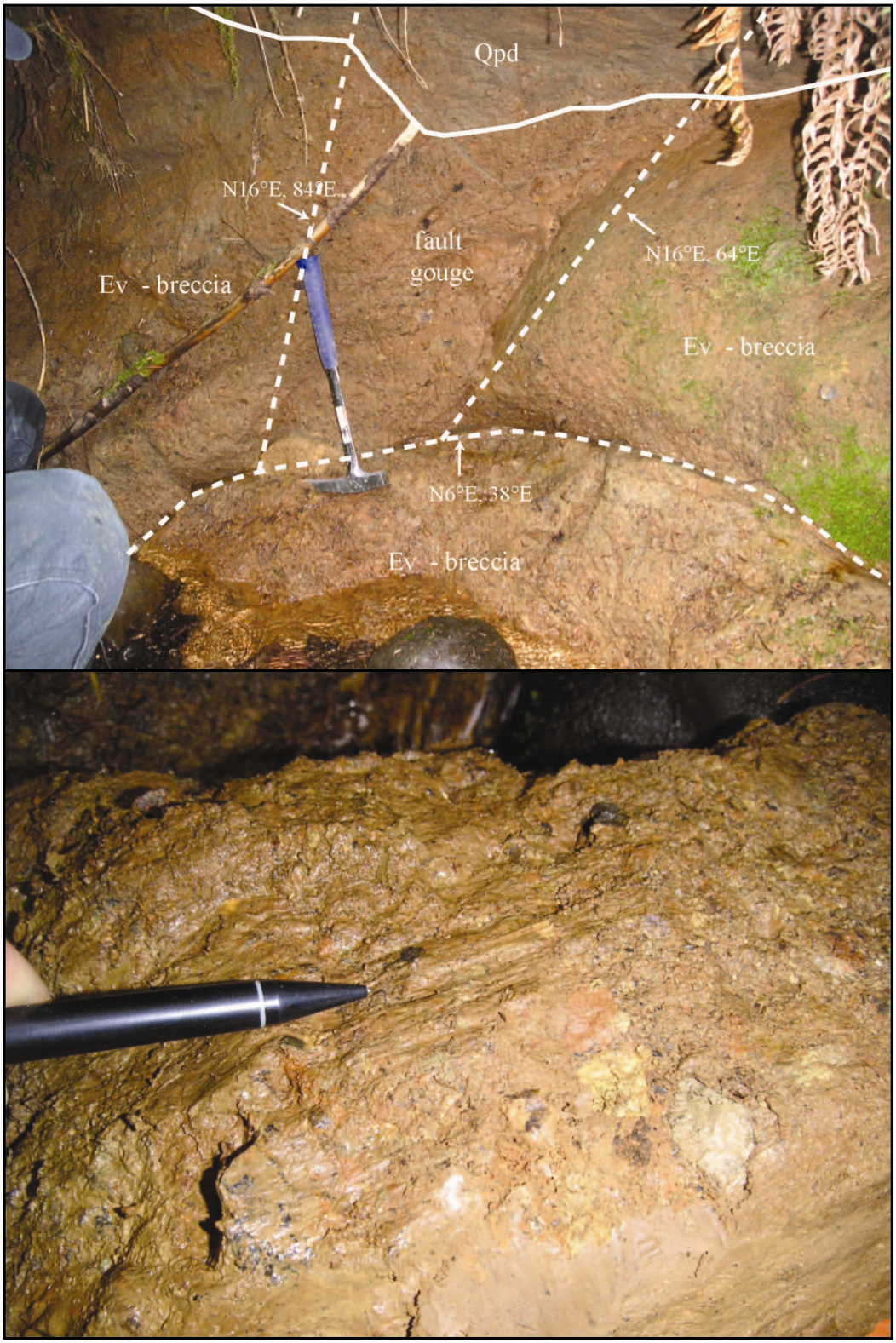

Figure F9. Quaternary faults (dashed white lines) in northern Eagle Creek at significant site S11, where highly fractured basalt breccia is faulted against pre-Vashon drift (top photo). Slickenlines on the fault, which strikes N16°E and dips east at 84°, have a trend and plunge of S46°E, 71°SW. The slickenlines suggest reverse subvertical movement (bottom photo). Hammer for scale in the upper photo is 16.5 in. long.

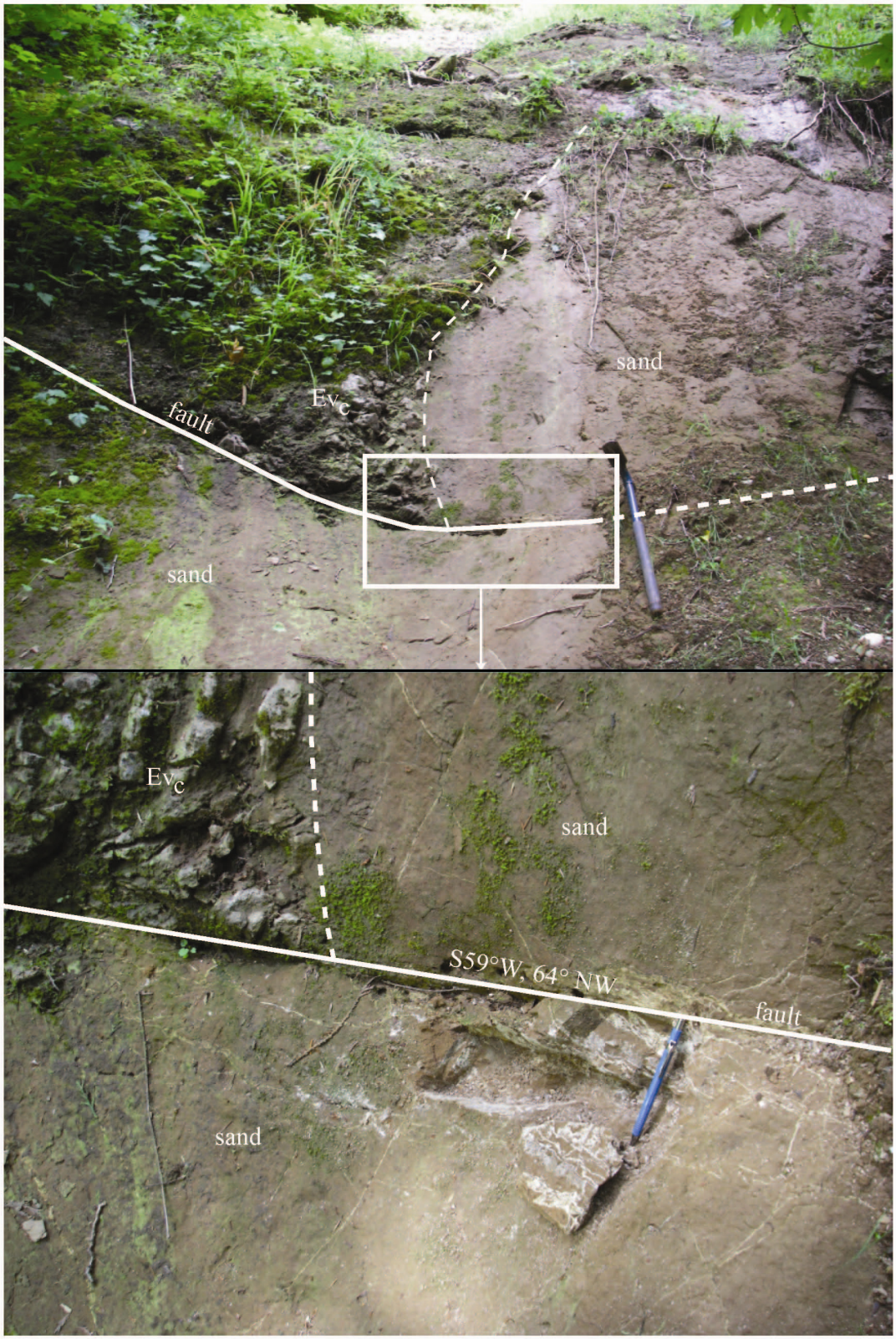

Figure F10. Quaternary fault in south Eagle Creek at significant site S12. At this location pre-Vashon sand is in fault contact with basalt of the Crescent Formation. Calcite slickensides indicate reverse movement with a trend and plunge of S31°W, 63°NW.

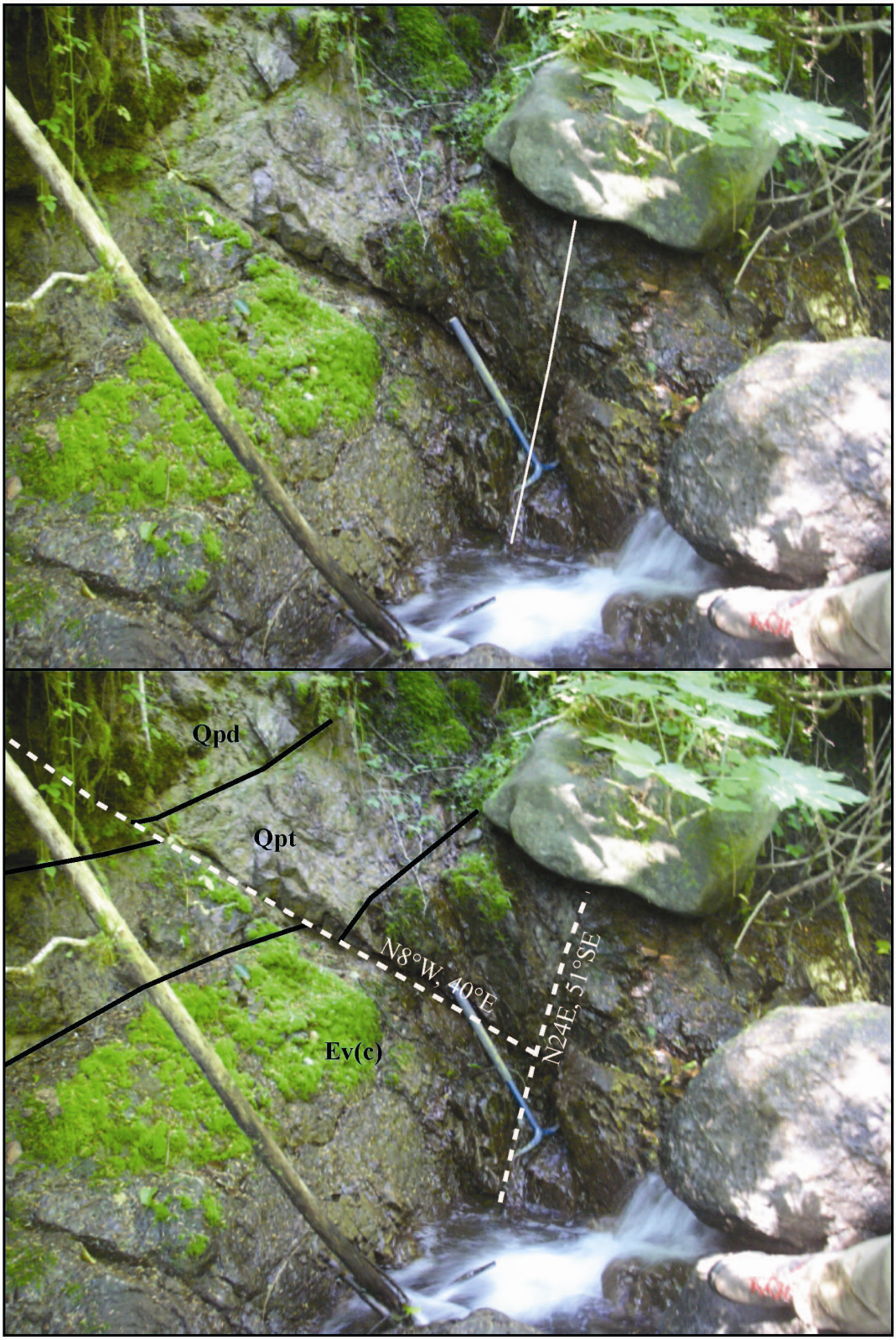

Figure F11. Quaternary fault in Eagle Creek at significant site S13. The fault strikes N8°W and dips 40°E. It cuts units Ev_c, Qpt, and Qpd. Note the offset of about 10 in. in unit Qpd at the upper left corner of the lower photograph.